

# Impact of QCD and PDF uncertainties on Standard Model Measurements

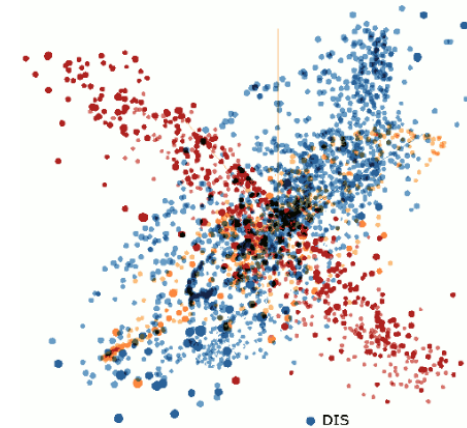
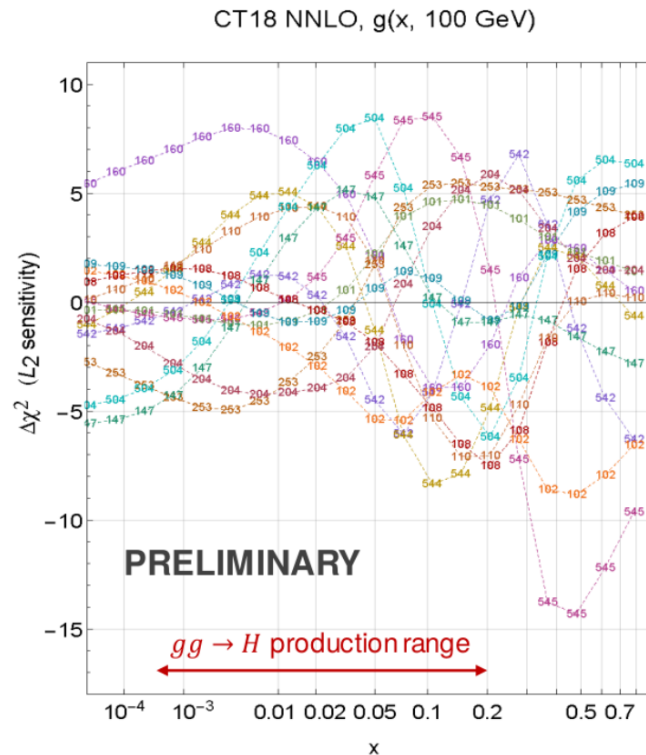
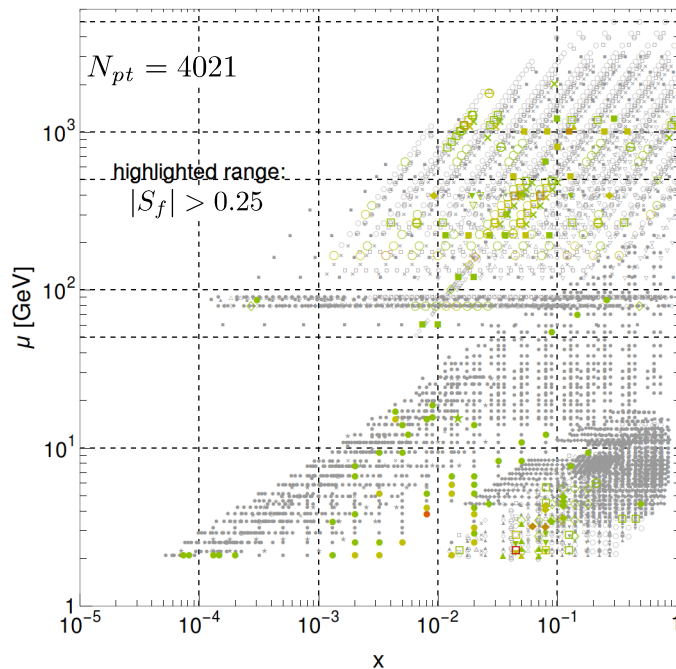
a theory/PDF analysis perspective.

**Tim Hobbs, SMU/CTEQ and JLab EIC Center**

July 17<sup>th</sup> 2019

Collaboration with Bo-Ting Wang, Pavel Nadolsky, Fred Olness  
...and **CTEQ-TEA**...

$|S_f|$  for  $\sigma_{H^0}$ , 14 TeV, CT14HERA2NNLO



QCD@LHC '19. Buffalo, NY; July 15-19, 2019.



# LHC has accumulated copious high-precision data

## LHC Performance 2017



“data deluge...”

this data is an opportunity, but also a challenge:

→ PDF uncertainties are a **double-edged sword**

(i.e., quantities for which PDF uncertainties are large are also PDF-sensitive, and can be constraining)

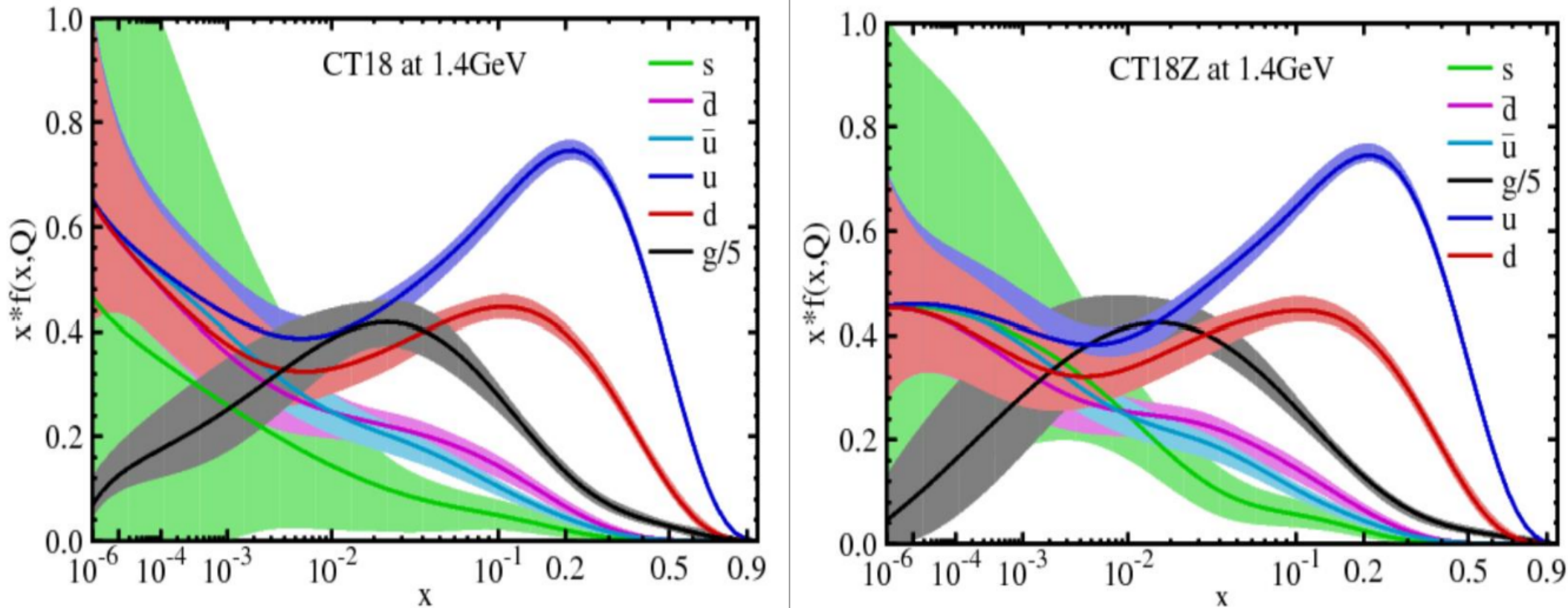
**this talk (mainly):**  $\sin^2 \theta_W$ ,  $M_W$ ,  $\sigma_H$ , ...

→ to reach precision objectives for HL-LHC, it will be crucial to understand pulls/tensions in modern PDF analyses

# CT18 parton distributions

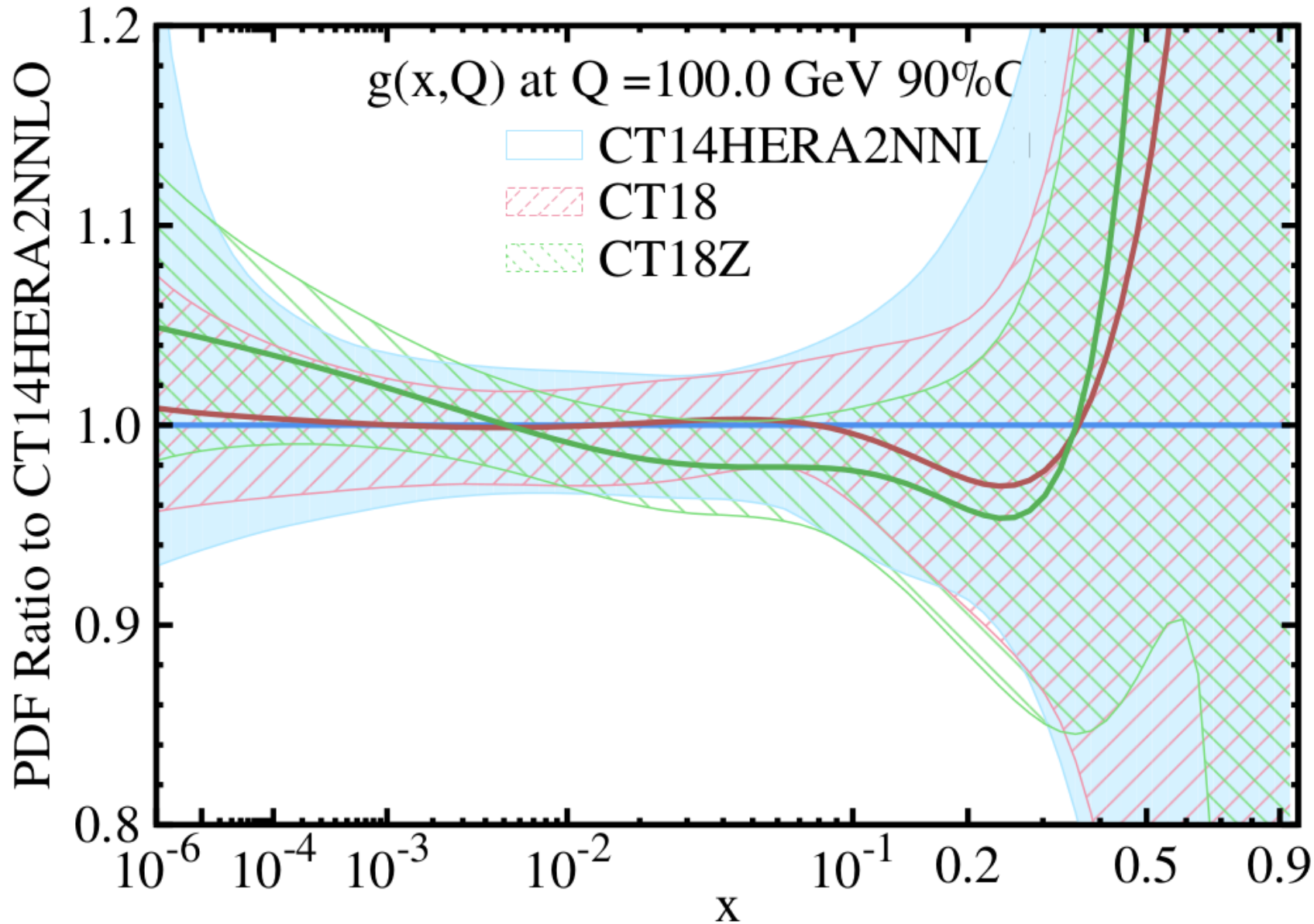
PDF analyses are challenging! (theoretically, computationally, statistically, ... )

## Four PDF ensembles: CT18 (default), A, X, and Z



CT18Z has enhanced gluon and strange PDFs at  $x \sim 10^{-4}$ , and reduced light-quark PDFs at  $x < 10^{-2}$ . The CT18Z fit is performed so as to maximize the differences from CT18 PDFs, while preserving about the same goodness-of-fit as for CT18. CT18A and CT18X include some features of CT18Z

(See talk by P. Nadolsky, July 15th.)



- LHC Run-1 data drive important PDF improvements, including for the gluon at high-, low- $x$
- BUT: performing/comparing fits is insufficient for understanding PDF sensitivities

# PDFSense: an impact-study framework complementary to reweighing approaches

(See ePUMP talk by C. Schmidt.)

→ quickly evaluate a HEP data set according to its PDF **sensitivity**,  $S_f$

("correlation 2.0"): an easy-to-compute **figure-of-merit** for data point sensitivity to PDFs in the presence of experimental errors

→ map these sensitivities in a kinematical parameter space to quantify/visualize origin and interplay of pulls and tensions

## an expanding set of calculations:

### 1. Mapping the sensitivity of hadronic experiments to nucleon structure

B.-T. Wang, T.J. Hobbs, S. Doyle, J. Gao, T.-J. Hou, P. M. Nadolsky, F. I. Olness  
[Phys.Rev. D98 \(2018\) 094030](#)

### 2. The coming synergy between lattice QCD and high-energy phenomenology

T.J. Hobbs, Bo-Ting Wang, Pavel Nadolsky, Fredrick Olness  
[arXiv:1904.00222](#)

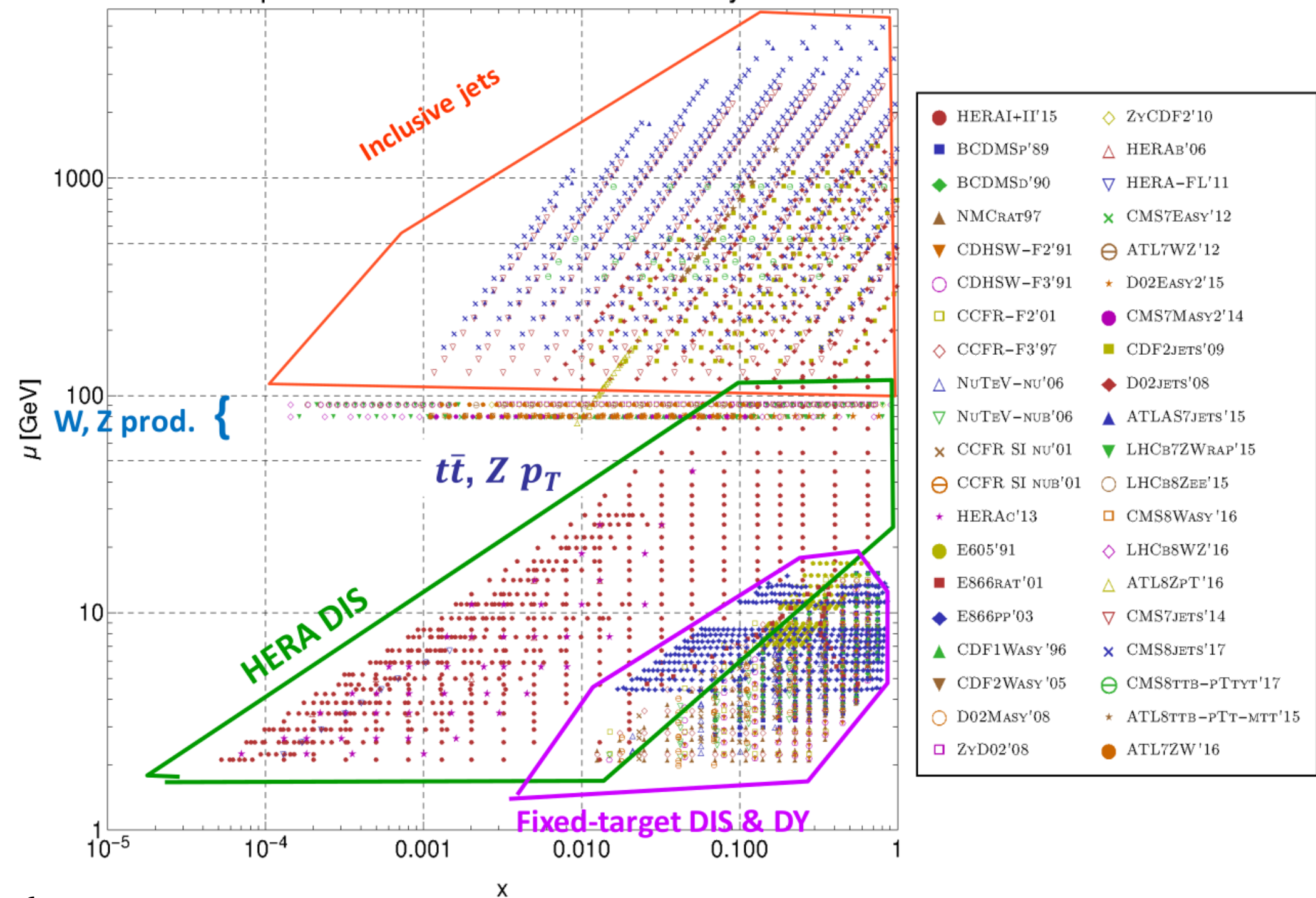
### 3. Mapping the PDF sensitivity of future facilities (HL-LHC, LHeC, and EIC)

T.J. Hobbs, Bo-Ting Wang, Pavel Nadolsky, Fredrick Olness  
[arxiv:1907.00988](#)

(more detailed work in preparation)

T  
O  
D  
A  
Y

# Experimental data in CT18 PDF analysis



# 1. New LHC datasets for CT18

---

1. 245 1505.07024 LHCb Z (W) muon rapidity at 7 TeV(applgrid)
2. 246 1503.00963 LHCb 8 TeV Z rapidity (applgrid);
3. 249 1603.01803 CMS W lepton asymmetry at 8 TeV (applgrid)
4. 250 1511.08039 LHCb Z (W) muon rapidity at 8 TeV(applgrid)
5. 253 1512.02192 ATLAS 7 TeV Z pT (applgrid)
6. 542 1406.0324 CMS incl. jet at 7 TeV with R=0.7 (fastNLO)
7. 544 1410.8857 ATLAS incl. jet at 7 TeV with R=0.6 (applgrid)
8. 545 1609.05331 CMS incl. jet at 8 TeV with R=0.7 (fastNLO)
9. 565 1511.04716 ATLAS 8 TeV tT pT diff. distributions (fastNNLO)
10. 567 1511.04716 ATLAS 8 TeV tT mtT diff. distributions (fastNNLO)
11. 573 1703.01630 CMS 8 TeV tT (pT , yt ) double diff. distributions (fastNNLO)

12. 248 1612.03016 ATLAS 7 TeV Z and W rapidity (applgrid)->CT18Z
  - also uses a special small-x factorization scale, charm mass  $m_c=1.4$  GeV
  - serious changes in PDFs, so warrants a separate PDF

---

PDFSense guided the selection and implementation of these data for CT18

how is this done? ... examine and map the sensitivities based on knowledge of Hessian **PDFs** and **residual** variations

- *idea* : study the **statistical correlation** between PDFs and the quality of the fit at a measured data point(s); fit quality encoded in a (Theory) – (shifted Data) *residual* :

$$r_i(\vec{a}) = \frac{1}{s_i} (T_i(\vec{a}) - D_{i,sh}(\vec{a}))$$

$s_i$  : uncorrelated uncert.

$\vec{a}$  : PDF parameters

- for each data point, calculate the correlation (and sensitivity) between the residual and PDFs based on Hessian variation over PDF replicas,

$$C_f \equiv \text{Corr}[f(x_i, \mu_i), r_i(x_i, \mu_i)] \quad \longrightarrow \quad S_f \equiv \frac{\Delta r_i}{\langle r_0 \rangle_E} C_f$$

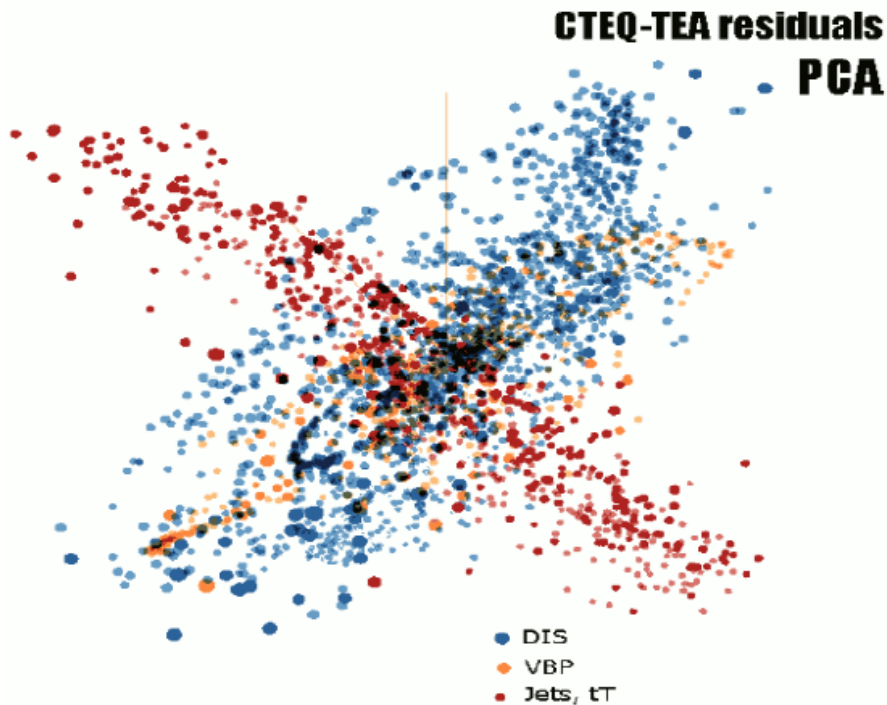
- map these in kinematical parameter space where, e.g., for DIS,

$$x_i \approx x_{Bi} \quad \mu_i \approx Q|_i$$

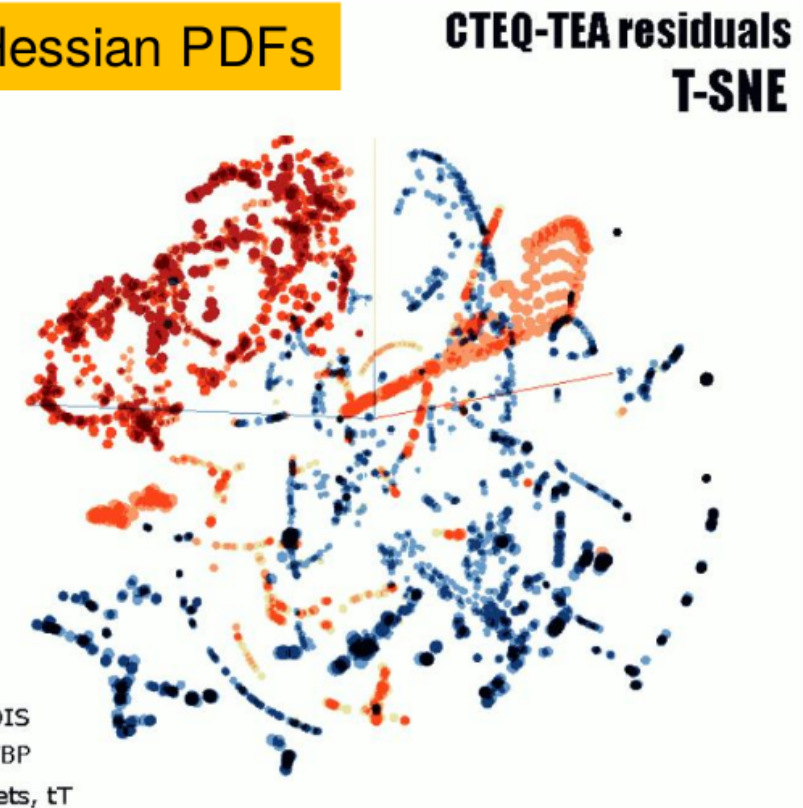
# Vectors of data point residuals...

... carry detailed information about sensitivity of individual experimental data points to PDFs; can be studied using statistical packages (TensorFlow, Mathematica,...)

Using Hessian PDFs



Principal Component Analysis (PCA) visualizes the 56-dim. manifold by reducing it to 10 dimensions (à la META PDFs)



Similarly, t-distributed Stochastic Neighbor embedding (t-SNE) distinguishes PDF pulls by process

# the sensitivity reveals a richer landscape than the correlation!

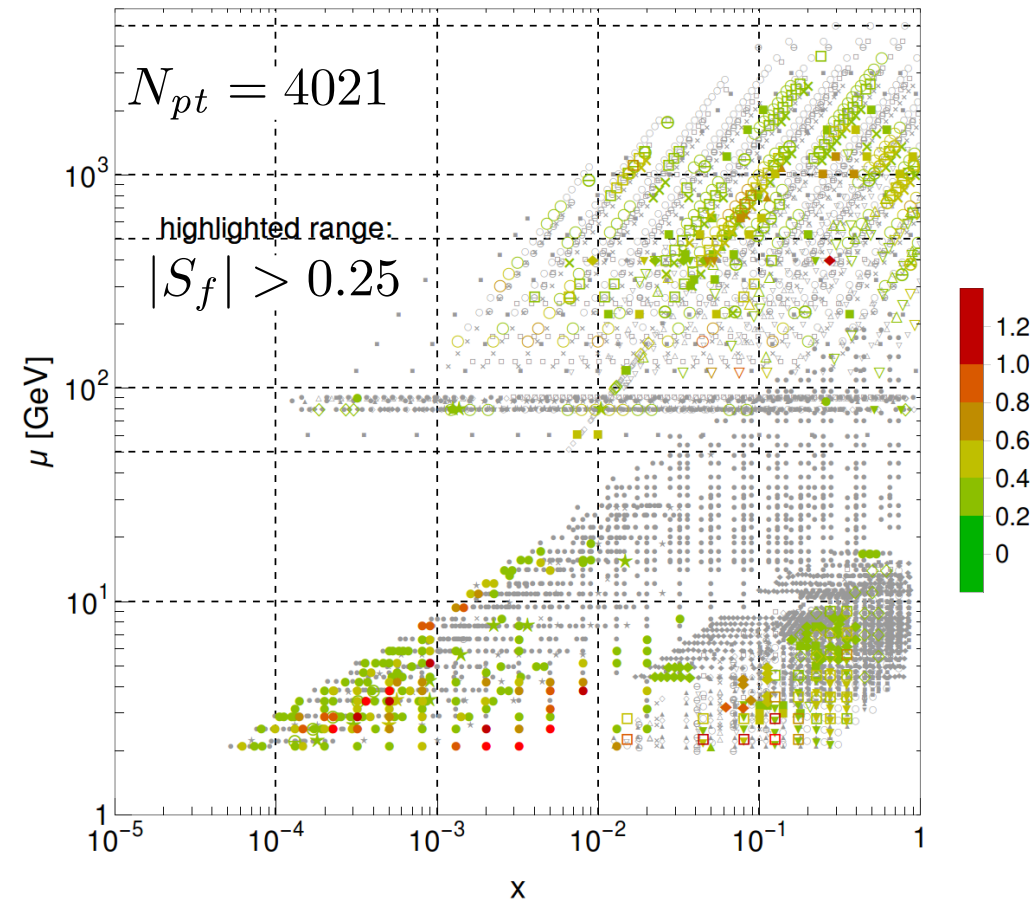
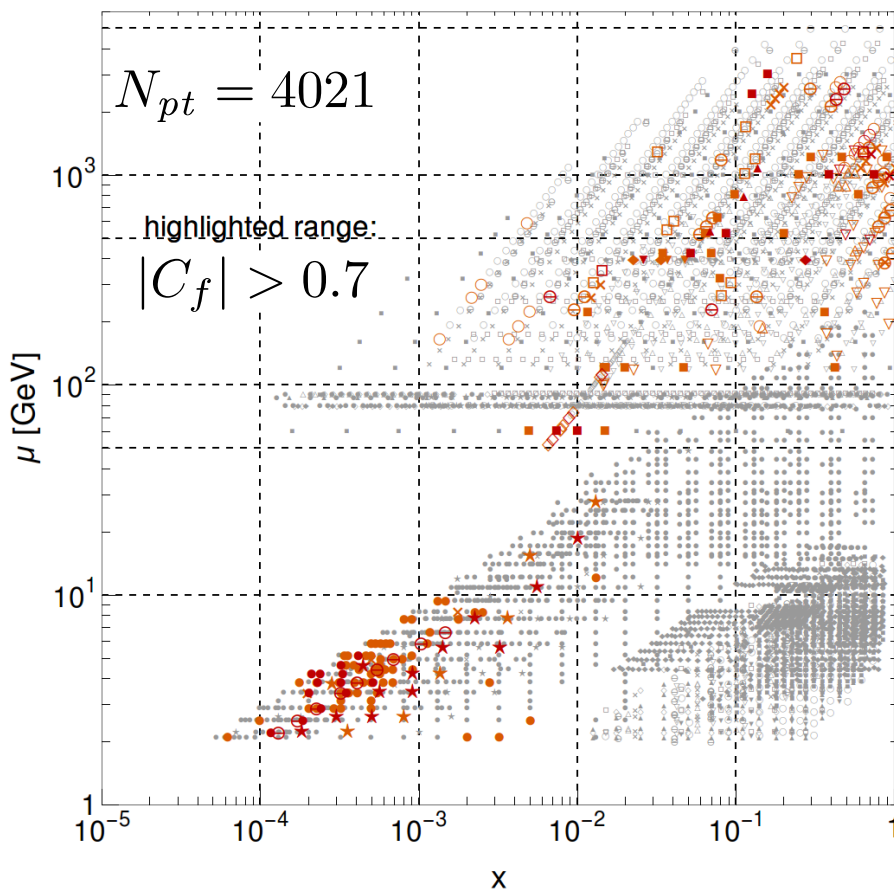
e.g., the substantial impact of inclusive jet data on gluon PDF is identified by  $S_f$

$$C_g(x_i, \mu_i)$$

$|C_f|$  for  $g(x, \mu)$ , CT14HERA2NNLO

$$S_g(x_i, \mu_i)$$

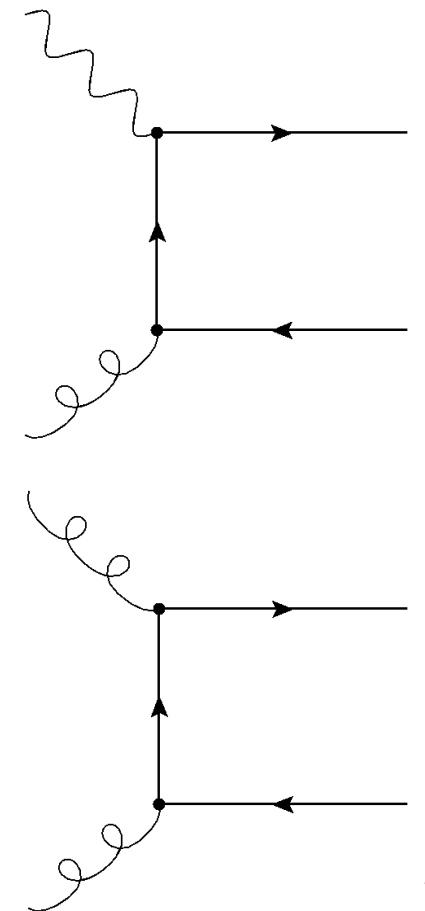
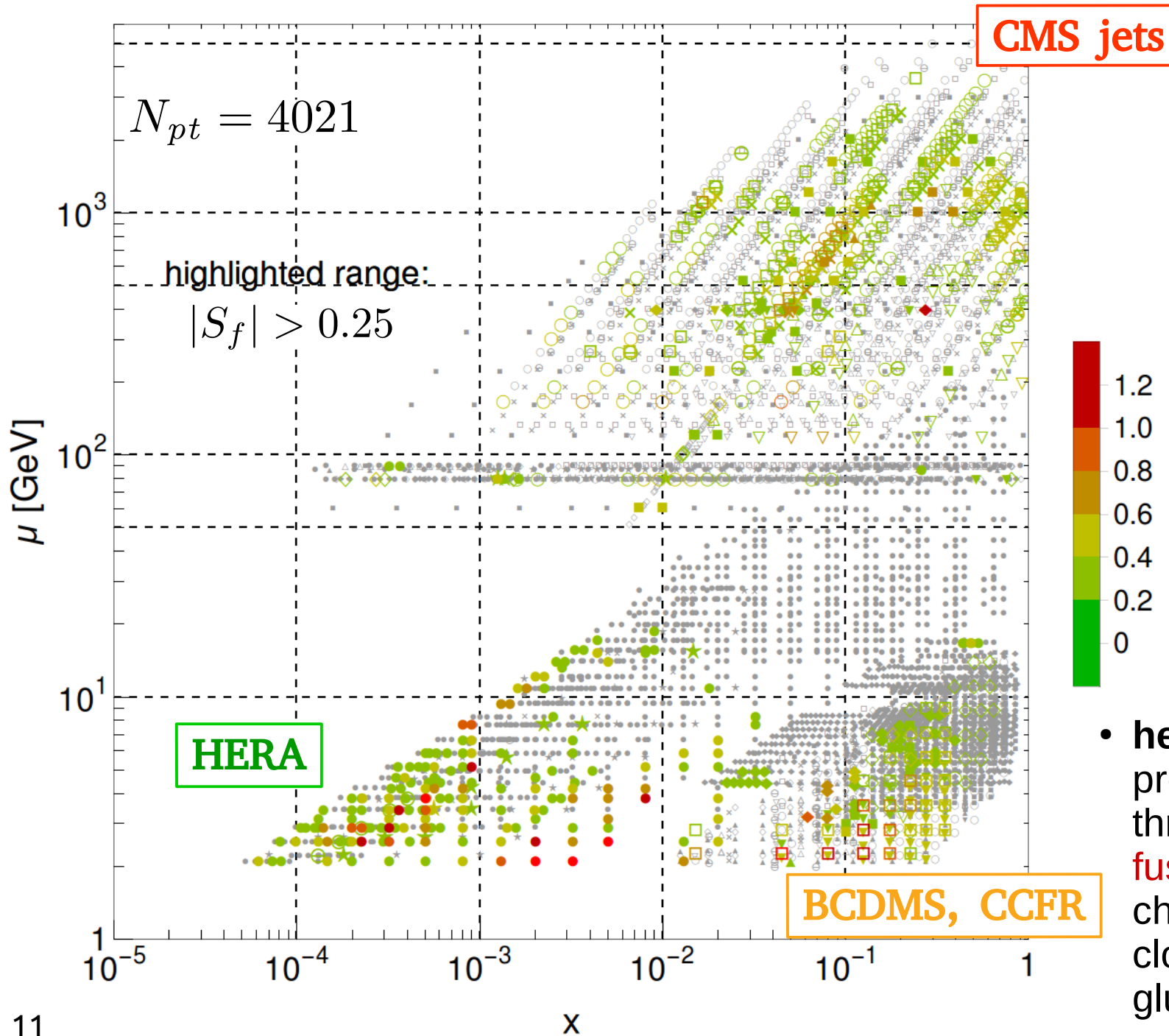
$|S_f|$  for  $g(x, \mu)$ , CT14HERA2NNLO



sensitivity maps reveal:

- (i) highest impact data points for specific PDFs/observables
- (ii) tensions/complementarities among data sets
- (iii) physical origin of PDF constraints

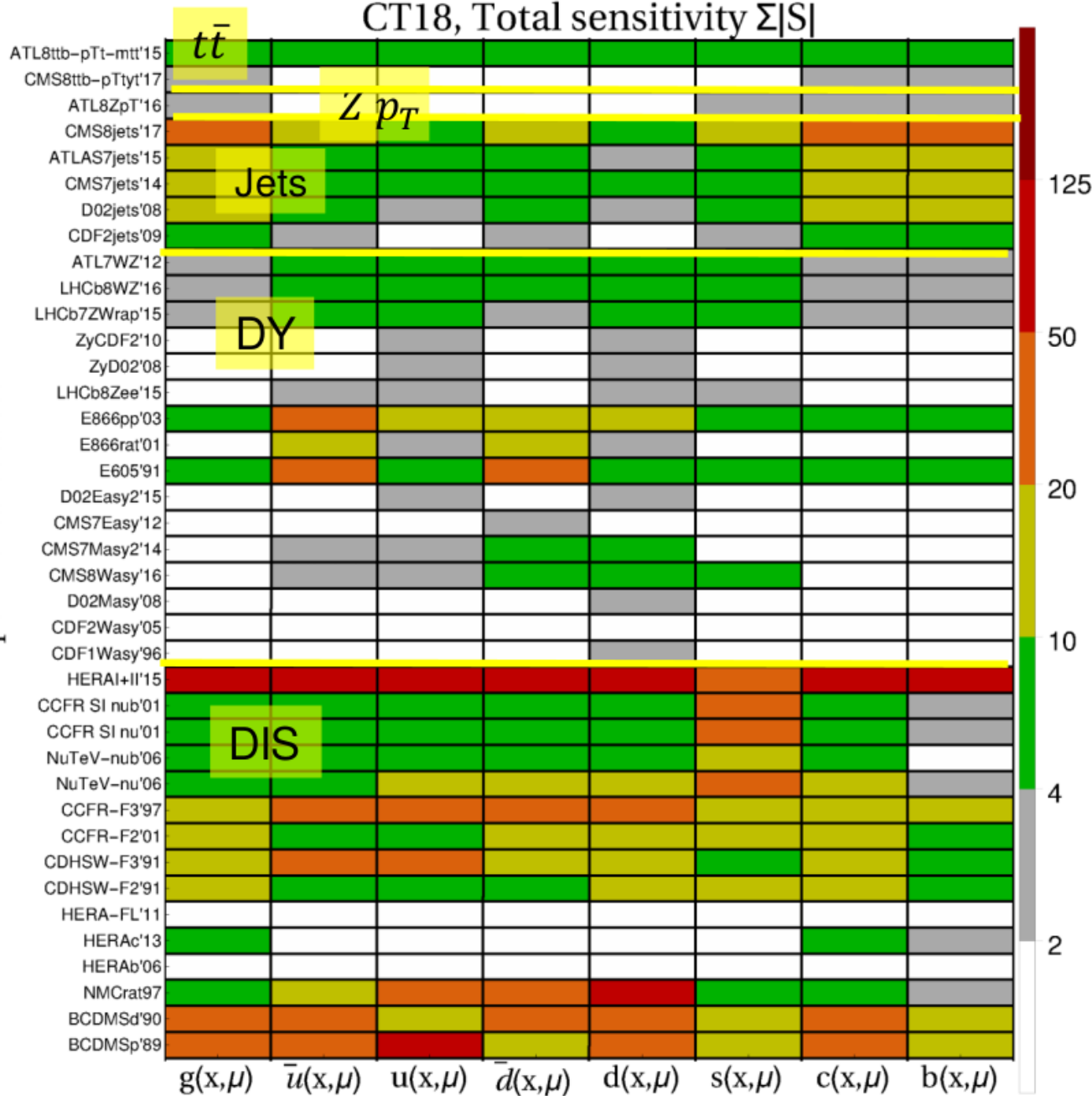
# $|S_f|$ for $c(x,\mu)$ , CT14HERA2NNLO



- **heavy quark** production proceeds through **boson fusion diagrams**: charm sensitivities closely track the gluon plot

# Sensitivity of hadronic experiments to PDFs

CT18, Total sensitivity  $\Sigma|S|$



Total sensitivity to  $f_a(x_i, \mu_i)$ , summed over data points

$$\sum_{\text{points}} |S_{f,i}|$$

Computed using the **PDFSense** code  
 [arXiv:1803.02777]

# we use this technology to examine implications for HEP phenomenology at LHC

---

esp., EW pheno., Higgs physics,  $g(x)$ , ...

➔ Mapping the sensitivity of hadronic experiments to nucleon structure  
B.-T. Wang, T.J. Hobbs, S. Doyle, J. Gao, T.-J. Hou, P. M. Nadolsky, F. I. Olness  
[Phys.Rev. D98 \(2018\) 094030](#)

*L2 sensitivity details in*

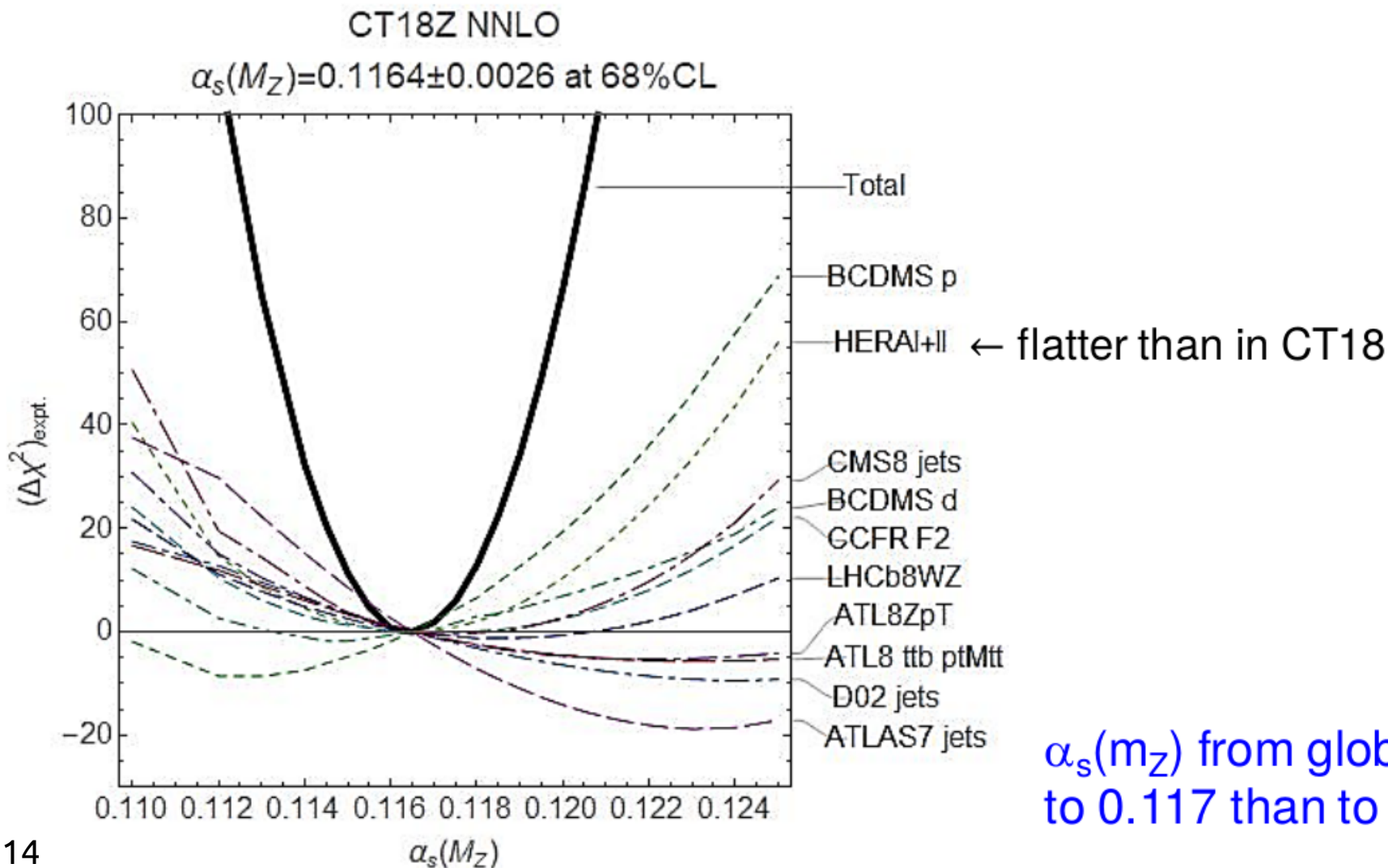
The coming synergy between lattice QCD and high-energy phenomenology  
T.J. Hobbs, Bo-Ting Wang, Pavel Nadolsky, Fredrick Olness  
[arXiv:1904.00222v2](#) (coming soon)

$$\alpha_S(\mu)$$

# Lagrange Multiplier (LM) Scans: $\alpha_S(M_Z)$

The LM scan technique is introduced in **Stump et al., Phys.Rev. D65 (2001) 014012**

- 😊 Detailed dependence of  $\chi^2$       😞 slow; refitting on a supercomputing cluster



$\alpha_S(m_Z)$  from global fit closer to 0.117 than to 0.118

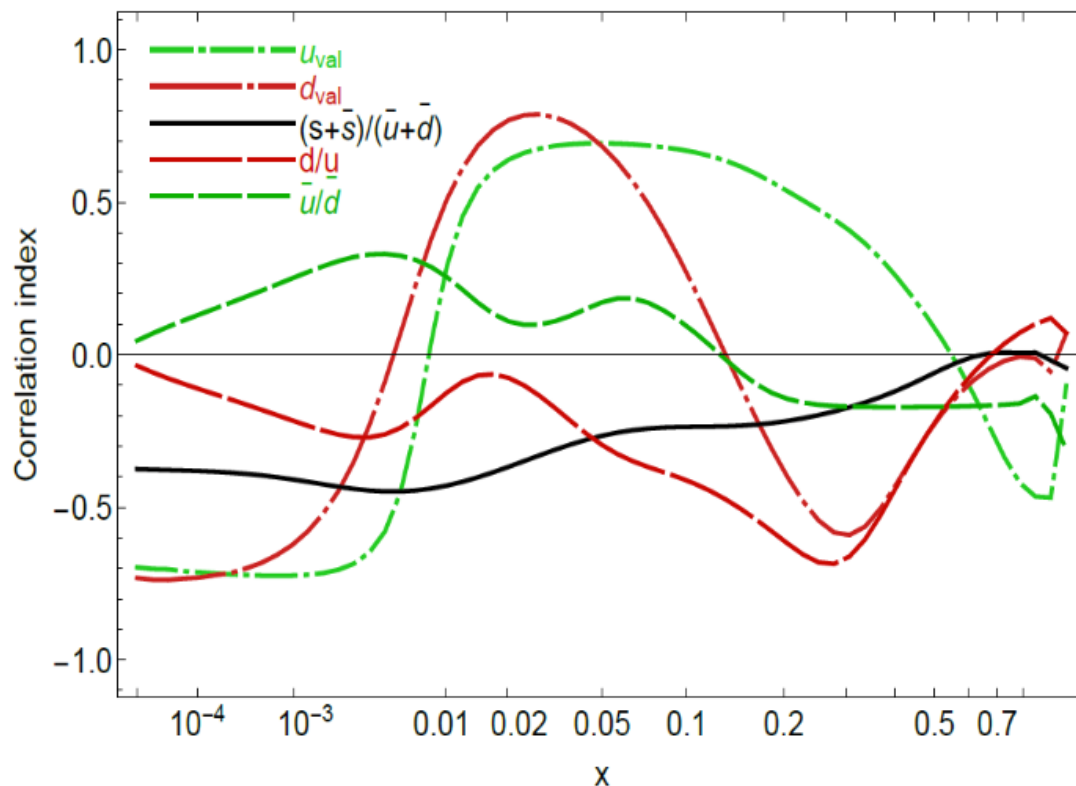
$\sin^2 \theta_W$  (and, eventually,  $M_W$ )

...as a follow-on to Alessandro's EW-focused overview:

important PDF correlations for the ATLAS extraction of  $\sin^2 \theta_W$

# Example: $\sin^2 \theta_{weak} \equiv s2w$ measured by ATLAS 8 TeV

Correlation,  $\sin \theta_W$  (ATLAS 8 TeV CB) and  $f(x,Q)$  at  $Q=81.45$  GeV  
2018/11/11, PRELIMINARY, CT14 NNLO



Strongest correlations of  $s2w$  with  $u_{val}, d_{val}$  at  $0.005 \lesssim x \lesssim 0.2$

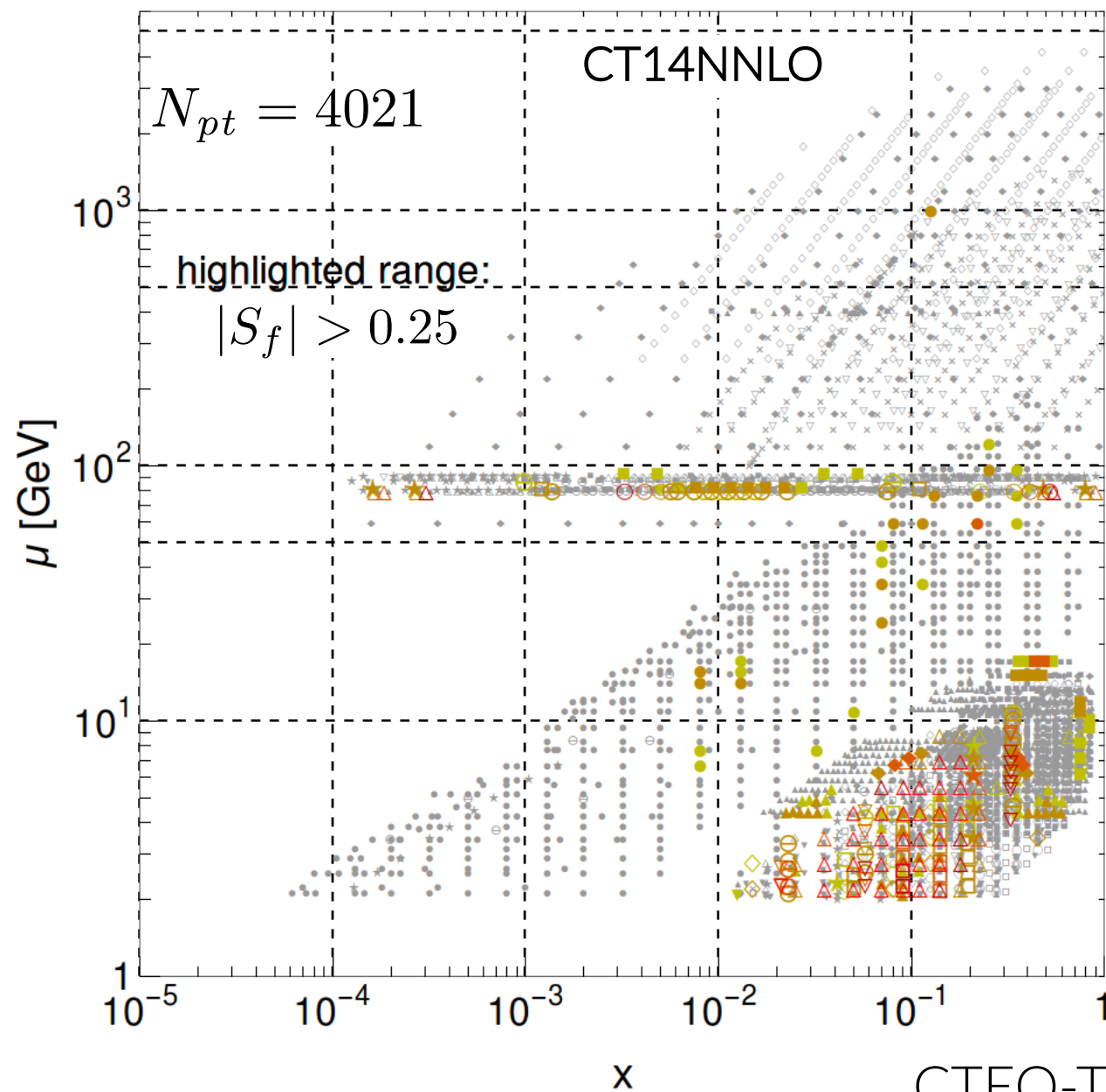
weak correlations with  $\bar{u}, \bar{d}, \bar{s}, g$

$u_{val}, d_{val}$  changed between CT10 and CT14 [1506.07433, Sec. 2B]

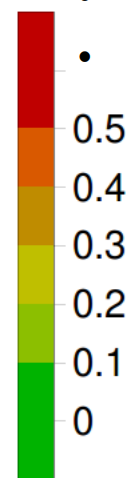
It is instructive to explore the data pulls on  $u_{val}, d_{val}$

$$\sin^2 \theta_W$$

PDF sensitivity of  $\sin^2 \theta_W$  from 7 TeV ATLAS data



- **combined HERA1 DIS [most sensitive]**
- CCFR  $\nu p$  DIS  $F_{3,2}$
- BCDMS  $F_2^{p,d}$
- NMC  $ep, ed$  DIS
- CDHSW  $\nu A$  DIS
- NuTeV  $\nu A \rightarrow \mu\mu X$
- CCFR  $\nu A \rightarrow \mu\mu X$
- E866  $pp \rightarrow \ell^+ \ell^- X$
- ATLAS 7 TeV W/Z ( $35 \text{ pb}^{-1}$ )

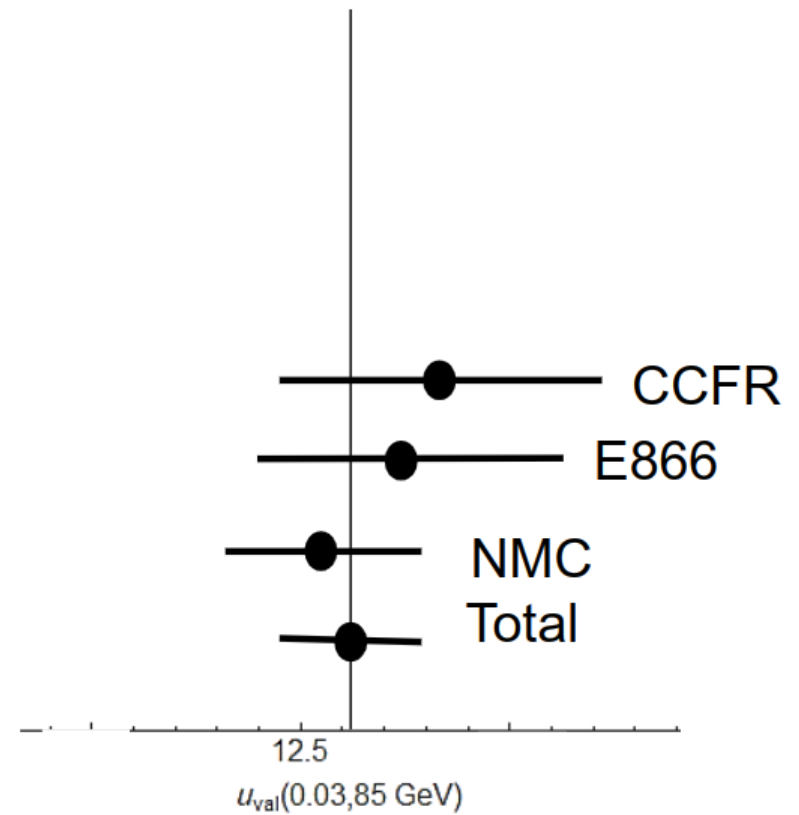
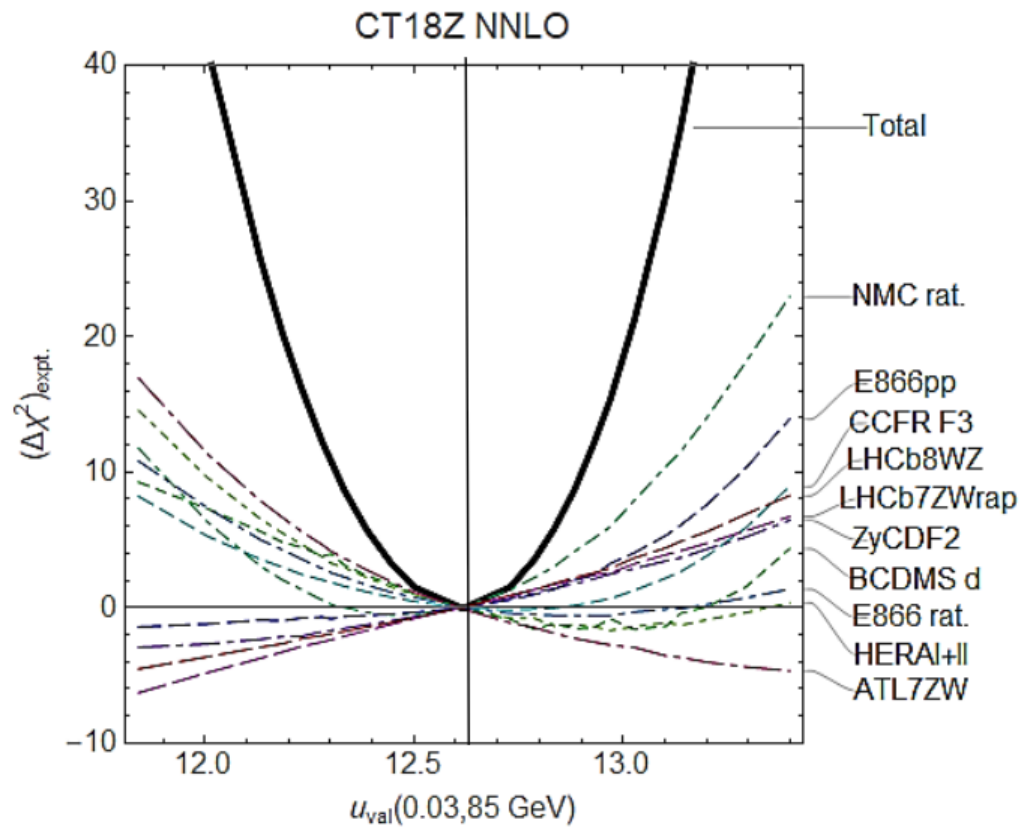


CTEQ-TEA sensitivities to  $\sin^2 \theta_W$

... using a Lagrange Multiplier scan...

... or using residuals for replicas

[errors and correlations; most replicas are not good fits]



PRELIMINARY

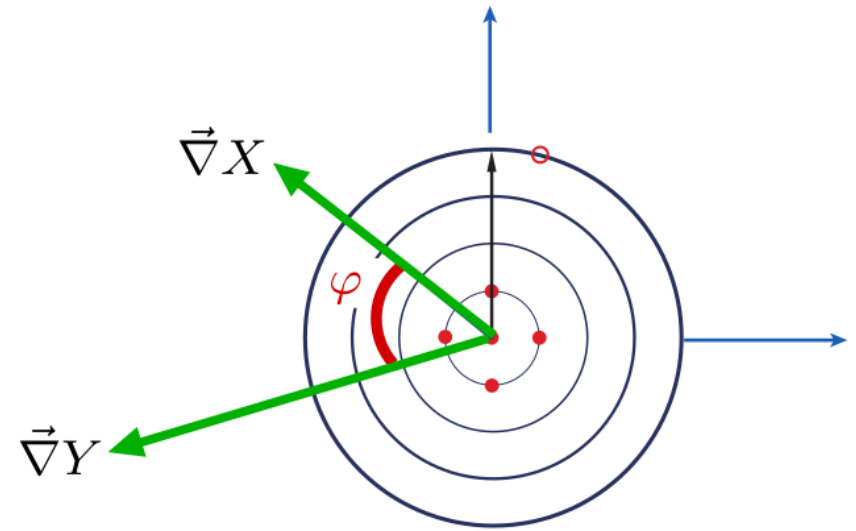
Can repeat for  $s_{2w}$ ,  $M_W$ , ...

rather than the costly LM scans, we can examine a “cheaper” measure which yields comparable information

---

the  $L_2$  sensitivity

---



$L_2$  sensitivity. Take  $X = f_a(x_i, Q_i)$  or  $\sigma(f)$ ;  $Y = \chi_E^2$  for experiment  $E$ . Find  $\Delta Y(\vec{z}_{m,X})$  for the displacement  $|\vec{z}_{m,X}| = 1$  along the direction  $\vec{\nabla} X / |\vec{\nabla} X|$  (corresponding to  $\Delta \chi_{tot}^2 = T^2$  and  $X(\vec{z}) = X(0) + \Delta X$ ):

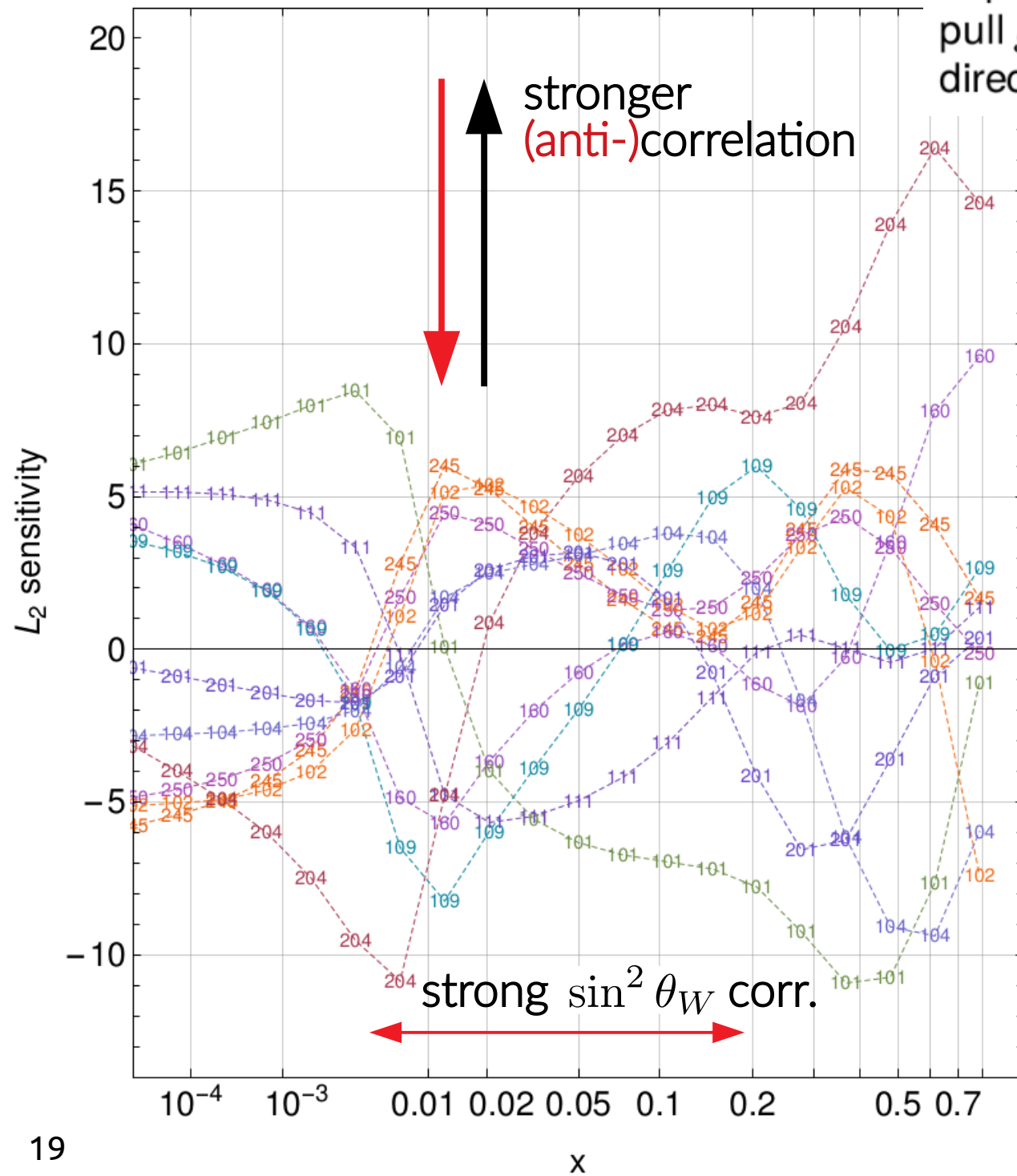
$$S_{f,L_2} \equiv \Delta Y(\vec{z}_{m,X}) = \vec{\nabla} Y \cdot \vec{z}_{m,X} = \vec{\nabla} Y \cdot \frac{\vec{\nabla} X}{|\vec{\nabla} X|}$$

$$= \Delta Y \cos \varphi$$

$$\text{or, } \sim \text{Corr}[f_a, \chi_E^2]$$

# CT18 NNLO, $u_V(x, Q)(x, 100 \text{ GeV})$

Experiments with large  $\Delta\chi^2 > 0$  [ $\Delta\chi^2 < 0$ ]  
pull  $g(x, Q)$  in the negative [positive]  
direction at the shown  $x$

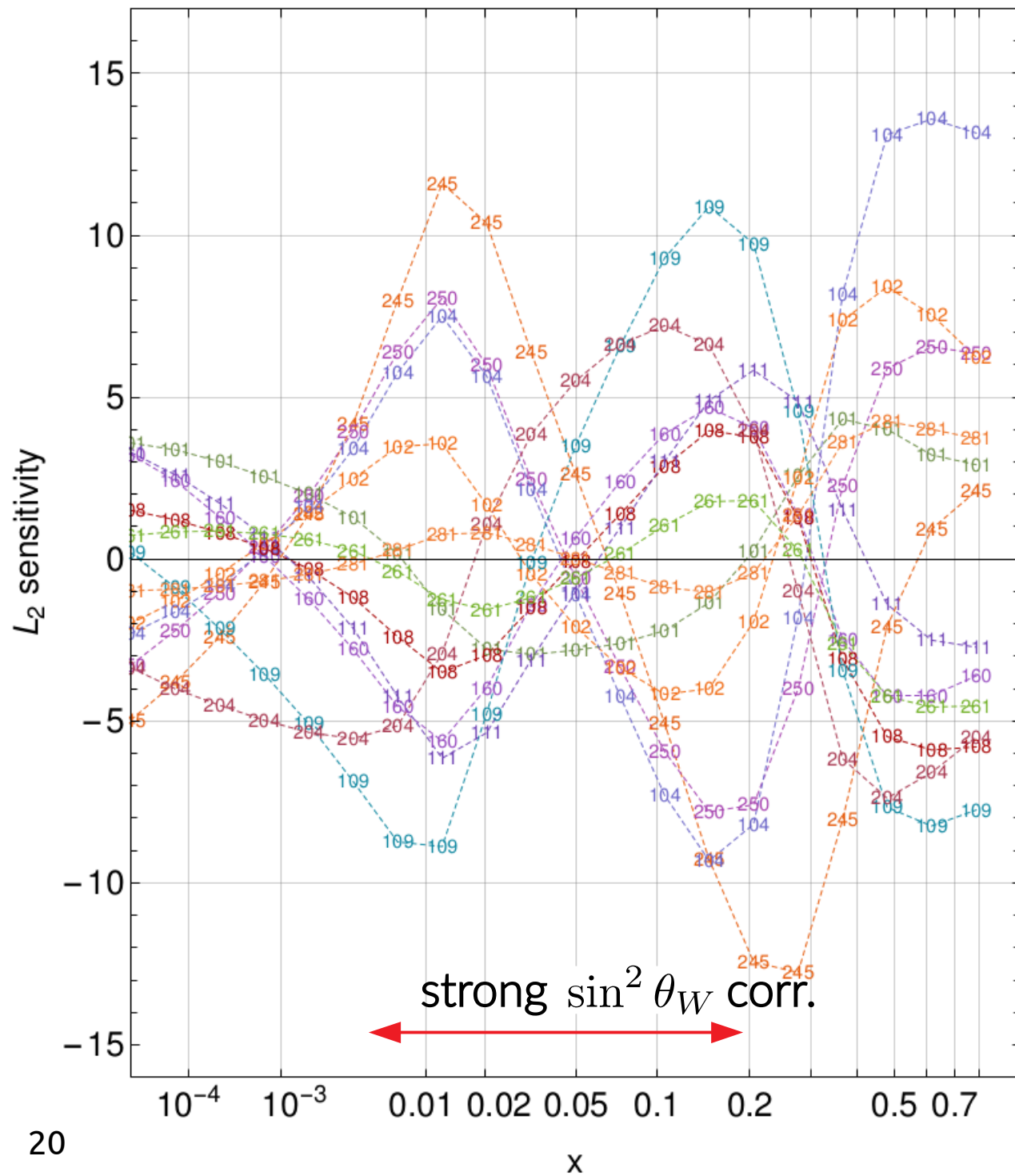


- 245--- LHCb7ZWrap
- 250--- LHCb8WZ
- 160--- HERAII
- 101--- BcdF2pCor
- 102--- BcdF2dCor
- 104--- NmcRatCor
- 109--- cdhswf3
- 111--- ccrf3.md
- 201--- e605
- 204--- e866ppxf

tension between  
LHCb W/Z  
data (245, 250);  
fixed-target DIS,  
Drell-Yan  
(CDHSW  $F_3$   
[109], E866pp  
[204])

→ in the region where  
 $\sin^2 \theta_W$  and  $u_v$   
are most correlated,  
opposing pulls from  
CCFR  $\nu$ DIS, BCDMS  
vs. E866  $pp$ , NMC rat.

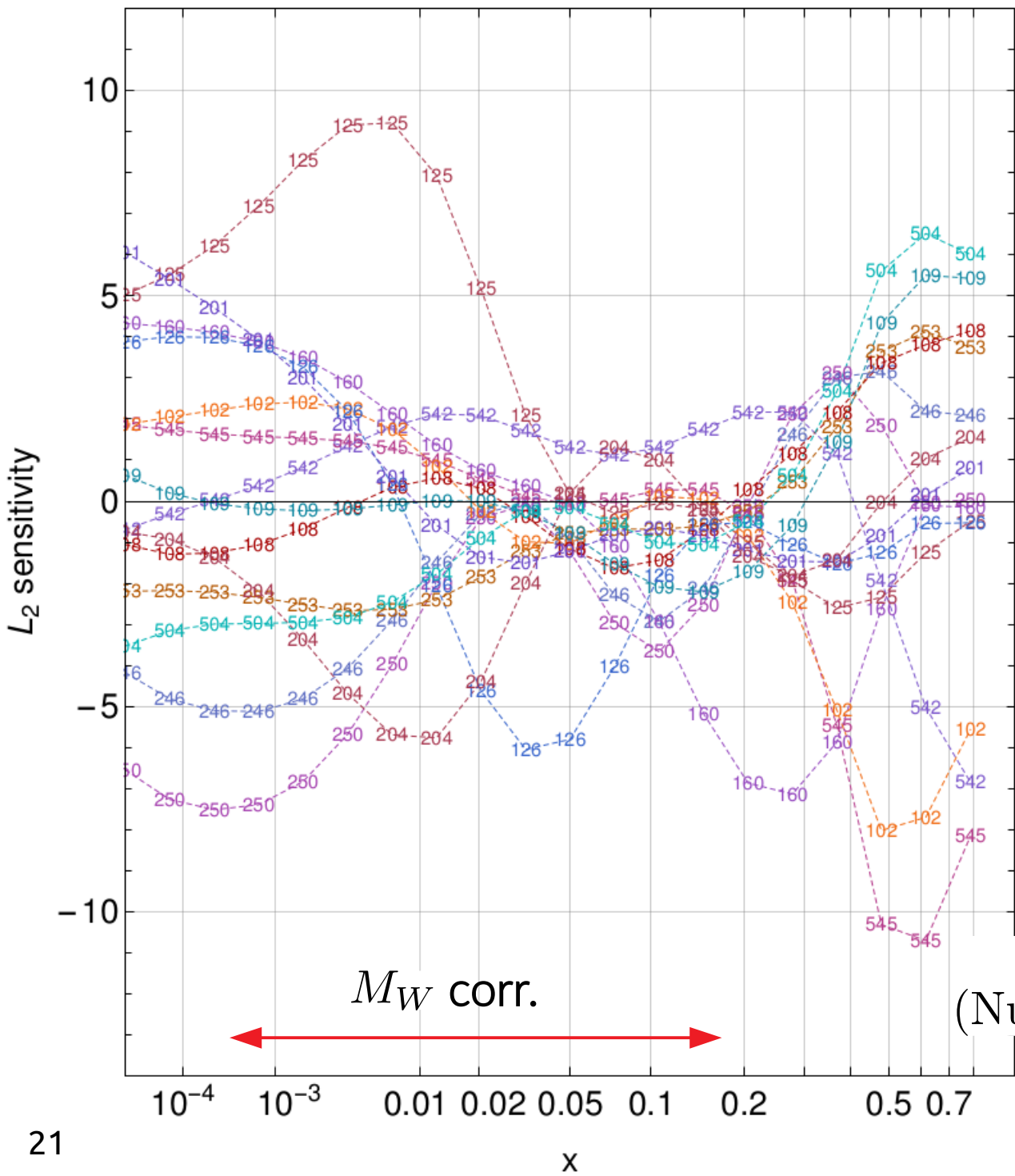
# CT18 NNLO, $d_V(x, Q)(x, 100 \text{ GeV})$



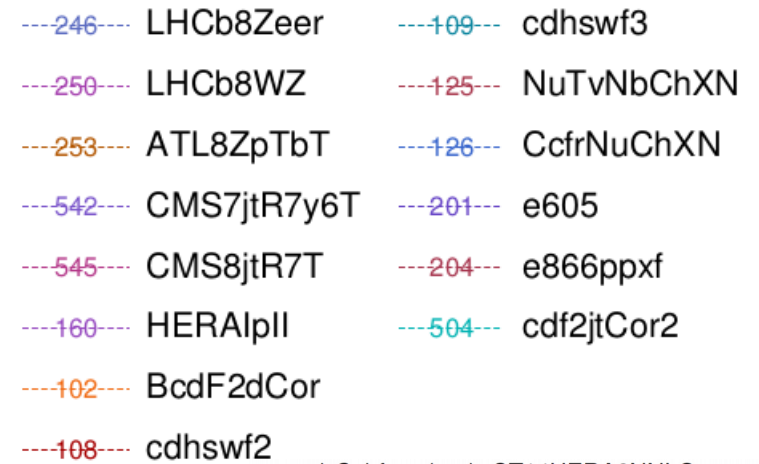
tension between LHCb W/Z data (245, 250); fixed-target DIS, Drell-Yan (CDHSW  $F_3$  [109], E866pp [204])

- 245--- LHCb7ZWrap
- 250--- LHCb8WZ
- 160--- HERAIIpII
- 101--- BcdF2pCor
- 102--- BcdF2dCor
- 104--- NmcRatCor
- 108--- cdhswf2
- 109--- cdhswf3
- 111--- ccfrf3.md
- 204--- e866ppxf
- 261--- ZyCDF2
- 281--- d02Easy5

again, tensions observed between, e.g., NMC ratio data and CDHSW, E866pp

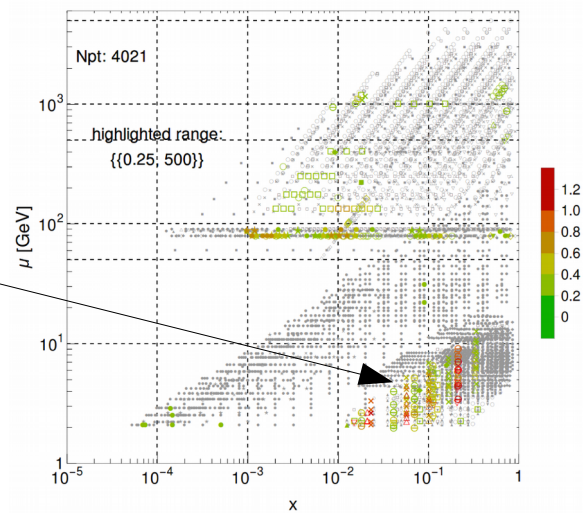


...this analysis can be extended to  $M_W$ ,  
 extractions of which are dependent upon  $s(x)$ ,  
 through Z-calibration

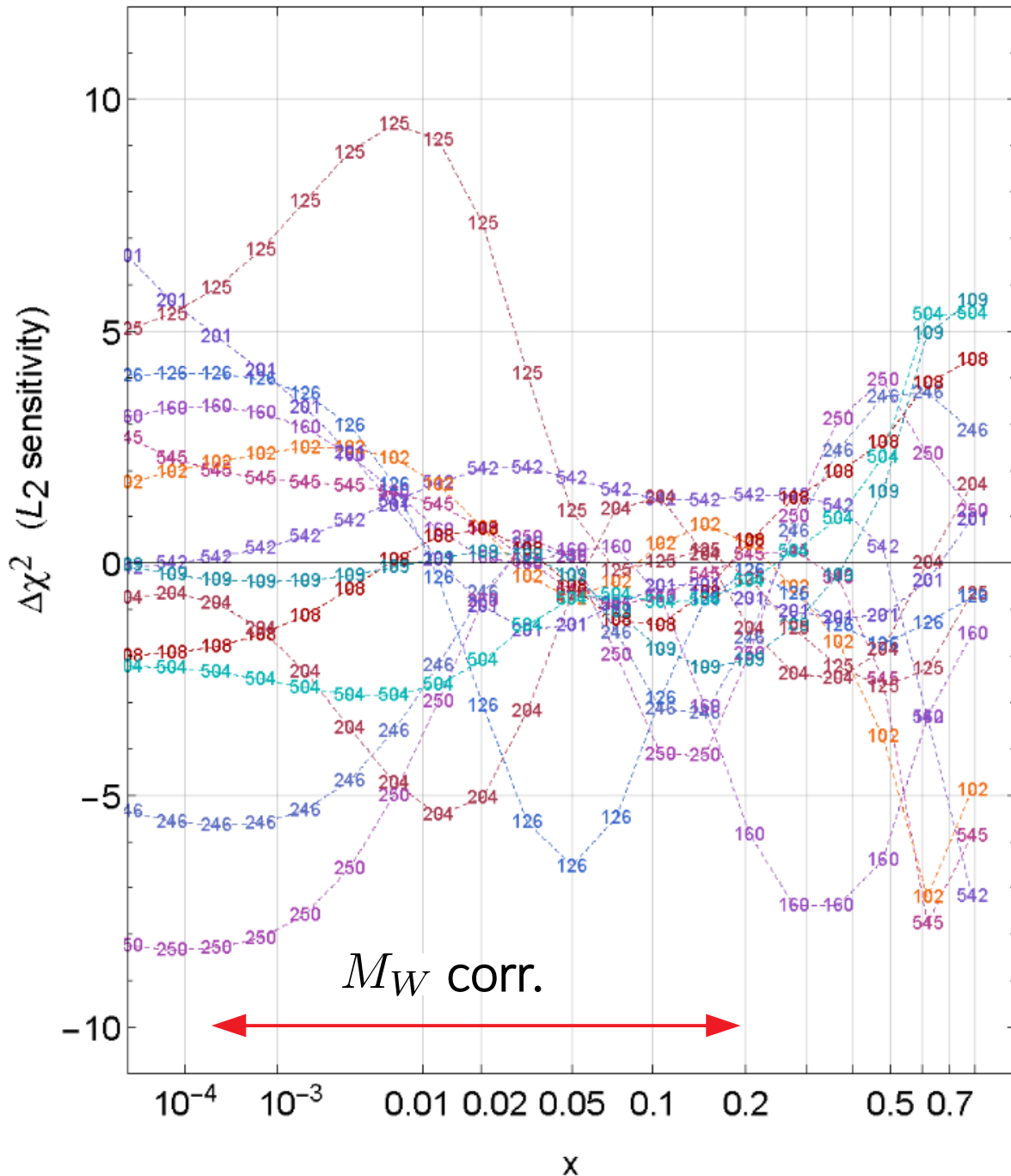


$\nu$ DIS  
 (NuTeV, ...)

$|S_f|$  for  $s(x, \mu)$ , CT14HERA2NNLO



CT18 NNLO,  $s(x, 2 \text{ GeV})$



# $L_2$ sensitivity, strangeness: CT18

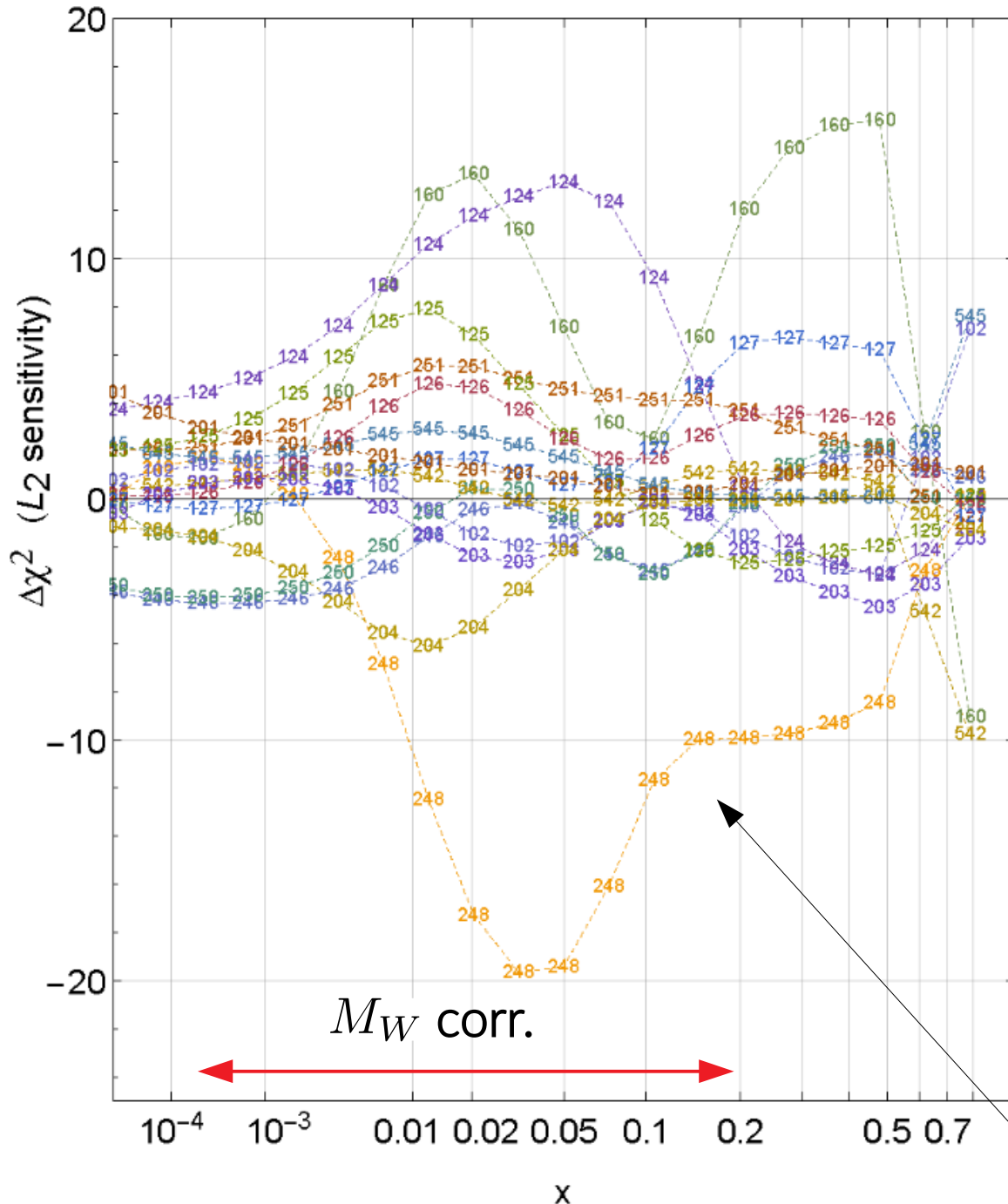
## Most sensitive experiments

- 246--- LHCb8Zeer
- 250--- LHCb8WZ
- 542--- CMS7jtR7y6T
- 545--- CMS8jtR7T
- 160--- HERAIplI
- 102--- BcdF2dCor
- 108--- cdhswf2
- 109--- cdhswf3
- 125--- NuTvNbChXN
- 126--- CcfrNuChXN
- 201--- e605
- 204--- e866ppxf
- 504--- cdf2jtCor2

A tension trend between DIS (HERA I+II, CCFR, NuTeV) and Drell-Yan (ATLAS 7 Z/W, LHCb W/Z, E866 pp, ...) experiments

CT18Z NNLO,  $s(x, 2 \text{ GeV})$

# $L_2$ sensitivity, strangeness: CT18Z



Most sensitive experiments

- 246--- LHCb8Zeer
- 248--- ATLAS7ZW.xF
- 250--- LHCb8WZ
- 251--- ATLAS8DY
- 542--- CMS7jtR7y6T
- 545--- CMS8jtR7T
- 160--- HERAIpII
- 102--- BcdF2dCor
- 124--- NuTeVNuChXN
- 125--- NuTeVNbChXN
- 126--- CcfrNuChXN
- 127--- CcfrNbChXN
- 201--- e605
- 203--- e866f
- 204--- e866ppxf

A tension trend between DIS (HERA I+II, CCFR, NuTeV) and Drell-Yan (ATLAS 7 Z/W, LHCb W/Z, E866 pp, ...) experiments

pronounced effect of ATLAS 7 TeV Z/W data!

- there remains considerable dependence (as large as  $\sim 13\%$ ) upon PDF parametrization and running coupling

→ the situation is such that precision in Higgs phenom. is significantly **PDF-limited**

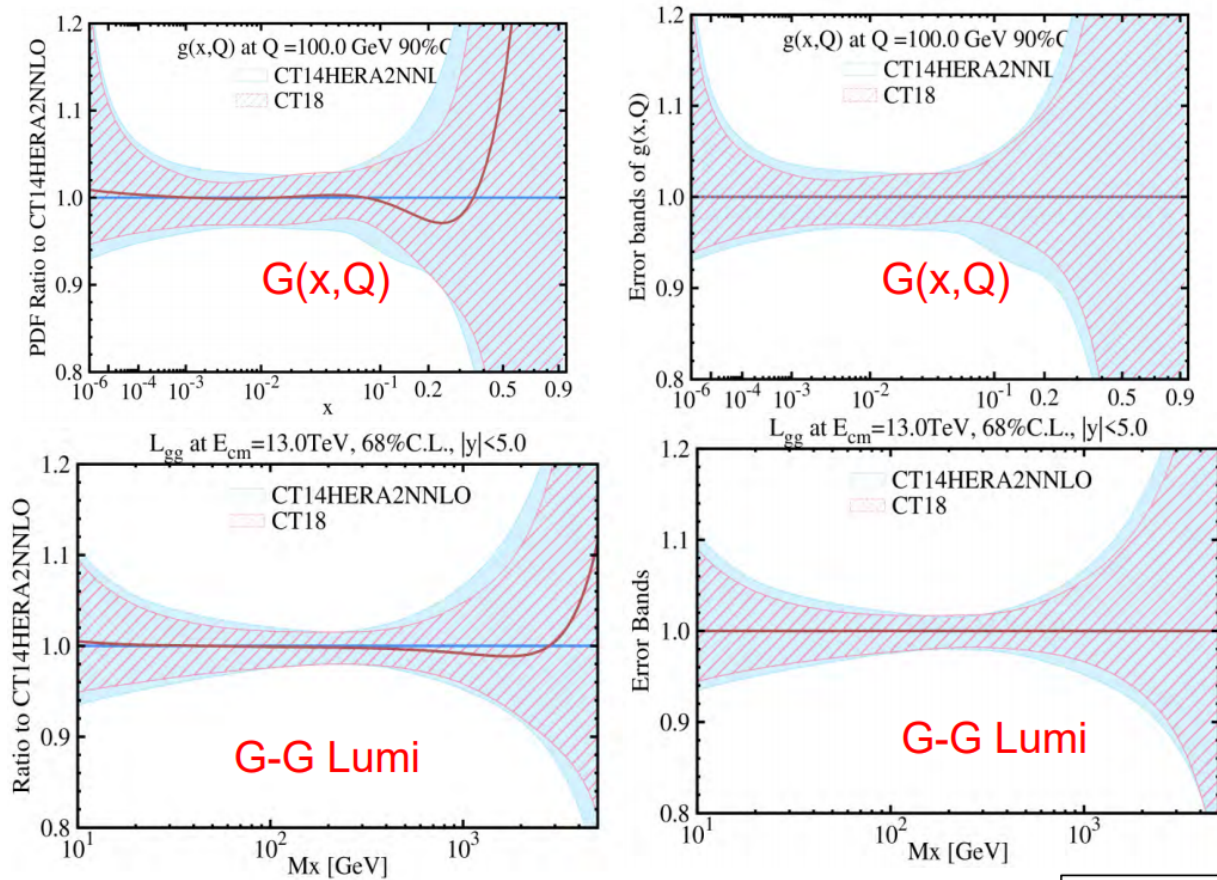
Accardi et al., EPJC76, 471 (2016).

PDF sets	$\sigma(H)^{\text{NNLO}}$ (pb) nominal $\alpha_s(M_Z)$	$\sigma(H)^{\text{NNLO}}$ (pb) $\alpha_s(M_Z) = 0.115$	$\sigma(H)^{\text{NNLO}}$ (pb) $\alpha_s(M_Z) = 0.118$
ABM12 [2]	$39.80 \pm 0.84$	$41.62 \pm 0.46$	$44.70 \pm 0.50$
CJ15 [1] <sup>a</sup>	$42.45^{+0.43}_{-0.18}$	$39.48^{+0.40}_{-0.17}$	$42.45^{+0.43}_{-0.18}$
CT14 [3] <sup>b</sup>	$42.33^{+1.43}_{-1.68}$	$39.41^{+1.33}_{-1.56}$ (40.10)	$42.33^{+1.43}_{-1.68}$
HERAPDF2.0 [4] <sup>c</sup>	$42.62^{+0.35}_{-0.43}$	$39.68^{+0.32}_{-0.40}$ (40.88)	$42.62^{+0.35}_{-0.43}$
JR14 (dyn) [5]	$38.01 \pm 0.34$	$39.34 \pm 0.22$	$42.25 \pm 0.24$
MMHT14 [6]	$42.36^{+0.56}_{-0.78}$	$39.43^{+0.53}_{-0.73}$ (40.48)	$42.36^{+0.56}_{-0.78}$
NNPDF3.0 [7]	$42.59 \pm 0.80$	$39.65 \pm 0.74$ (40.74 $\pm$ 0.88)	$42.59 \pm 0.80$
PDF4LHC15 [8]	$42.42 \pm 0.78$	$39.49 \pm 0.73$	$42.42 \pm 0.78$

$\sigma_H$  at NNLO and  $\sqrt{s} = 13 \text{ TeV}$ ;  $\mu_F = \mu_R = m_H$

→ enhancing the discovery potential in the Higgs sector will require improving these uncertainties!

# CT14 → CT18 modestly shifts Higgs cross sections and slightly reduces PDF uncertainties

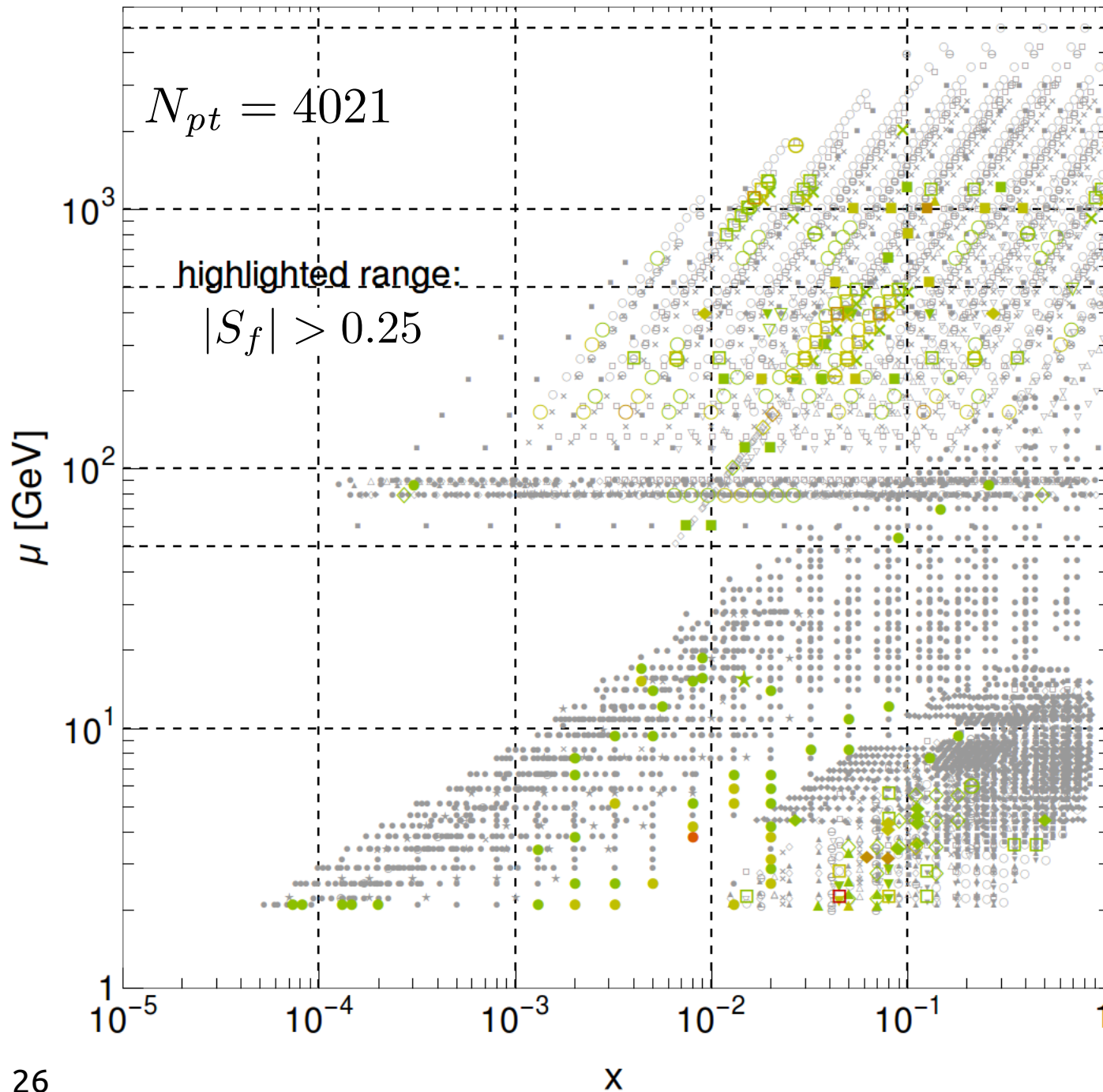


7 TeV		
	$\sigma(\text{gg-h})$	$\delta\sigma \text{ sym}(90\% \text{C.L.})$
CT14NNLO	14.67	0.46
CT18	14.57	0.44
8 TeV		
	$\sigma(\text{gg-h})$	$\delta\sigma \text{ sym}(90\% \text{C.L.})$
CT14NNLO	18.70	0.57
CT18	18.45	0.55
13 TeV		
	$\sigma(\text{gg-h})$	$\delta\sigma \text{ sym}(90\% \text{C.L.})$
CT14NNLO	42.78	1.32
CT18	42.43	1.26
14 TeV		
	$\sigma(\text{gg-h})$	$\delta\sigma \text{ sym}(90\% \text{C.L.})$
CT14NNLO	48.23	1.50
CT18	47.91	1.42

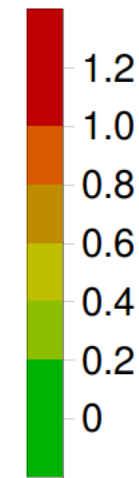
PDF induced errors (at 90% CL) are reduced by about 5% as compared to CT14 predictions.

can we disentangle elements of the global analysis responsible for these improvements?

# $|S_f|$ for $\sigma_{H^0}$ 14 TeV, CT14HERA2NNLO



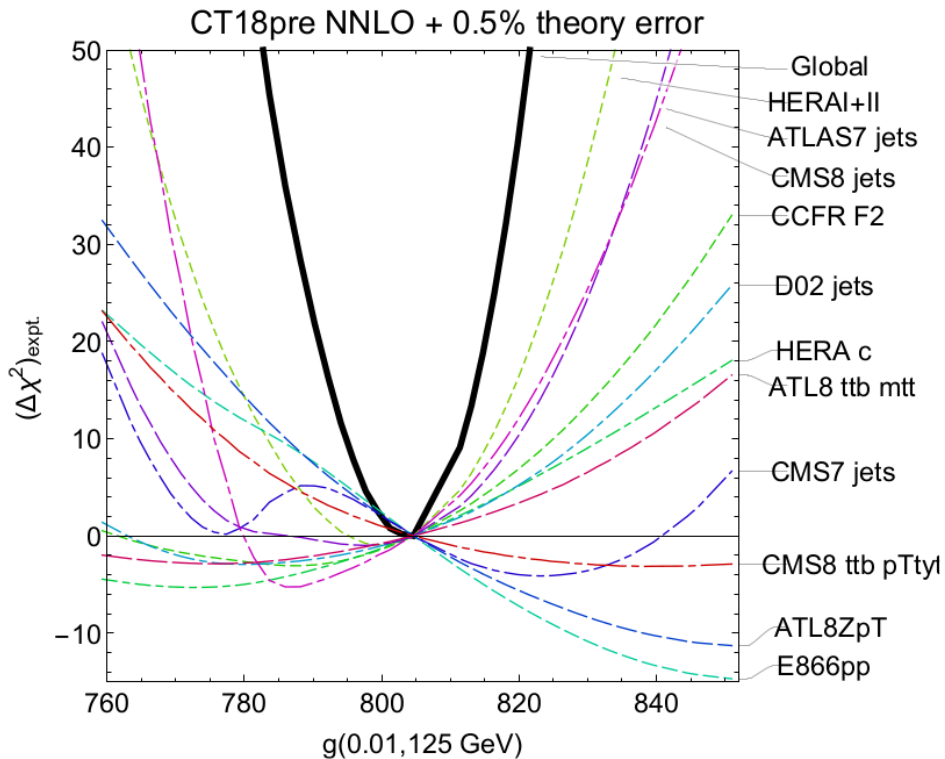
- after the aggregated HERA data, inclusive jet production have greatest total sensitivity!



- large correlations for E866, BCDMS, CCFR, CMS WASY, Z  $p_T$  and  $t\bar{t}$  production, but smaller numbers of highly-sensitive points

we use the Higgs region  $g(x)$  to validate PDFSense

...for the gluon PDF in the Higgs region,  $g(0.01, m_H)$



$g(x=0.01, \mu=125 \text{ GeV})$		
PDFSENSE		LM scan
CT14HERA2	CT18pre	CT18pre
HERAI+II'15	HERAI+II'15	HERAI+II'15
CMS8jets'17	CMS8jets'17	CMS8jets'17
CMS7jets'14	CMS7jets'14	ATLAS7jets'15
ATLAS7jets'15	E866pp'03	E866pp'03
E866pp'03	ATLAS7jets'15	ATLAS7jets'15
BCDMSd'90	BCDMSd'90	CCFR-F2'01
CCFR-F3'97	BCDMSp'89	D02jets'08
D02jets'08	D02jets'08	HERAc'13
NMCrat'97	NMCrat'97	NuTeV-nub'06
BCDMSp'89	CDHSW-F2'91	CCFR-F3'97

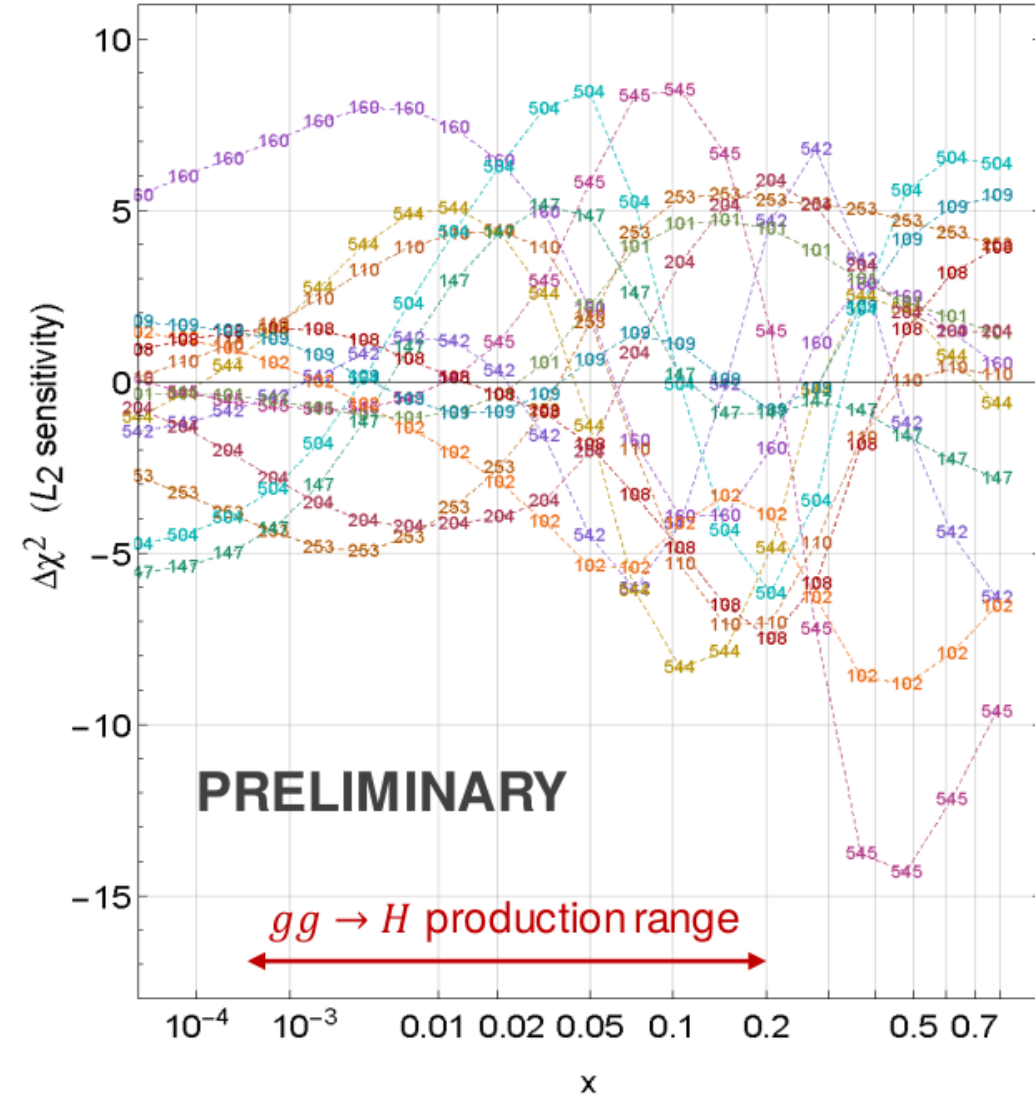
- PDFSense identifies the most sensitive experiments with high confidence and in accord with other methods such as the LM scans. It works the best when the uncertainties are nearly Gaussian, and experimental constraints agree among themselves [arXiv:1803.02777]

# Estimated $\chi^2$ pulls from experiments

( $L_2$  sensitivity, arXiv:1904.00222, v. 2)

CT18 NNLO,  $g(x, 100 \text{ GeV})$

CT18 NNLO, gluon at  $Q=100 \text{ GeV}$



Most sensitive experiments

- 253--- ATL8ZpTbT
- 542--- CMS7jtR7y6T
- 544--- ATL7jtR6uT
- 545--- CMS8jtR7T
- 160--- HERAplI
- 101--- BcdF2pCor
- 102--- BcdF2dCor
- 108--- cdhswf2
- 109--- cdhswf3
- 110--- ccfrf2.mi
- 147--- Hn1X0c
- 204--- e866ppxf
- 504--- cdf2jtCor2

Experiments with large  $\Delta\chi^2 > 0$  [ $\Delta\chi^2 < 0$ ] pull  $g(x, Q)$  in the negative [positive] direction at the shown  $x$

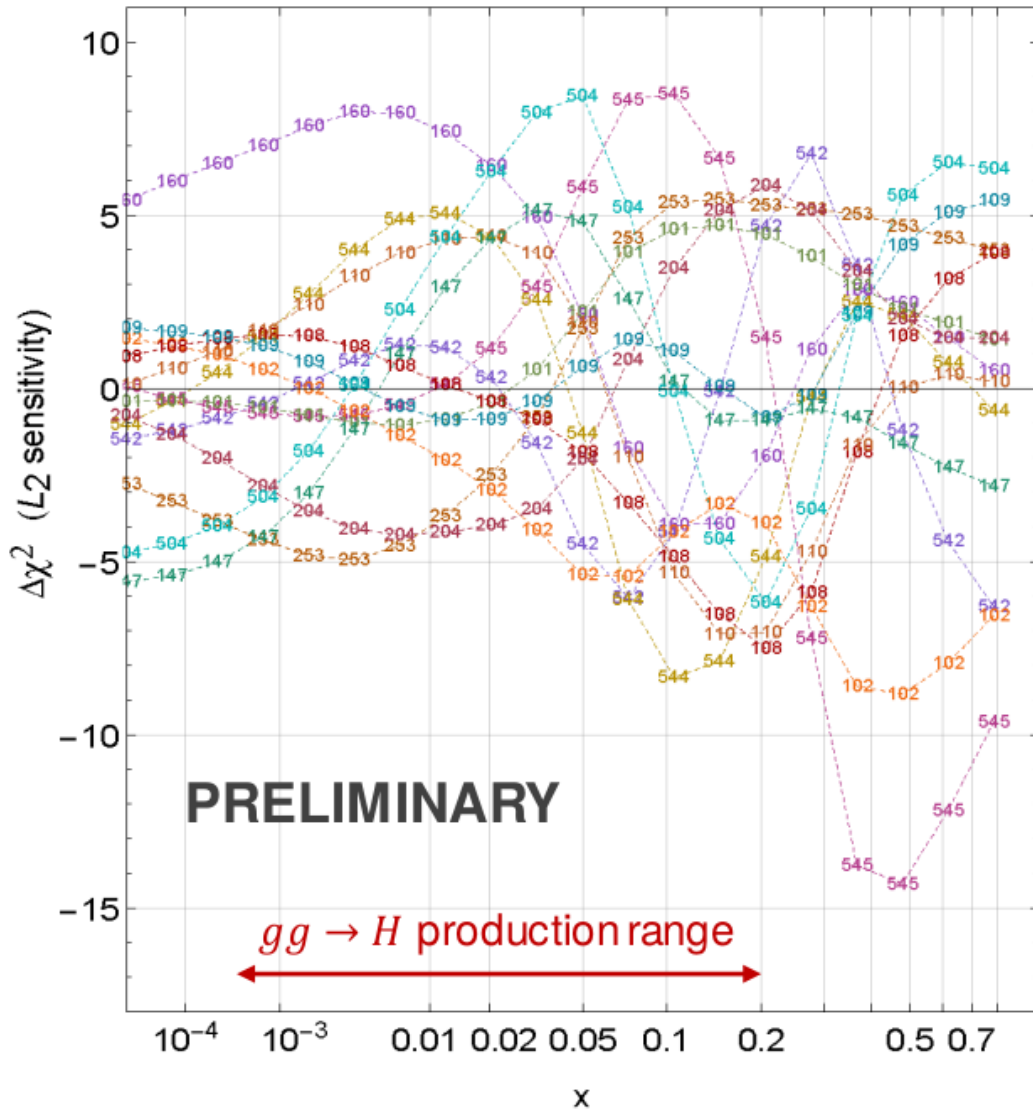
Estimated using CT18 Hessian PDFs

# Estimated $\chi^2$ pulls from experiments

( $L_2$  sensitivity, arXiv:1904.00222, v. 2)

CT18 NNLO,  $g(x, 100 \text{ GeV})$

CT18 NNLO, gluon at  $Q=100 \text{ GeV}$



## Most sensitive experiments

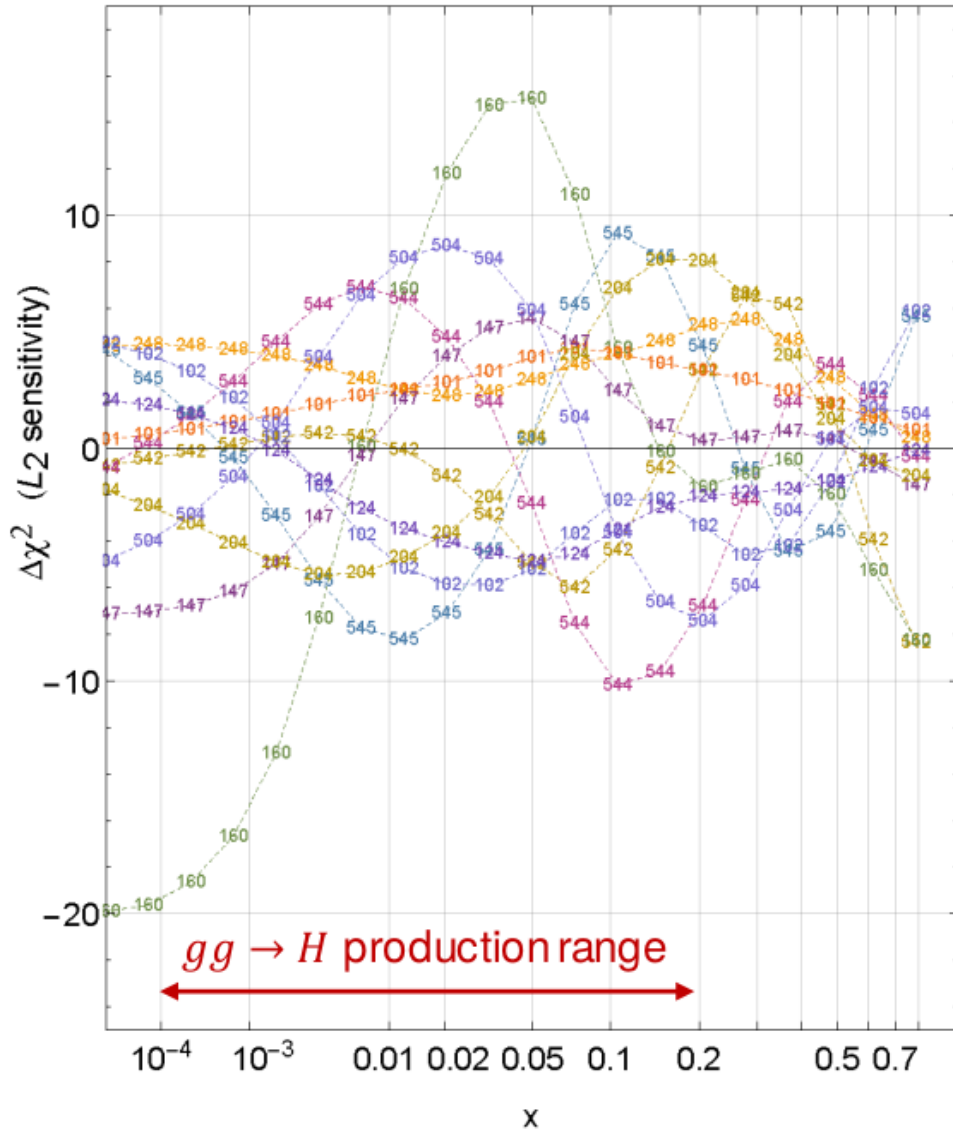
- 253--- ATLAS8ZpTbT
- 109--- cdhswf3
- 542--- CMS7jtR7y6T
- 110--- ccrf2.mi
- 544--- ATLAS7jtR6uT
- 147--- Hn1X0c
- 545--- CMS8jtR7T
- 204--- e866ppxf
- 160--- HERAIpII
- 504--- cdf2jtCor2
- 101--- BcdF2pCor
- 102--- BcdF2dCor
- 108--- cdhswf2

Note opposite pulls (tensions) in some  $x$  ranges between HERA I+II DIS (ID=160); CDF (504), ATLAS 7 (544), CMS 7 (542), CMS 8 jet (545) production; E866pp DY (204); ATLAS 8 Z pT (253) production; BCDMS and CDHSW DIS

# Estimated $\chi^2$ pulls from experiments

( $L_2$  sensitivity, arXiv:1904.00222, v. 2)

CT18Z NNLO,  $g(x, 100 \text{ GeV})$



Same for CT18Z NNLO

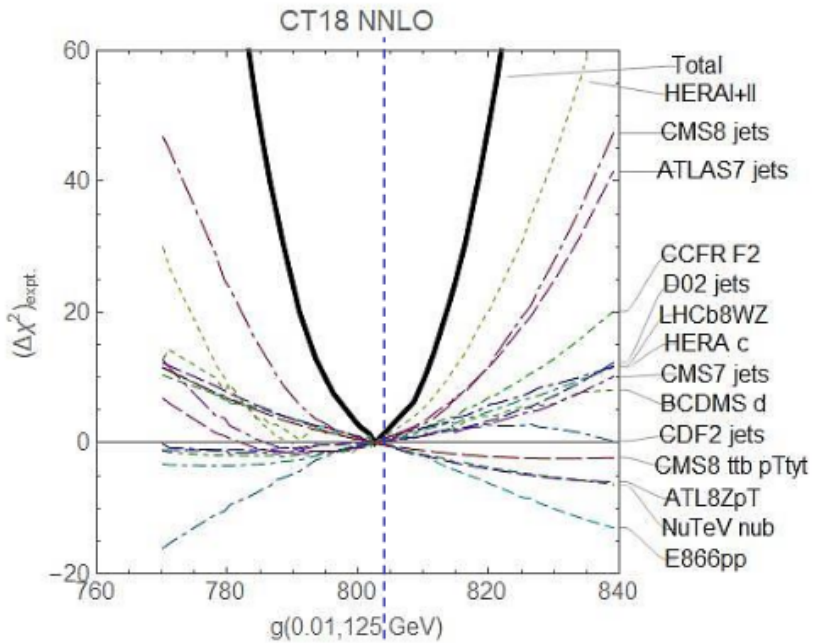
Most sensitive experiments

- 248--- ATL7ZW.xF
- 542--- CMS7jtR7y6T
- 544--- ATL7jtR6uT
- 545--- CMS8jtR7T
- 160--- HERA I+II
- 101--- BcdF2pCor
- 102--- BcdF2dCor
- 124--- NuTvNuChXN
- 147--- Hn1X0c
- 204--- e866ppxf
- 504--- cdf2jtCor2

Constraints from HERA I+II DIS (ID=160) follow a different trend from CT18 NNLO

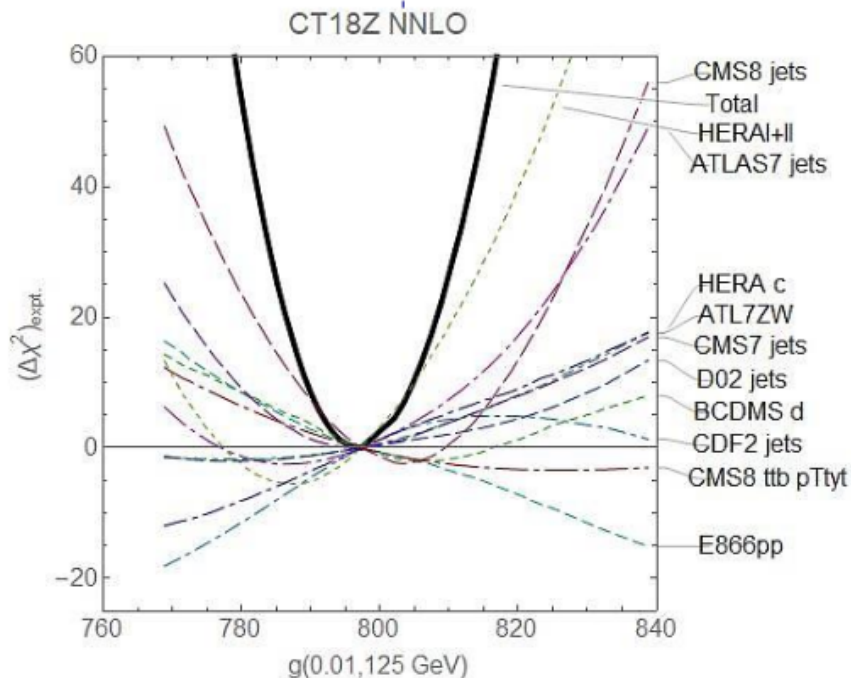
**PRELIMINARY**

# Lagrange Multiplier scan: $g(0.01, 125 \text{ GeV})$



## Upper row: CT18

- HERAI+II data set provides the dominant constraint, followed by ATLAS, CDF2, CMS, D02 jet production, HERA charm,...
- $t\bar{t}$  double-diff. cross sections provide weaker constraints



## Lower row: CT18Z

- CT18Z: a 1% lower NNLO gluon in the Higgs production region than for CT14/CT18

(a consequence of using a "saturation" factorization scale in NNLO DIS for CT18Z)

more speculatively, BSM searches and SMEFT represent possibilities for analogous sensitivity analyses

---

- SMEFiT analyses fit a generic parametrization of BSM physics,  
e.g., van Beek, Nocera, Rojo, Slade, arXiv:1906.05296

$$\mathcal{L}_{\text{SMEFT}} = \mathcal{L}_{\text{SM}} + \sum_i^{N_{\text{op}}} \frac{c_i}{\Lambda^2} \mathcal{O}_i^{(6)}$$

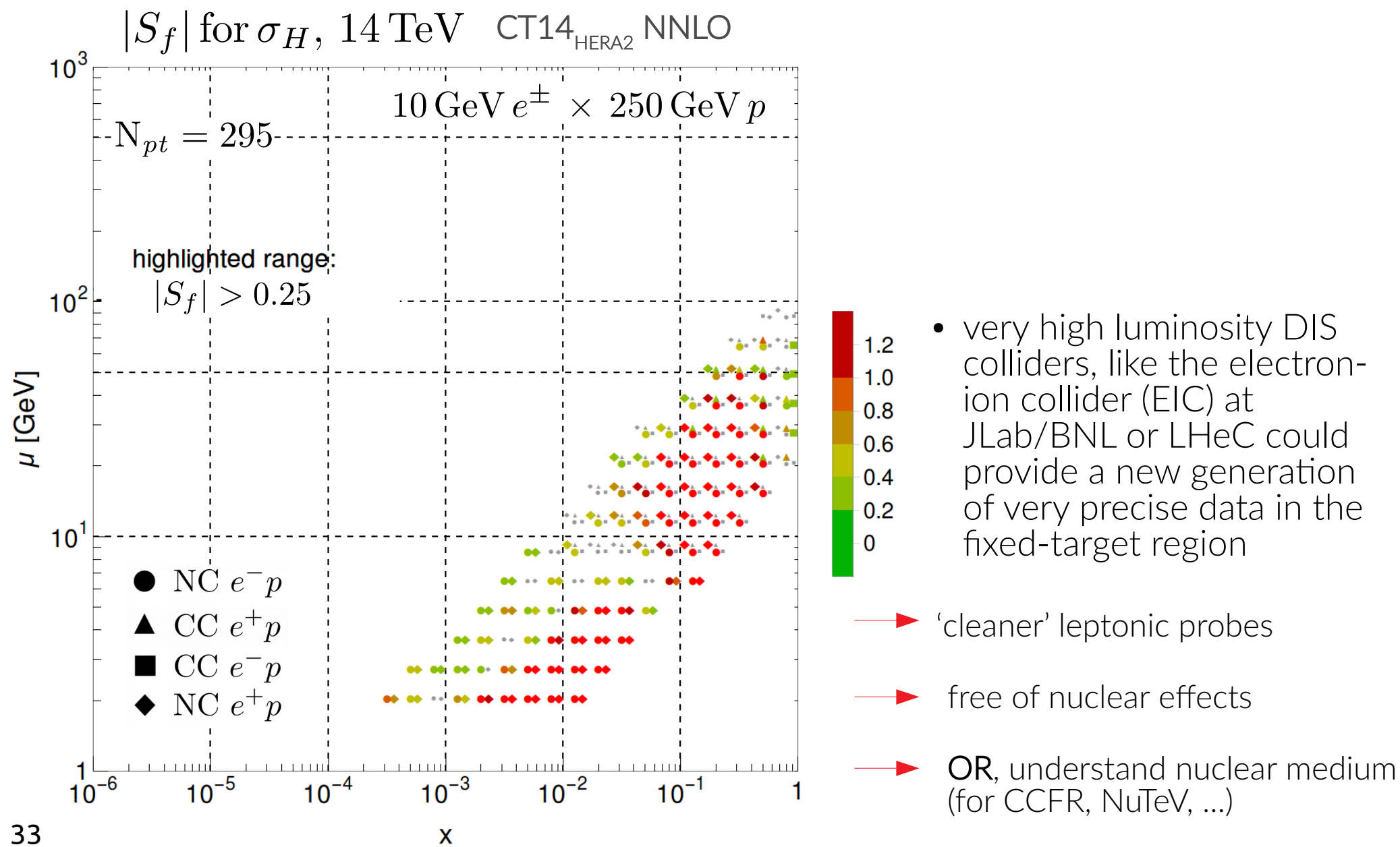
dependent upon Wilson coefficients for dim-6 operators:

$$\{ c_i^{(k)} \}, \quad i = 1, \dots, N_{\text{op}}, \quad k = 1, \dots, N_{\text{rep}}$$

---

—► with error replicas in the space of  $\{c_i^{(k)}\}$ , one could analyze data pulls on SMEFiT ingredients à la PDFSense

→ a systematic approach to reconcile LHC experiments will be imperative to reducing PDF uncertainties for the precision EW era at **HL-LHC**



# concluding observations

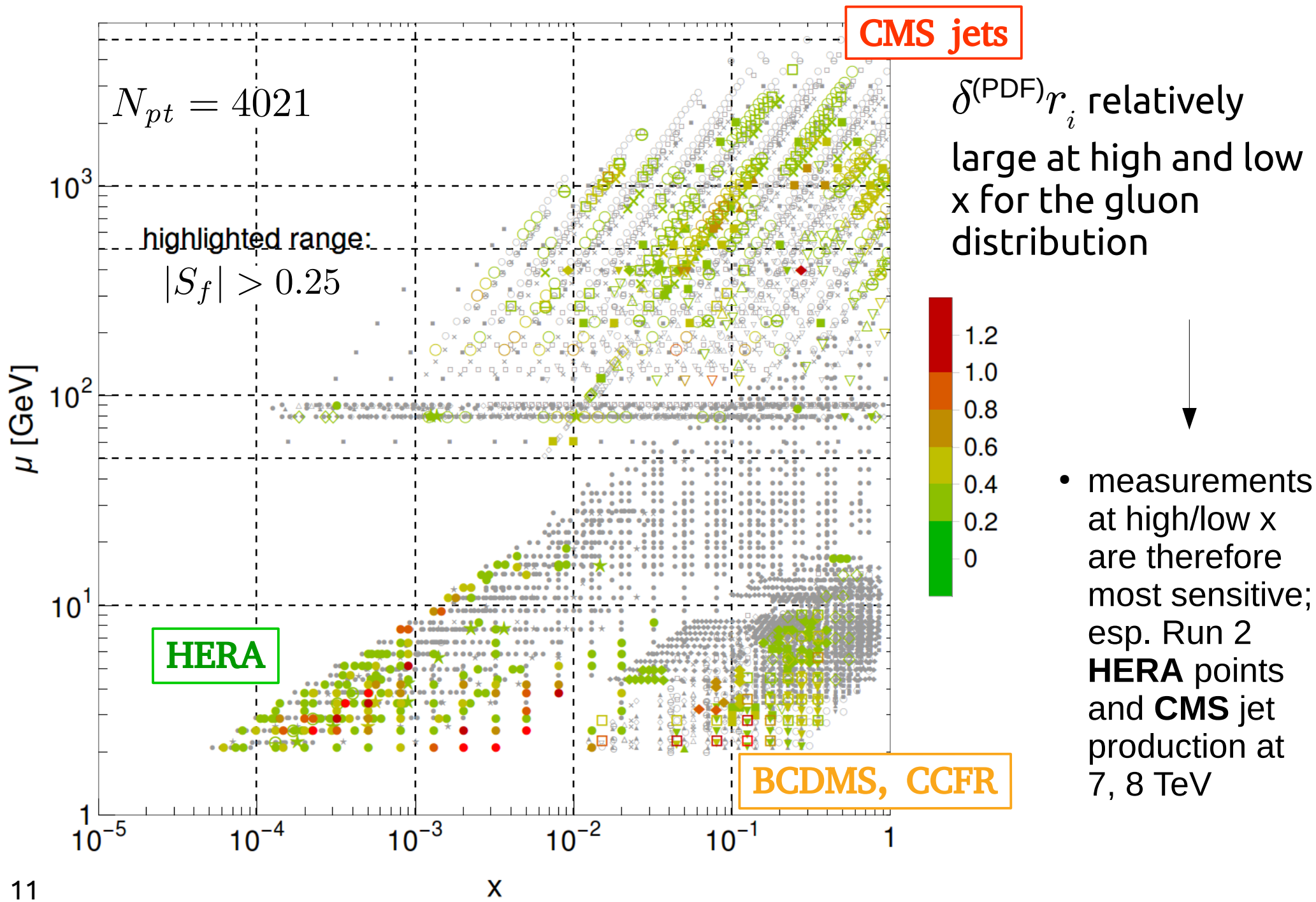
---

- PDFSense produces kinematic maps and summary charts of data-point sensitivities to PDFs and PDF-dependent quantities; readily extendable
  - fast; public code: <http://metapdf.hepforge.org/PDFSense>
- PDF uncertainties of HEP observables can be opportunities for sensitive PDF measurements
- heightened constraining power (on  $\sin^2\theta_W$ ,  $\sigma_H$ , ...) will require smoothing data tensions that are now being explored
  - $\sin^2\theta_W$  driven by  $u_{\text{val}}$ ,  $d_{\text{val}}$ , which, e.g., E866pp, BCDMS have opposing pulls
    - a community effort to understand systematic tensions needed
  - we find important improvements  $\sigma_H$  from incl. jet prod.; resolution of tensions will further tighten constraints
- dealing with these issues will be essential for HL-LHC program

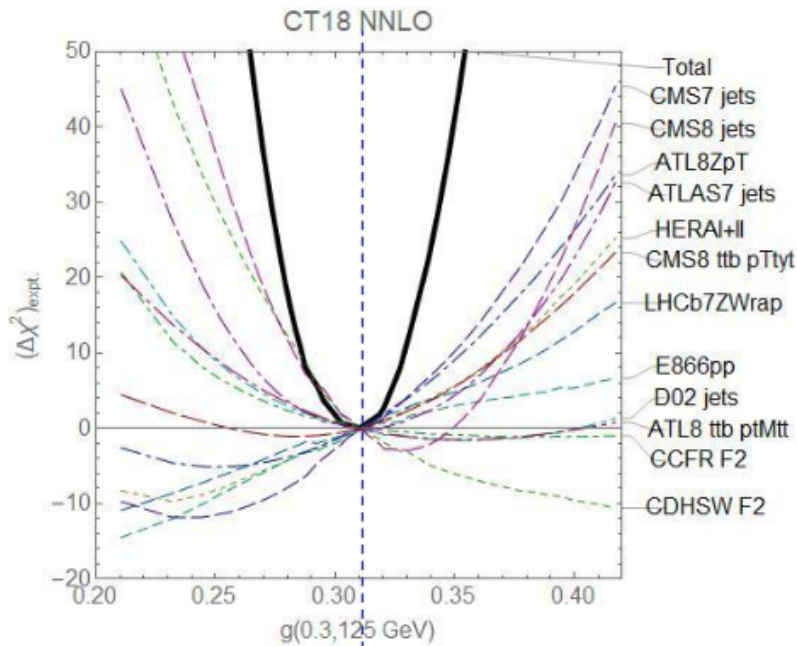
supplemental material

---

# $|S_f|$ for $g(x, \mu)$ , CT14HERA2NNLO



# Lagrange Multiplier scan: $g(0.3, 125 \text{ GeV})$

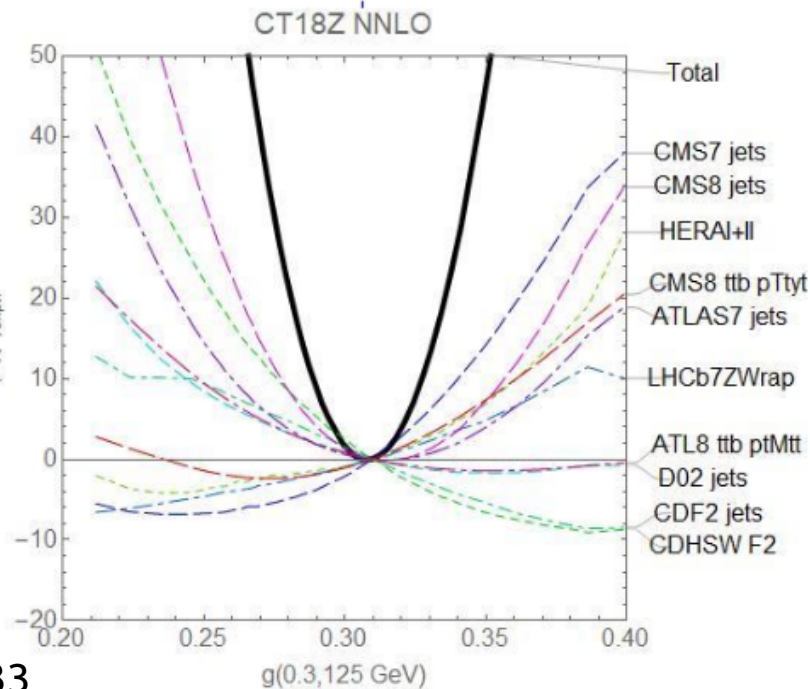


**Upper/lower rows: CT18/CT18Z**

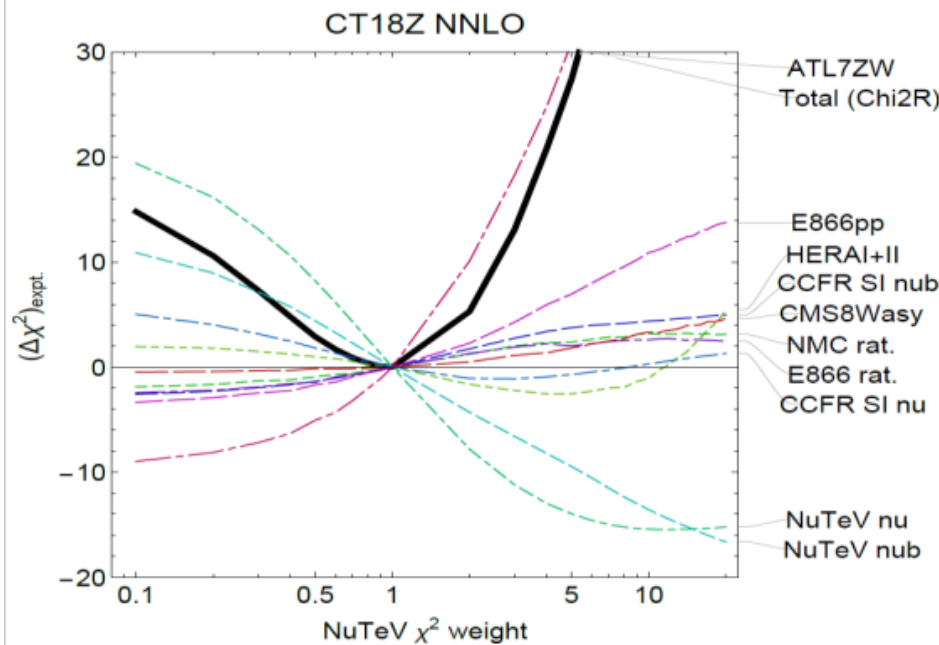
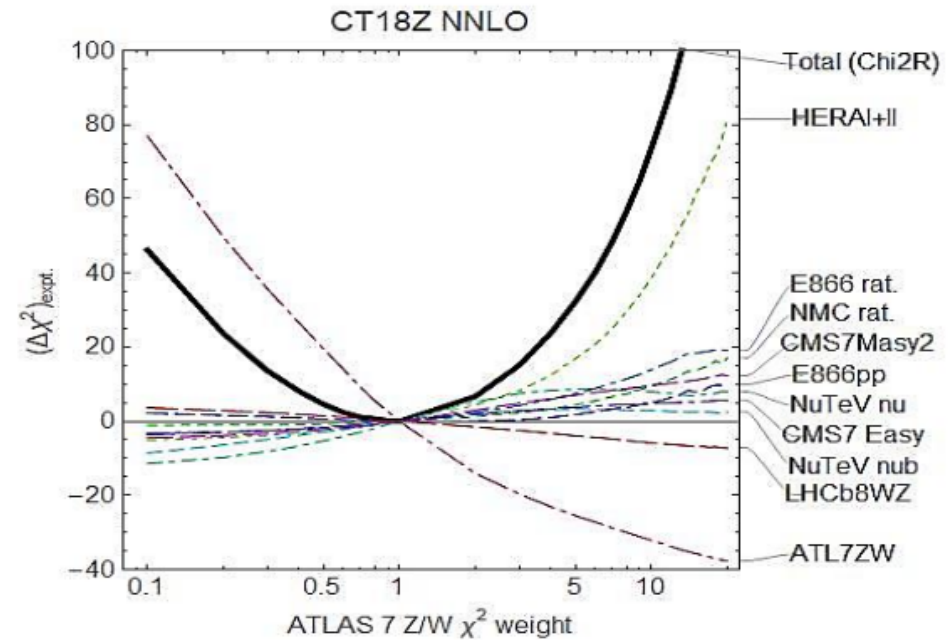
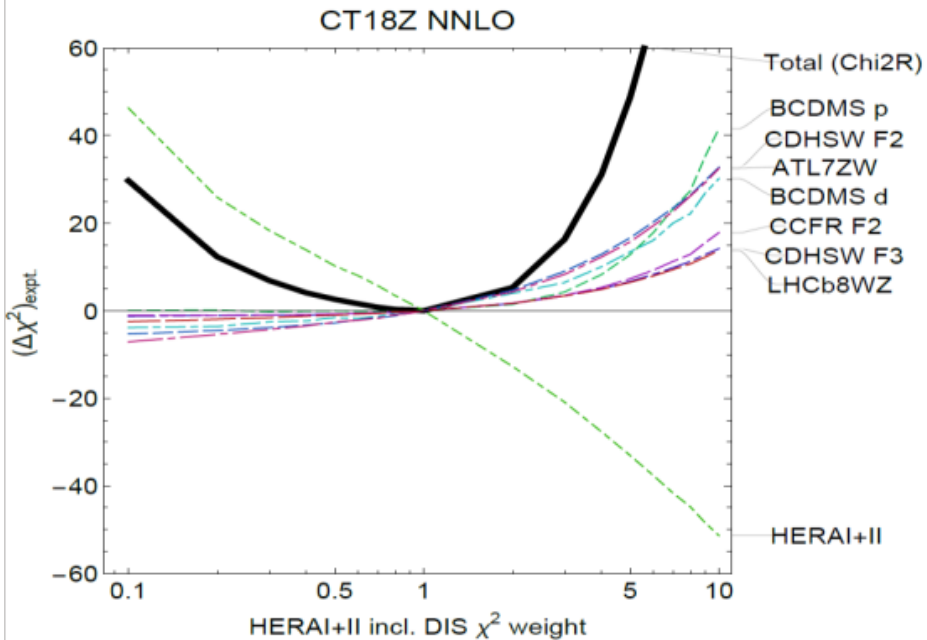
Good overall agreement. But observe opposite pulls from ATLAS7/CMS7 jet production and CMS8 jet production

Similarly, ATLAS  $t\bar{t}$  distributions  $d^2\sigma/(dp_{T,t}dm_{t\bar{t}})$  and CMS  $t\bar{t}$  distributions  $d^2\sigma/(dp_{T,t}dy_{t,ave})$  at 8 TeV impose weak opposite pulls

Constraints from ATLAS 8  $Z p_T$  production data are moderate and still affected by NNLO scale uncertainty



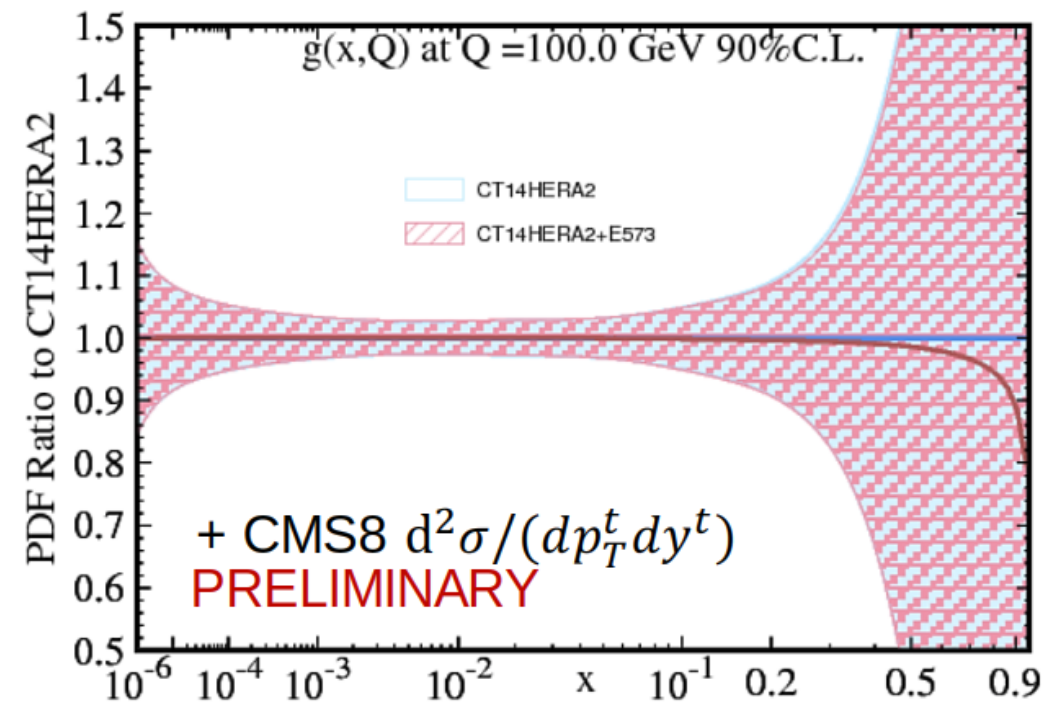
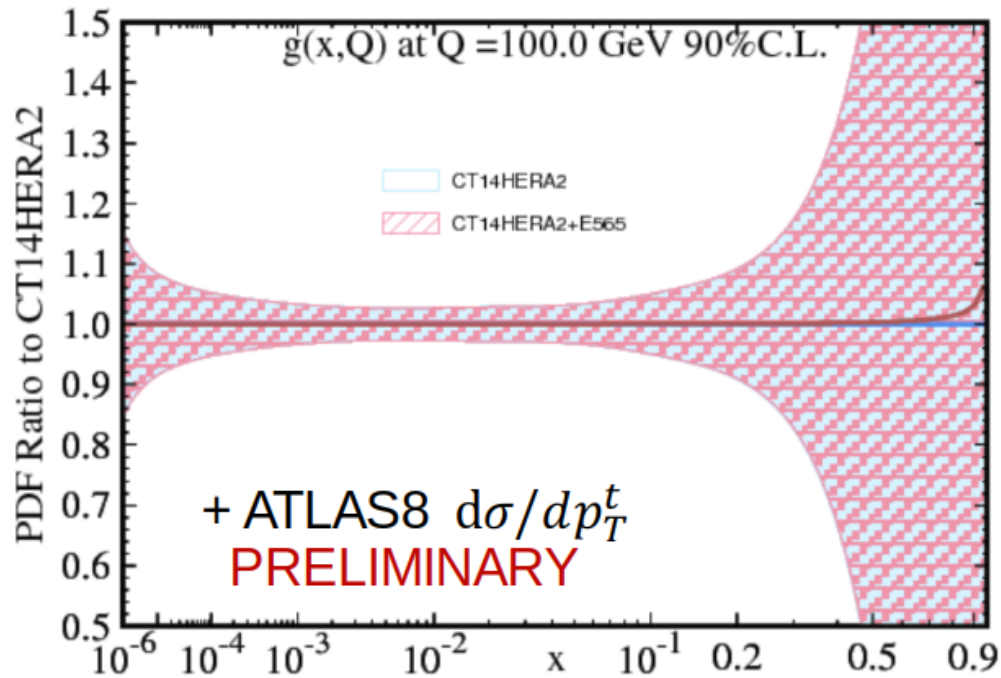
# LM scans on $\chi^2$ weights of HERA I+II, ATLAS 7 Z/W, and NuTeV data



Fits with varied weights and LM scans reveal a disagreement between important DIS [primarily HERA, CCFR, NuTeV,...] and DY [primarily ATL7ZW, E866, LHCb8WZ,...] experiments. This is more pronounced for large- $x$  gluon as well as strangeness.

## ePump estimates of impact of $t\bar{t}$ data

When the  $t\bar{t}$  data were added to the CT14HERA2 NNLO data set according to the **ePump** Hessian reweighting method (CT14nn+E<sub>XXX</sub>), no significant change in the PDF uncertainty was observed



FastNNLO calculation from **Csakon, Mitov, et al.**

Slight reduction in gluon PDF uncertainty at  $x \sim 0.2$ ; weaker than for the other groups because of also including jet production data

Top-antitop production experiments have **strong** sensitivity per data point, offer a **novel** independent measurement of the gluon PDF in several channels

## 2<sup>nd</sup> aside: kinematical matchings

- residual-PDF correlations and sensitivities are evaluated at parton-level kinematics determined according to leading-order matchings with physical scales in measurements

deeply-inelastic scattering:

$$\mu_i \approx Q|_i, \quad x_i \approx x_B|_i$$

$x_i$  : parton mom. fraction

$\mu_i$  : factorization scale

hadron-hadron collisions:

$AB \rightarrow CX$

$$\mu_i \approx Q|_i, \quad x_i^\pm \approx \frac{Q}{\sqrt{s}} \exp(\pm y_C)|_i$$

single-inclusive jet production:

$$Q = 2p_{Tj}, \quad y_C = y_j$$

$t\bar{t}$  pair production:

$$Q = m_{t\bar{t}}, \quad y_C = y_{t\bar{t}}$$

etc...

$d\sigma/dp_T^Z$  measurements:

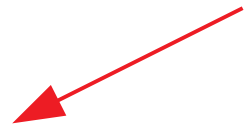
$$Q = \sqrt{(p_T^Z)^2 + (M_Z)^2}, \quad y_C = y_Z$$

the goal is to **quantify the strength of the constraints** placed on a particular set of PDFs by both individual and aggregated measurements *without direct fitting*

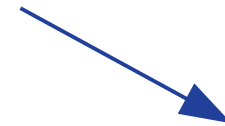
- for single-particle hadroproduction of gauge bosons at, *e.g.*, LHC, factorization gives

$$\sigma(AB \rightarrow W/Z+X) = \sum_n \alpha_s^n(\mu_R^2) \sum_{a,b} \int dx_a dx_b$$

$$\times f_{a/A}(x_a, \mu^2) \hat{\sigma}_{ab \rightarrow W/Z+X}(\hat{s}, \mu^2, \mu_R^2) f_{b/B}(x_b, \mu^2)$$



PDFs determined by fits to data; *e.g.*, "CT14H2"



pQCD matrix elements – specified by theoretical formalism in a given fit

- idea*: study the **statistical correlation** between PDFs and the quality of the fit at a measured data point(s); fit quality encoded in a (Theory) – (shifted Data) *residual*:

$$r_i(\vec{a}) = \frac{1}{s_i} (T_i(\vec{a}) - D_{i,sh}(\vec{a}))$$

$s_i$  : uncorrelated uncert.

$\vec{a}$  : PDF parameters

# a brief statistical aside, i

- the CTEQ-TEA global analysis relies on the **Hessian formalism** for its error treatment

$$\chi_E^2(\vec{a}) = \sum_{i=1}^{N_{pt}} r_i^2(\vec{a}) + \sum_{\alpha=1}^{N_\lambda} \bar{\lambda}_\alpha^2(\vec{a}) \longrightarrow \text{nuisance parameters to handle correlated errors}$$

$$r_i(\vec{a}) = \frac{1}{s_i} (T_i(\vec{a}) - D_{i,sh}(\vec{a}))$$

these result in systematic shifts to data central values:

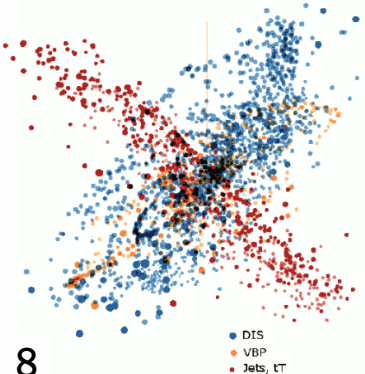
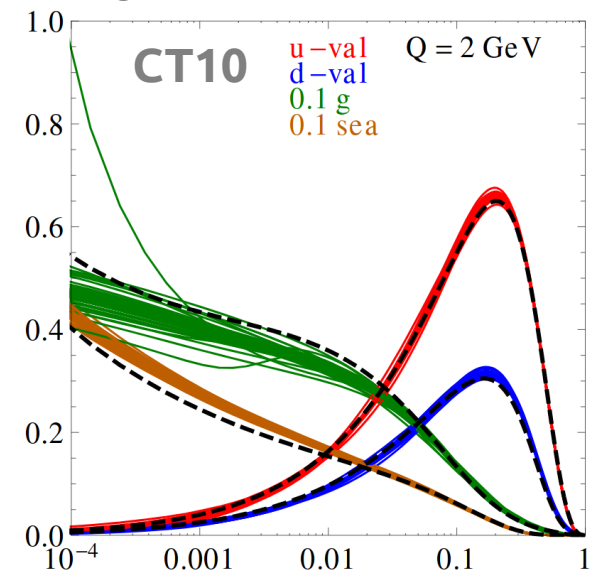
$$D_i \rightarrow D_{i,sh}(\vec{a}) = D_i - \sum_{\alpha=1}^{N_\lambda} \beta_{i\alpha} \bar{\lambda}_\alpha(\vec{a})$$

- a 56-dimensional parametric basis  $\vec{a}$  is obtained by diagonalizing the Hessian matrix H determined from  $\chi^2$  (following a 28-parameter fit)

use this basis to compute 56-component "normalized" residuals:

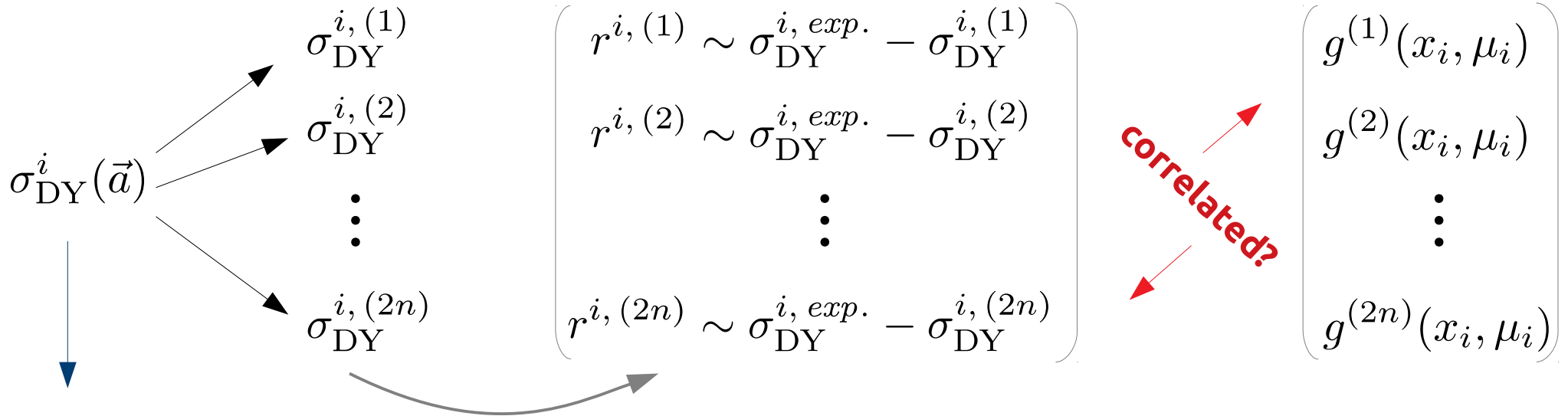
$$\delta_{i,l}^\pm \equiv (r_i(\vec{a}_l^\pm) - r_i(\vec{a}_0)) / \langle r_0 \rangle_E$$

$$\text{where } \langle r_0 \rangle_E \equiv \sqrt{\frac{1}{N_{pt}} \sum_{i=1}^{N_{pt}} r_i^2(\vec{a}_0)}$$



# a brief statistical aside, i [a]

## error replicas



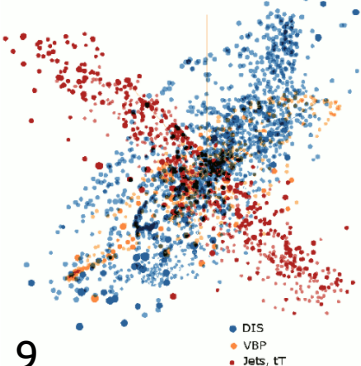
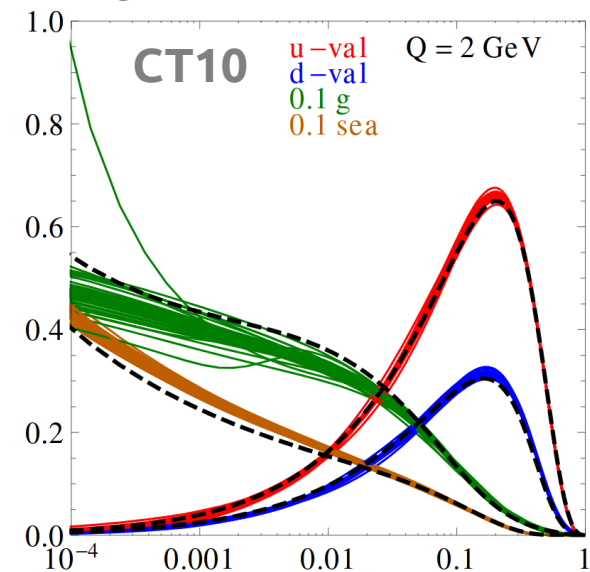
PDF prediction for  $i^{th}$  empirical measurement kinematically matched to a specific  $(x_i, \mu_i)$

- a 56-dimensional parametric basis  $\vec{a}$  is obtained by diagonalizing the Hessian matrix  $H$  determined from  $\chi^2$  (following a 28-parameter fit)

use this basis to compute 56-component "normalized" residuals:

$$\delta_{i,l}^{\pm} \equiv (r_i(\vec{a}_l^{\pm}) - r_i(\vec{a}_0)) / \langle r_0 \rangle_E$$

$$\text{where } \langle r_0 \rangle_E \equiv \sqrt{\frac{1}{N_{pt}} \sum_{i=1}^{N_{pt}} r_i^2(\vec{a}_0)}$$

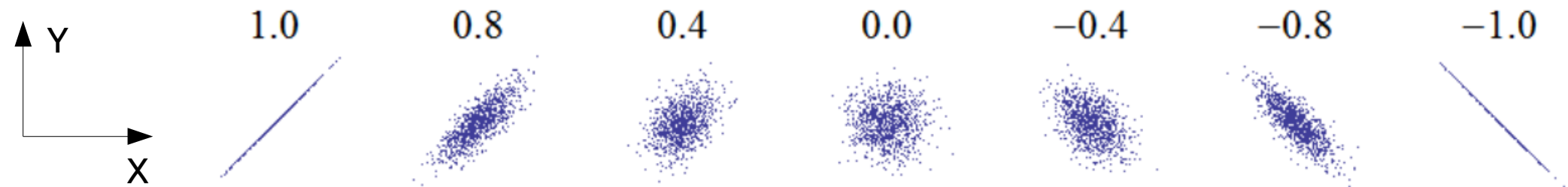


## a brief statistical aside, ii

- ... but how does the behavior of these residuals relate to the fitted PDFs and their uncertainties?

→ for example, how does the PDF uncertainty (at specific  $x$ ,  $\mu$ ) correlate with the residual associated with a theoretical prediction at the same  $x$ ,  $\mu$ ?

examine the Pearson correlation over the 56-member PDF error set between a PDF of given flavor and the residual



[X,Y] are exactly (anti-)correlated at the far (right) left above.

- we may then evaluate correlations between arbitrary PDF-derived quantities over the ensemble of error sets ([X,Y] may be PDFs, cross sections, residuals,...):

$$\text{Corr}[X, Y] = \frac{1}{4\Delta X \Delta Y} \sum_{j=1}^N (X_j^+ - X_j^-)(Y_j^+ - Y_j^-) \quad \Delta X = \frac{1}{2} \sqrt{\sum_{j=1}^N (X_j^+ - X_j^-)^2}$$

# Correlation $C_f$ and sensitivity $S_f$

The relation of data point  $i$  on the PDF dependence of  $f$  can be estimated by:

- $C_f \equiv \text{Corr}[\rho_i(\vec{a}), f(\vec{a})] = \cos\varphi$

$\vec{\rho}_i \equiv \vec{\nabla}r_i / \langle r_0 \rangle_E$  -- gradient of  $r_i$  normalized to the r.m.s. average residual in expt E;

$$(\vec{\nabla}r_i)_k = (r_i(\vec{a}_k^+) - r_i(\vec{a}_k^-)) / 2$$

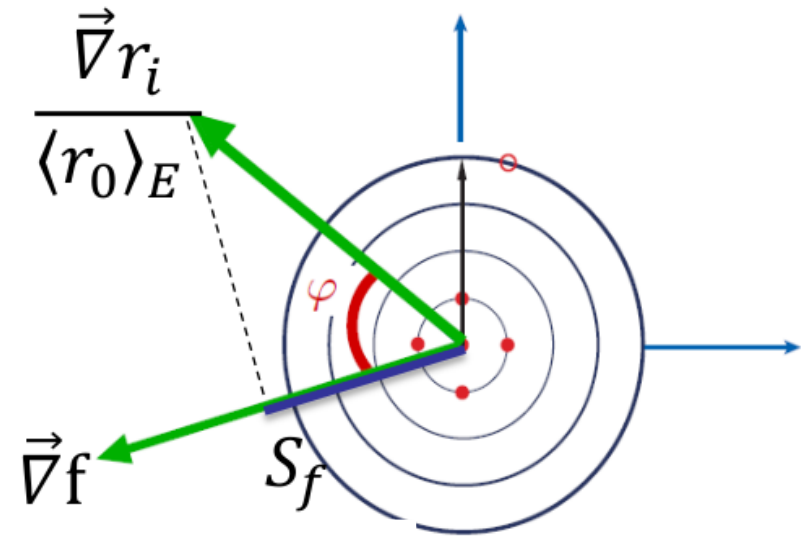
$$\text{Corr}[X, Y] = \frac{1}{4\Delta X \Delta Y} \sum_{j=1}^N (X_j^+ - X_j^-)(Y_j^+ - Y_j^-)$$

$C_f$  is **independent** of the experimental and PDF uncertainties. In the figures, take  $|C_f| \gtrsim 0.7$  to indicate a large correlation.

- $S_f \equiv |\vec{\rho}_i| \cos\varphi = C_f \frac{\Delta r_i}{\langle r_0 \rangle_E}$  -- projection of  $\vec{\rho}_i(\vec{a})$  on  $\vec{\nabla}f$

$S_f$  is proportional to  $\cos\varphi$  and the ratio of the PDF uncertainty to the experimental uncertainty. We can sum  $|S_f|$ .

In the figures, take  $|S_f| > 0.25$  to be significant.



independent of some fitting/reweighting ambiguities  
– e.g., the tolerance

more tomorrow on LHC implications

today: what about future experiments?

---

e.g., HL-LHC, LHeC, and beyond...

Mapping the PDF sensitivity of future facilities (HL-LHC, LHeC, and EIC)

T.J. Hobbs, Bo-Ting Wang, Pavel Nadolsky, Fredrick Olness

[arxiv:1907.00988](https://arxiv.org/abs/1907.00988)

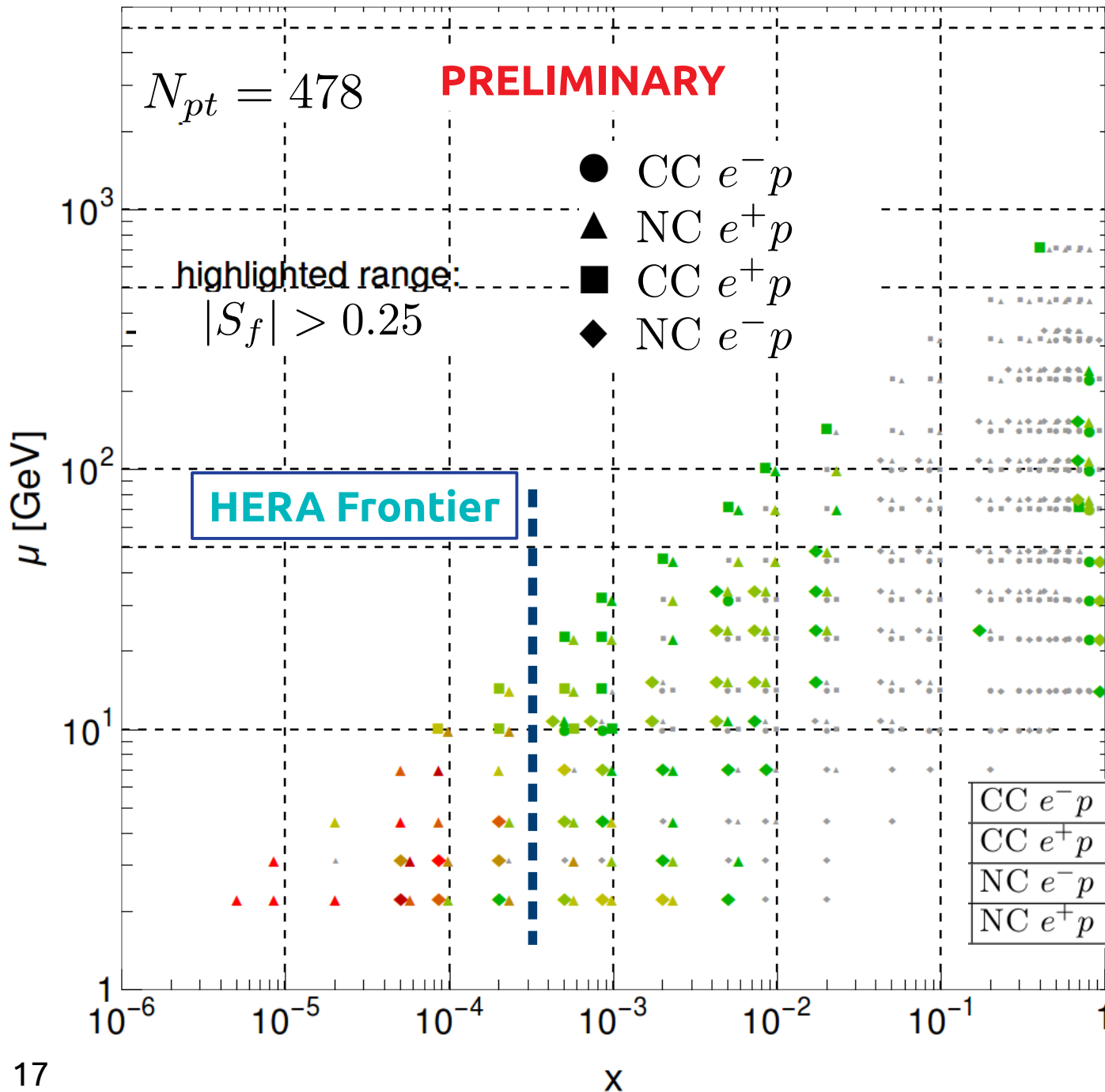
(more detailed work in preparation)

- an electron-proton (or electron-ion) collider to achieve **high luminosities**  $\gtrsim 1000$  times that of HERA
  - access a wide range of  $x$ , including  $x \simeq 10^{-6}$
  - explore the dynamics of gluon saturation; greatly improve PDF precision; perform SM tests; and many other physics goals
- can perform a sensitivity analysis of Monte Carlo generated  $ep$  reduced NC/CC cross sections (Klein & Radescu, LHeC-Note-2013-002 PHY)

$$60 \text{ GeV } e^{\pm} \text{ on } 1 \text{ or } 7 \text{ TeV } p$$

- to minimize the impact of large  $\chi^2$  of unfitted data (especially at low  $x$ ), we study the sensitivities for **fluctuated data** – i.e., pseudodata randomly fluctuated about the PDF4LHC15 NNLO prediction according to putative LHeC uncorrelated errors – based on **100 fb<sup>-1</sup>** of data

# $|S_f|$ for $g(x, \mu)$ , PDF4LHC15 NNLO

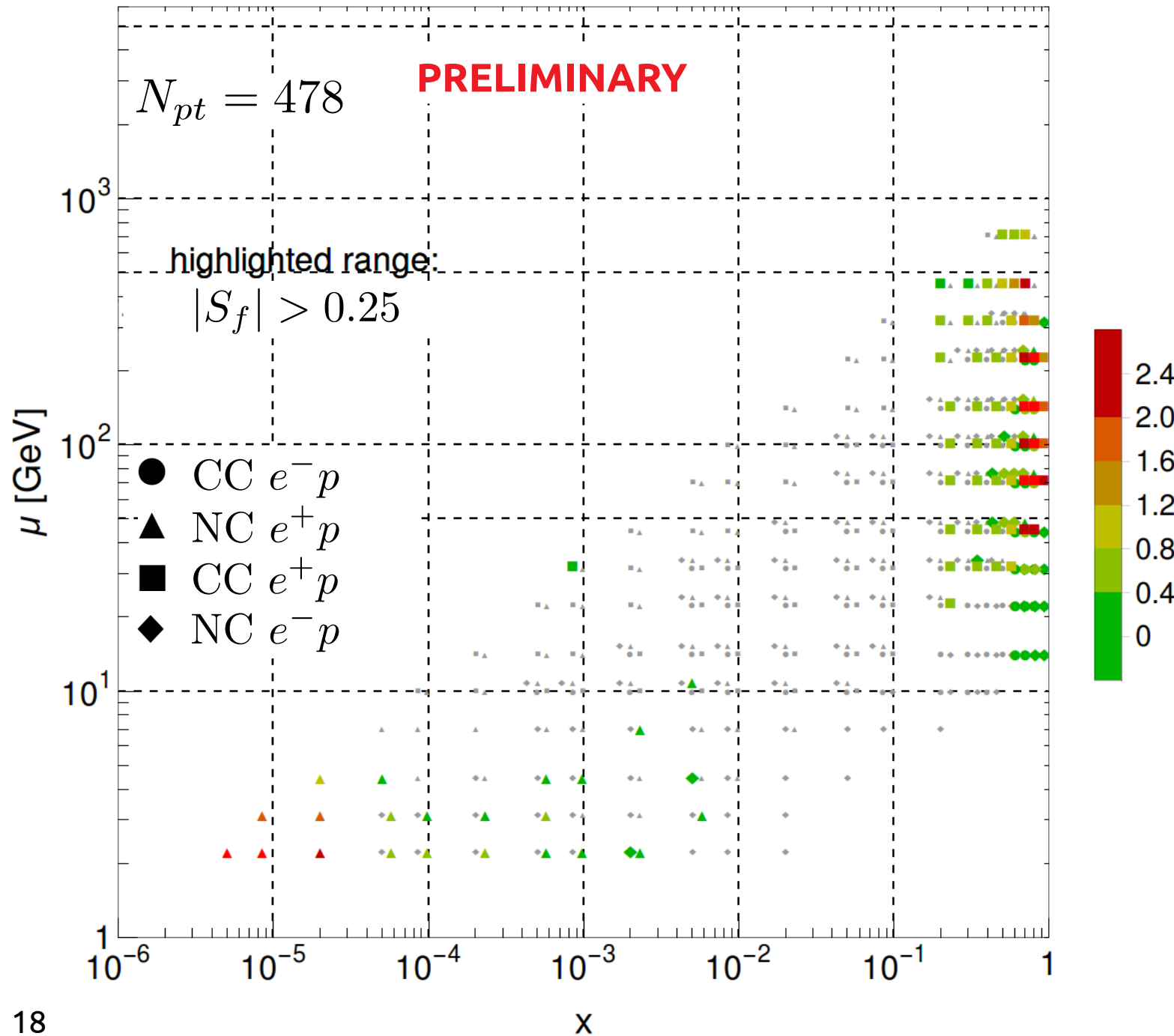


- very strong sensitivities along the frontier of the HERA Run II data,  $x \lesssim 10^{-4}$

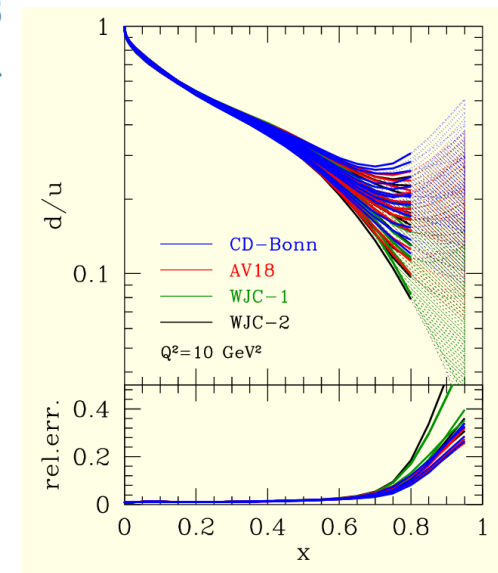
however, there are important constraints in general for  $x \lesssim 10^{-2}$

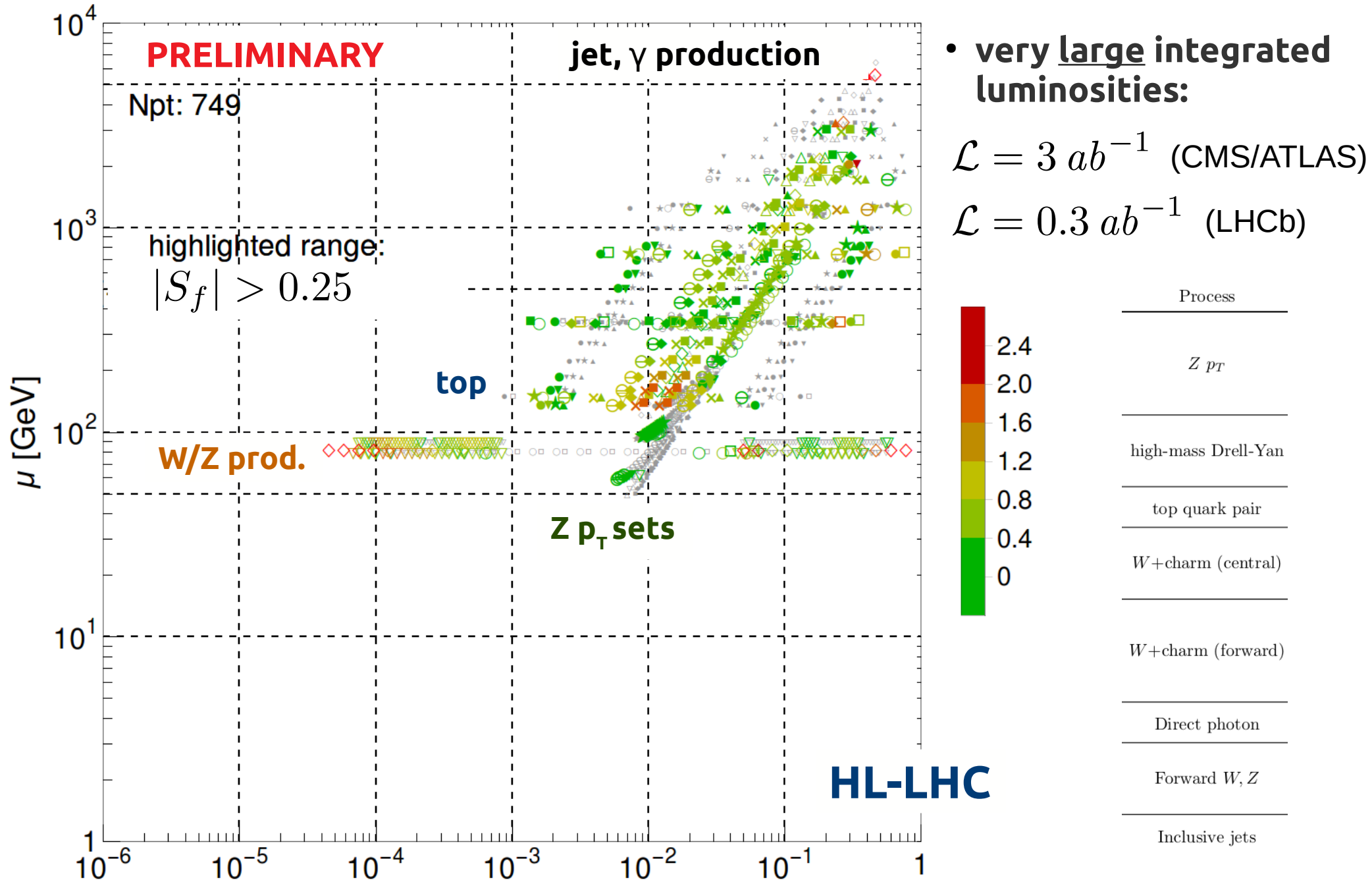
...and high  $x, \mu$

# $|S_f|$ for $d/u(x,\mu)$ , PDF4LHC15 NNLO



- LHeC's high luminosity may give it a reach to high enough  $x$  to help resolve the stubborn  $d/u$  question
- ...without a nuclear target...





- **very large integrated luminosities:**

$\mathcal{L} = 3 \text{ ab}^{-1}$  (CMS/ATLAS)

$\mathcal{L} = 0.3 \text{ ab}^{-1}$  (LHCb)

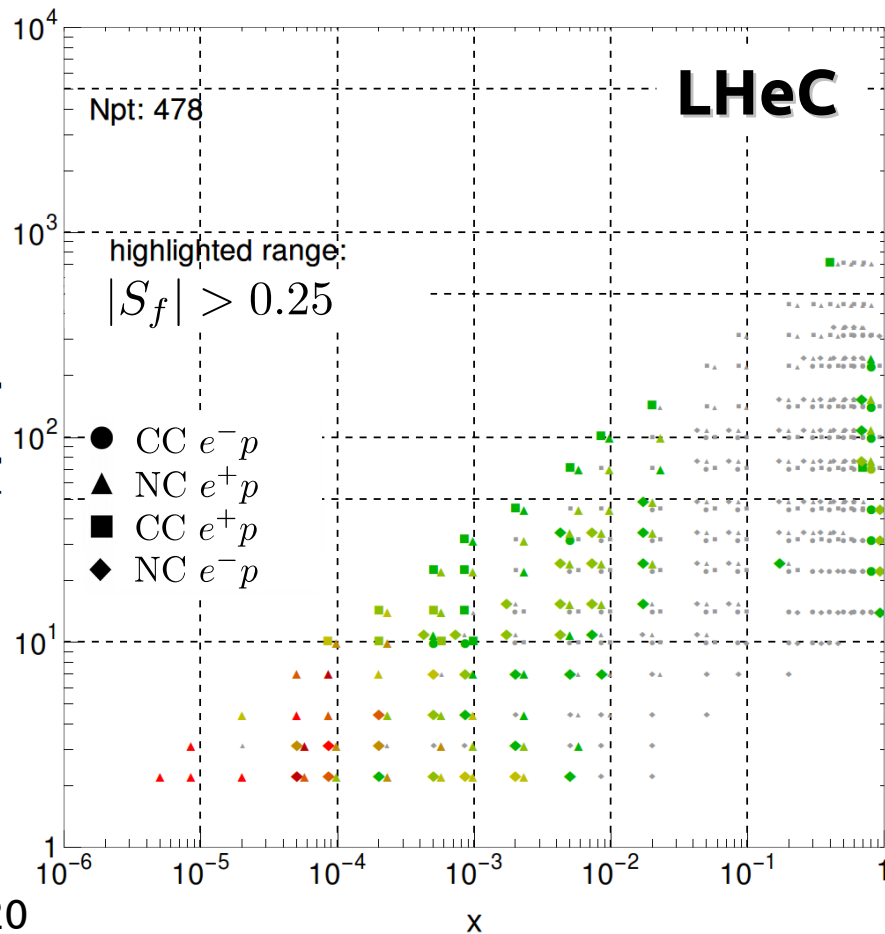
# now directly compare the LHeC vs. HL-LHC flavor sensitivities\*

\* noting the much larger integrated luminosity of the HL-LHC pseudo-data

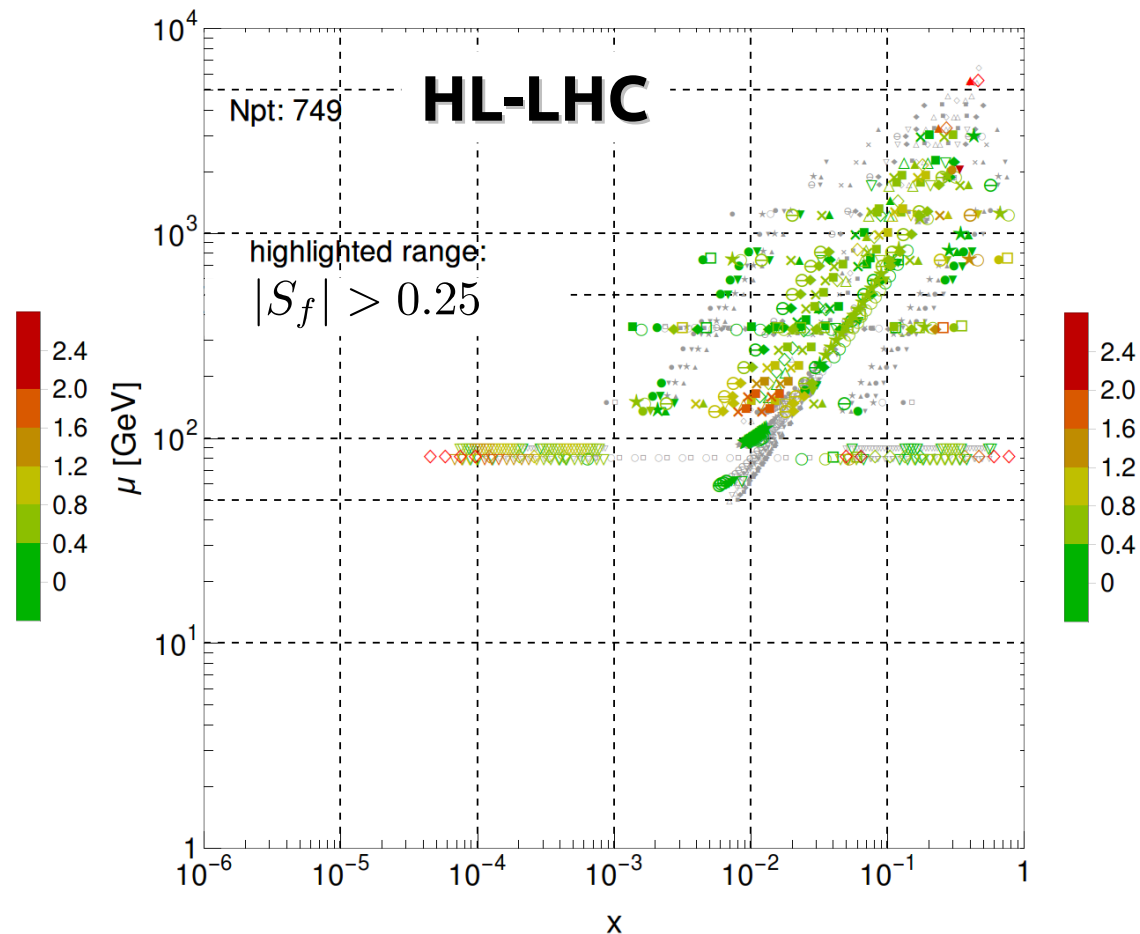
→ we compare both kinematic regions of especially strong sensitivity, and the aggregated impact of each experiment:

$$|S_g^{\text{LHeC}}| = 151.4 < |S_g^{\text{HL-LHC}}| = 244.6$$

$|S_f|$  for  $g(x, \mu)$ , PDF4LHC15 NNLO



$|S_f|$  for  $g(x, \mu)$ , PDF4LHC15 NNLO

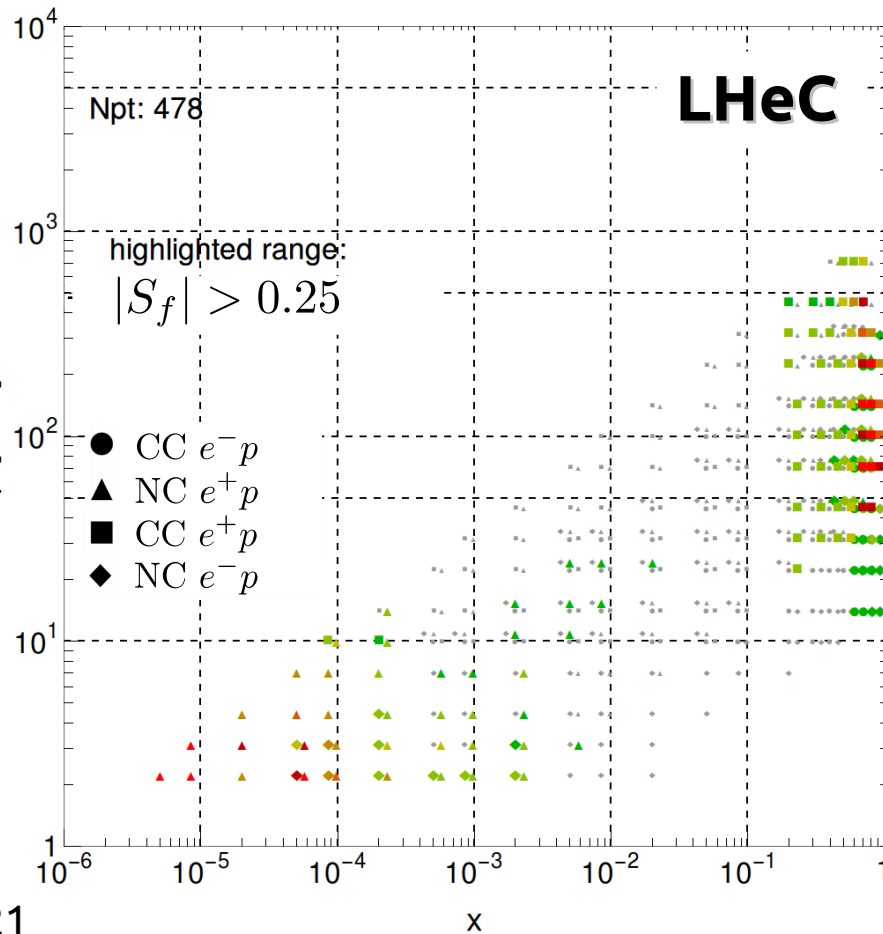


even with a small (pseudo)data set, LHeC enjoys strong sensitivity to down-type distributions!

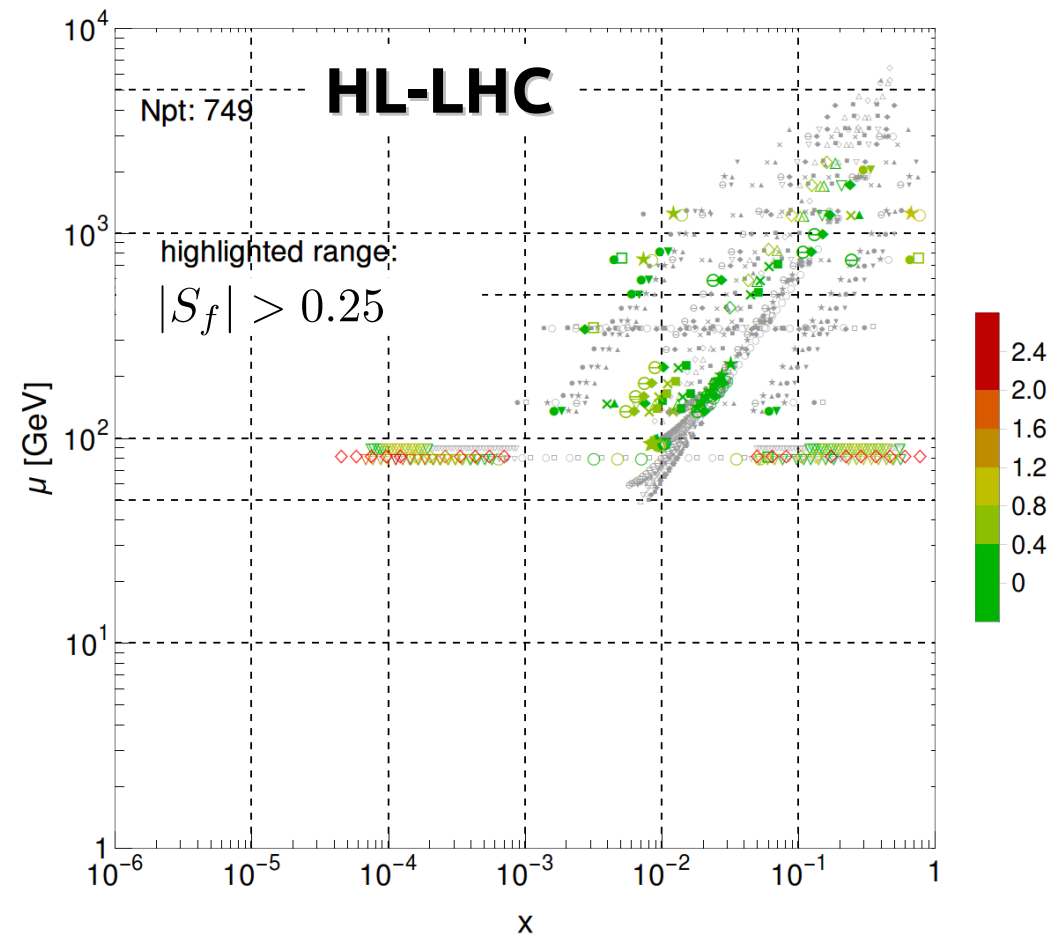
→ especially in a fashion complementary to HL-LHC, at very high/low  $x$

$$|S_d^{\text{LHeC}}| = 214.3 > |S_d^{\text{HL-LHC}}| = 170.8$$

$|S_f|$  for  $d(x, \mu)$ , PDF4LHC15 NNLO

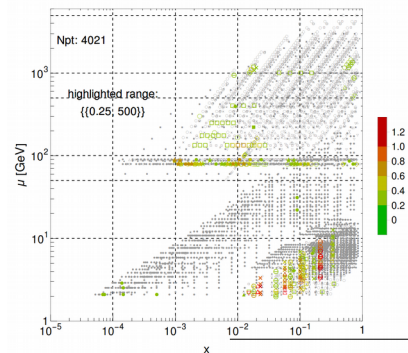


$|S_f|$  for  $d(x, \mu)$ , PDF4LHC15 NNLO



→ LHeC especially portends significantly heightened knowledge of nucleon strangeness

- CTEQ-TEA constraints come primarily through older fixed-target data and Tevatron data (and LHC Run I)



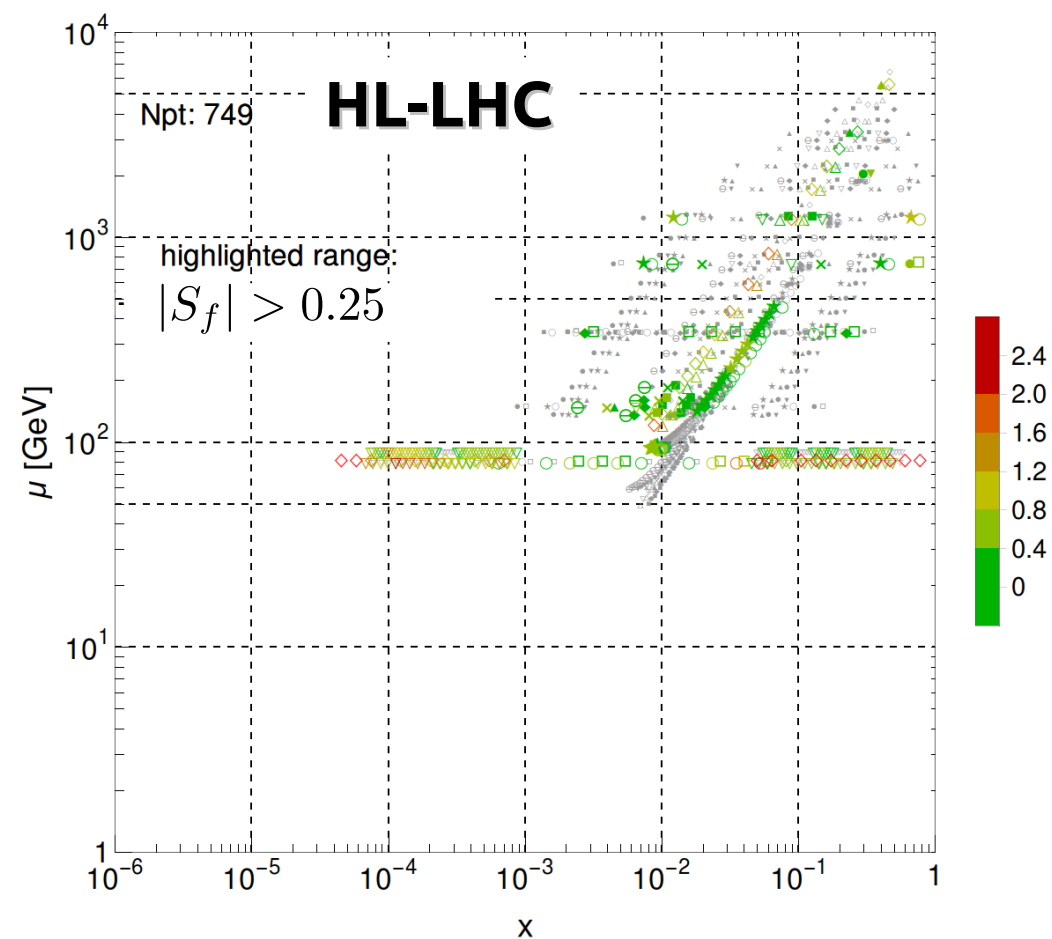
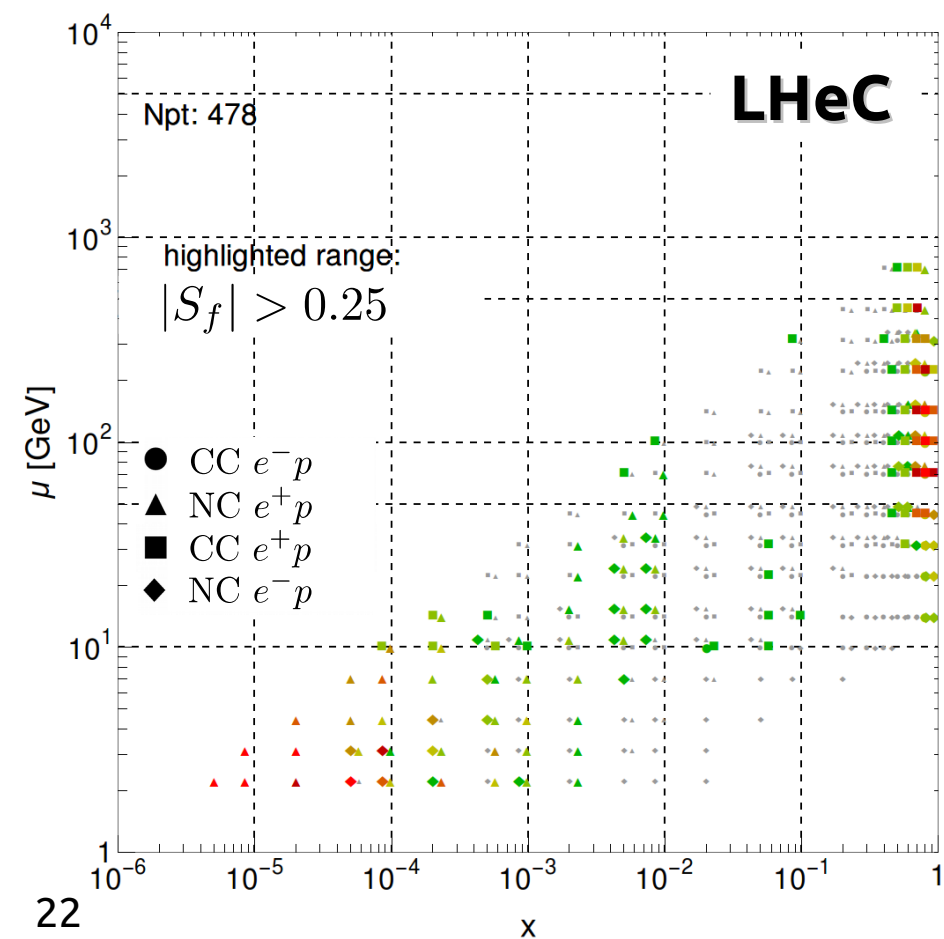
$$|S_s^{\text{LHeC}}| = 214.1$$

$\gg$

$$|S_s^{\text{HL-LHC}}| = 184.8$$

$|S_f|$  for  $s(x,\mu)$ , PDF4LHC15 NNLO

$|S_f|$  for  $s(x,\mu)$ , PDF4LHC15 NNLO

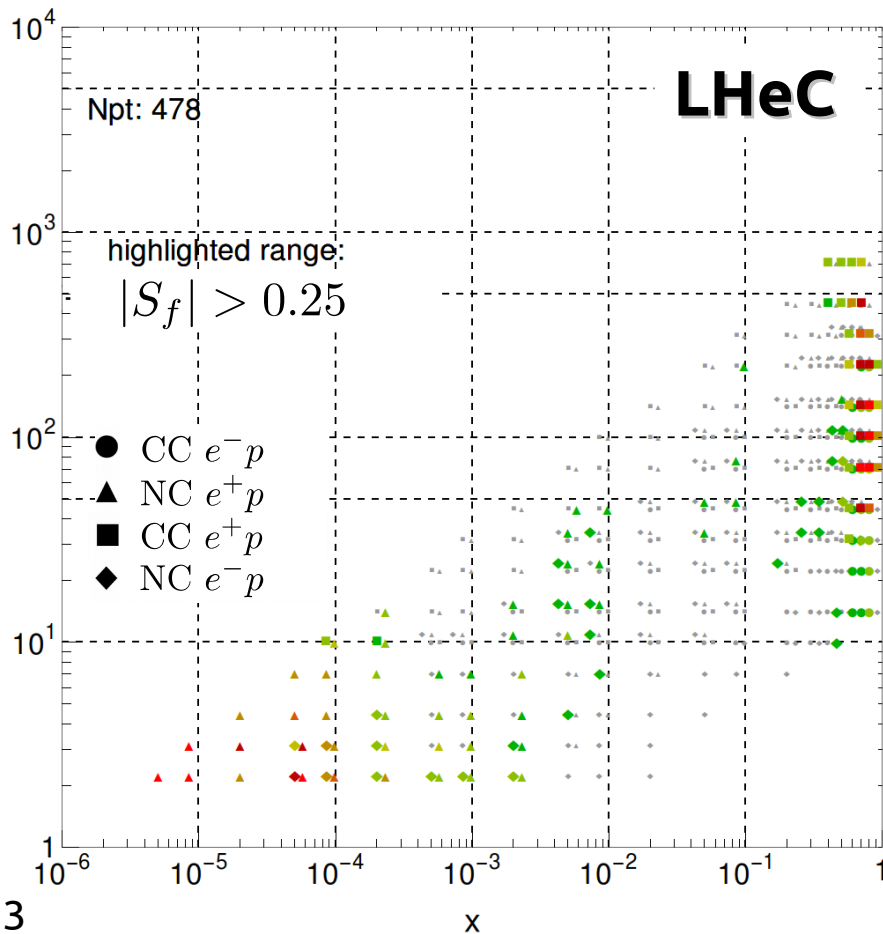


# in the SU(2) quark sea, the LHeC 100 fb<sup>-1</sup> set imposes constraints of magnitude comparable to HL-LHC

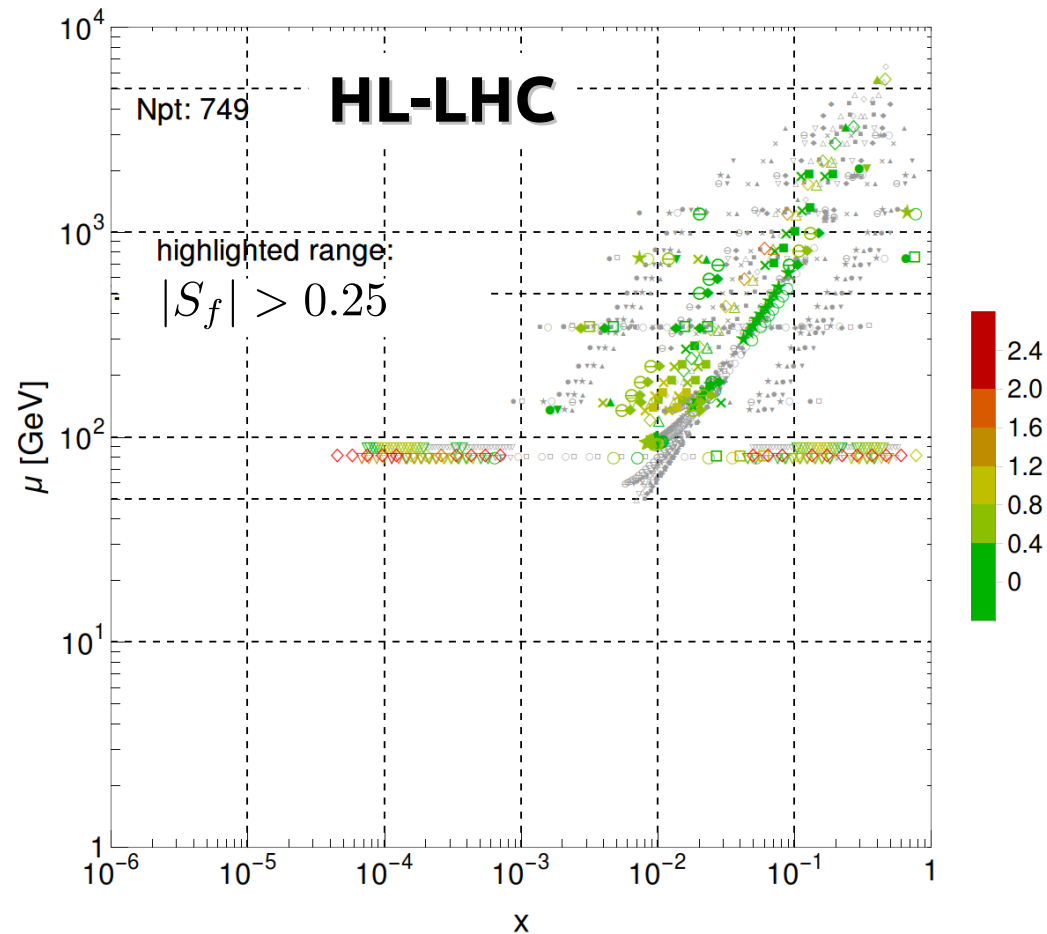
...these again predominate at the extrema of  $x$

$$|S_{\bar{d}}^{\text{LHeC}}| = 192.7 \quad \sim \quad |S_{\bar{d}}^{\text{HL-LHC}}| = 199.4$$

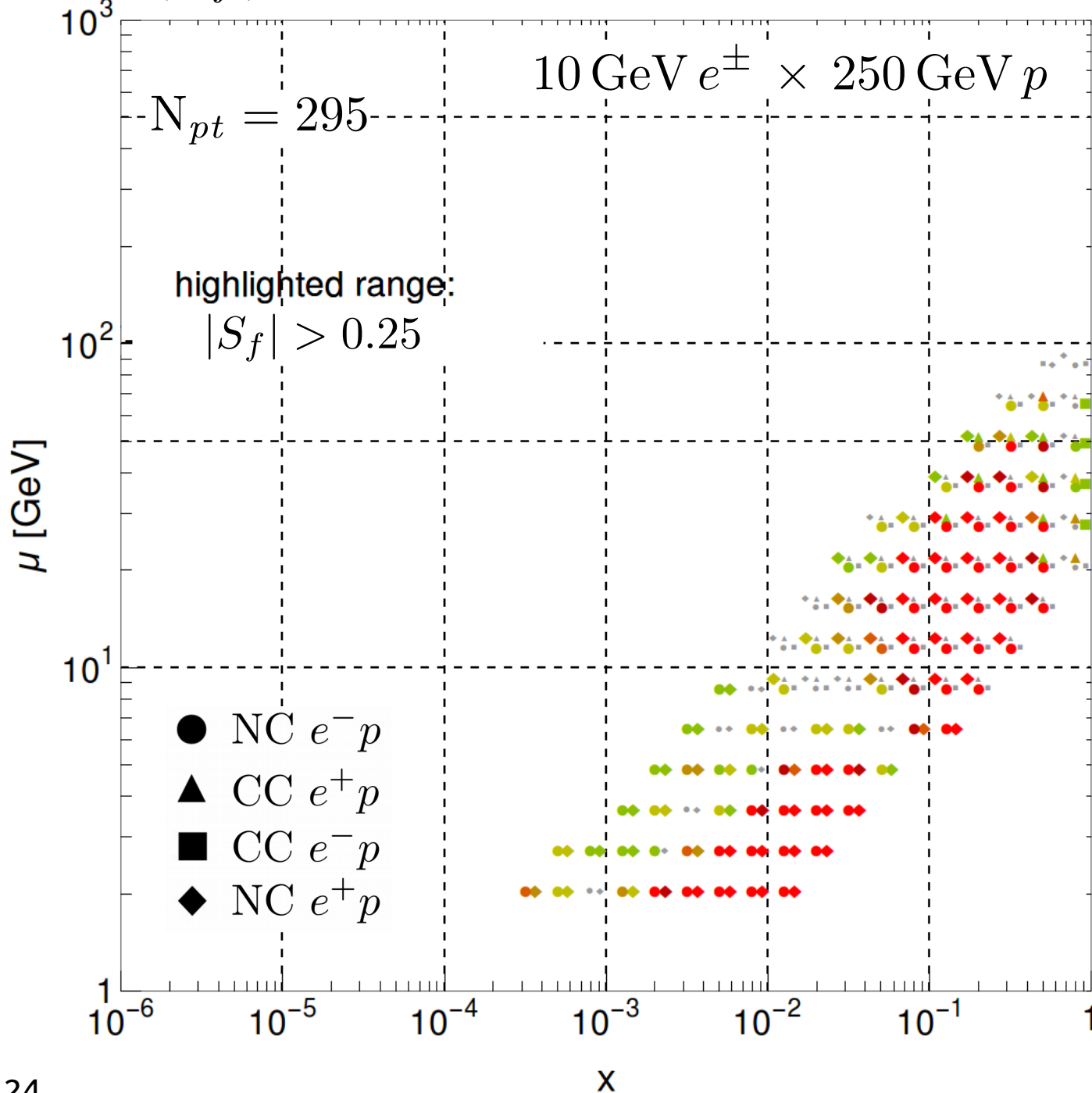
$|S_f|$  for  $\bar{d}(x,\mu)$ , PDF4LHC15 NNLO



$|S_f|$  for  $\bar{d}(x,\mu)$ , PDF4LHC15 NNLO



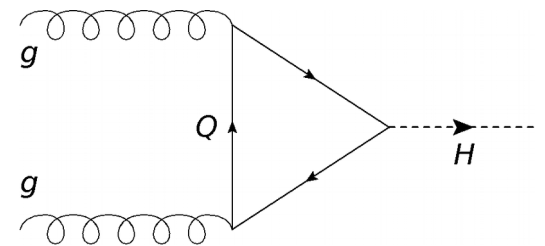
$|S_f|$  for  $\sigma_H$ , 14 TeV CT14 HERA2 NNLO



epilogue: a US-based EIC will have important HEP consequences, e.g., on Higgs physics

- the impact of an EIC upon the theoretical predictions for inclusive Higgs production arises from a very broad region of the kinematical space it can access

- impact rather closely tied to that of the integrated gluon PDF:



- **lattice QCD** calculations continue to improve and will be increasingly useful as <sup>4</sup> inputs into QCD global analyses

PDF-Lattice whitepaper – Lin et al., PNP100, 107 (2018); arXiv:1711.07916.

- the PDF-Lattice relationship will be *synergistic* :

→ PDF phenomenologists deliver improving benchmarks to challenge the Lattice



→ Lattice calculations for PDF Mellin **moments** and **quasi-PDFs** can be theoretical priors for QCD global fits

PDFSense analysis – Hobbs, Wang, Nadolsky and Olness, arXiv:1904.00022.

- moments from lattice can help unravel PDF flavor dependence, constrain phenom. PDFs:

$$(i) \quad \langle x^n \rangle_q = \int_0^1 dx x^n [q(x) + (-1)^{n+1} \bar{q}(x)] \rightarrow \langle x^{1,3,\dots} \rangle_{q^+}, \langle x^{2,4,\dots} \rangle_{q^-}$$

$$\mu_F = \mu^{\text{lat.}} = 2 \text{ GeV}$$

- lattice can also now compute x-dependent quantities – the quasi-PDFs (qPDFs):

$$(ii) \quad \tilde{q}(x, P_z, \tilde{\mu}) = \int_{-\infty}^{\infty} \frac{dz}{4\pi} e^{ixP_z z} \langle P | \bar{\psi}(z) \gamma^z U(z, 0) \psi(0) | P \rangle$$

## (i) PDF moments can be evaluated on the QCD lattice

- in lattice gauge theory, the accessible moments are C-odd/even combinations,

$$\langle x^n \rangle_q = \int_0^1 dx x^n [q(x) + (-1)^{n+1} \bar{q}(x)]$$

$$\left\{ \begin{array}{l} \langle x^n \rangle_{q^+} = \langle x^n \rangle_q \quad \text{for } n = 2\ell - 1 \\ \langle x^n \rangle_{q^-} = \langle x^n \rangle_q \quad \text{for } n = 2\ell \end{array} \right. \quad \ell \in \mathbb{Z}^+$$

- the PDF moments are related to hadronic matrix elements of twist-2 operators:

$$\frac{1}{2} \sum_s \langle p, s | \mathcal{O}_{\{\mu_1, \dots, \mu_{n+1}\}}^q | p, s \rangle = 2v_q^{n+1} [p_{\mu_1} \cdots p_{\mu_{n+1}} - \text{traces}]$$

PDF Mellin moments

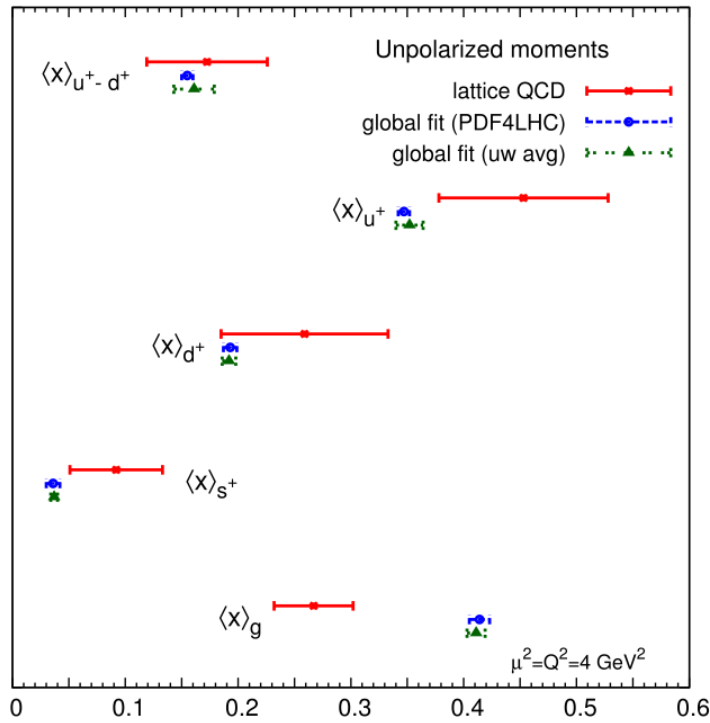
$$\mathcal{O}_{\{\mu_1, \dots, \mu_{n+1}\}}^q = \left( \frac{i}{2} \right)^n \bar{q}(x) \gamma_{\mu_1} \overleftrightarrow{D}_{\mu_2} \cdots \overleftrightarrow{D}_{\mu_{n+1}} q(x)$$

gauge-covariant derivatives

# the status of lattice QCD calculations

PDF-Lattice whitepaper – Lin et al., Prog. Part. Nucl. Phys. **100**, 107 (2018).

Mom.	Collab.	Ref.	$N_f$	Status	Disc [fm]	QM	FV	Ren	ES	
$\langle x \rangle_{u^+ - d^+}$	ETMC 15	[263]	2+1+1	P	0.06, 0.08	–	■, ★	★, ★	■, ★	
	ETMC 15	[263]	2	P	0.06–0.09	–	○	★	■	
	RQCD 14	[251]	2	P	0.06–0.08	–	○	★	○	
Mom.	Collab.	Ref.	$N_f$	Status	Disc	QM	FV	Ren	ES	
$\langle x^2 \rangle_{u^- - d^-}$	LHPC and SESAM 02	[279]	2	P	■	■	■	○	■	0.145(69)
	QCDSF 05	[93]	0	P	■	■	■	★	■	0.083(17)
	LHPC and SESAM 02	[279]	0	P	■	■	■	○	■	0.090(68)



- depending upon flavor and order, lattice extractions of Mellin moments have varying status (above, FLAG evaluations)
  - e.g., the first isovector moment has been computed by numerous groups
  - but the second, by relatively few
- systematic lattice effects are similarly widely varied

however, improvements are being made rapidly!

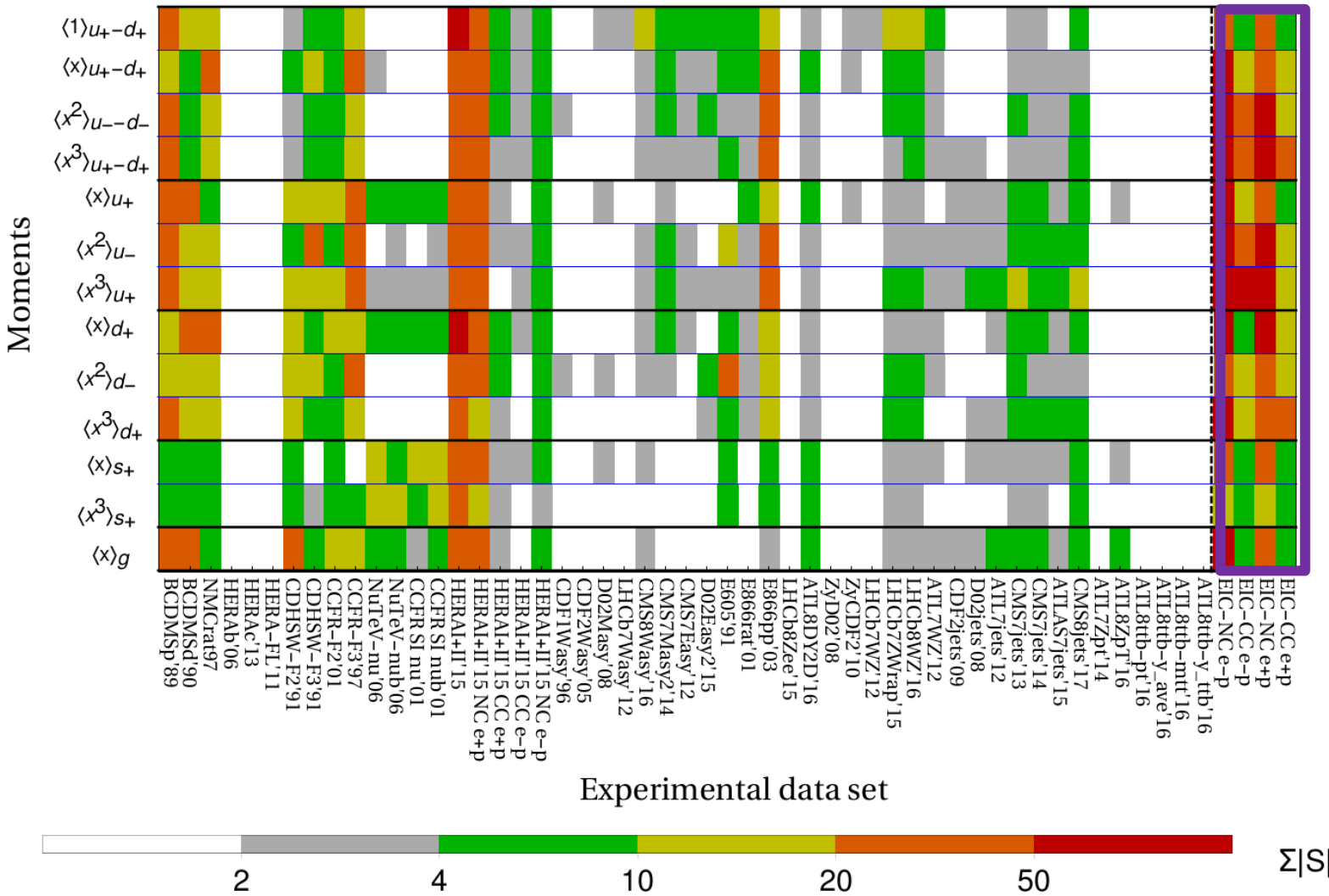
# sensitivity to Mellin moments

CT14HERA2, Total sensitivity  $\Sigma|S|$

Future

we show Mellin moments computable on the lattice at the scale  $\mu_F = 2 \text{ GeV}$

HERA, BCDMS, NMC, E866 DY pair production are most sensitive to the moments



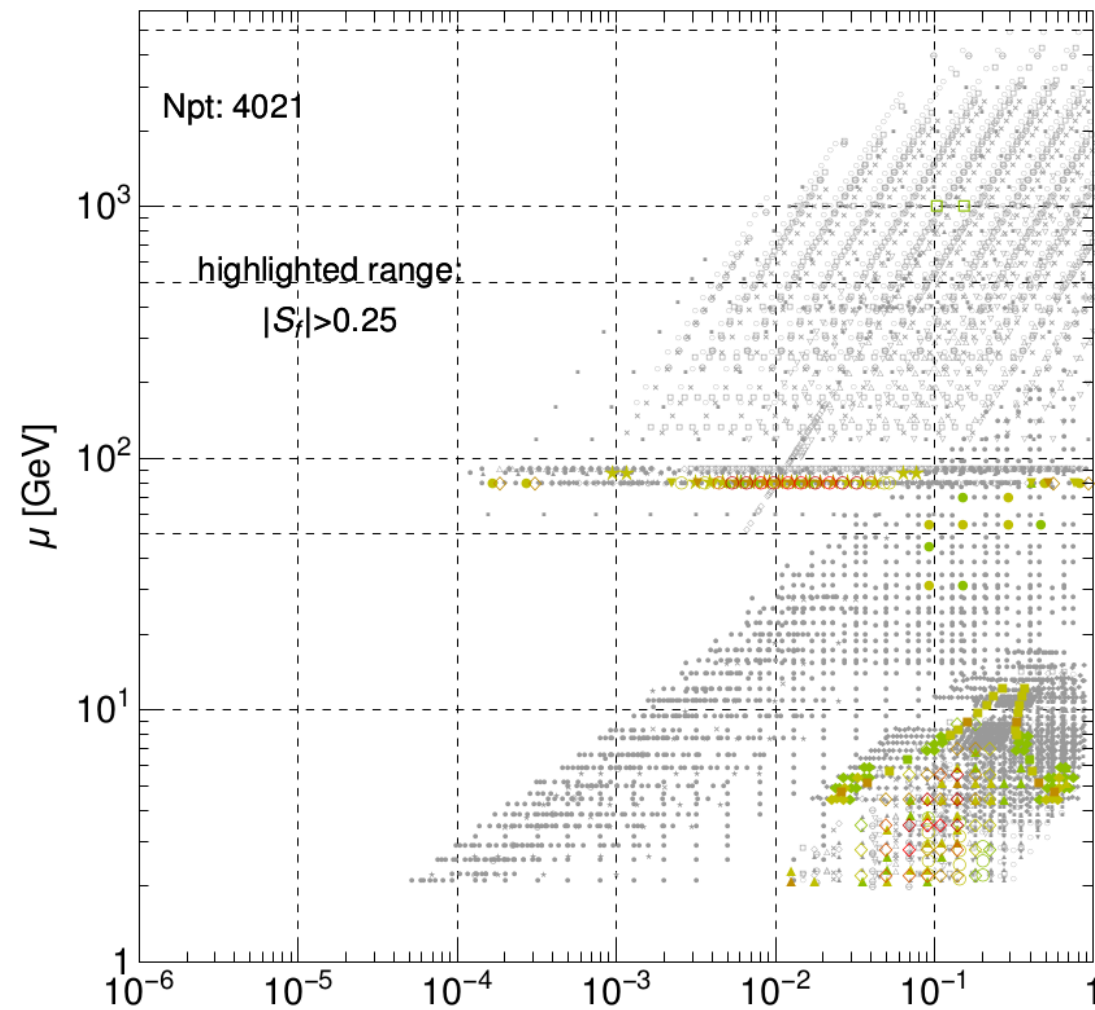
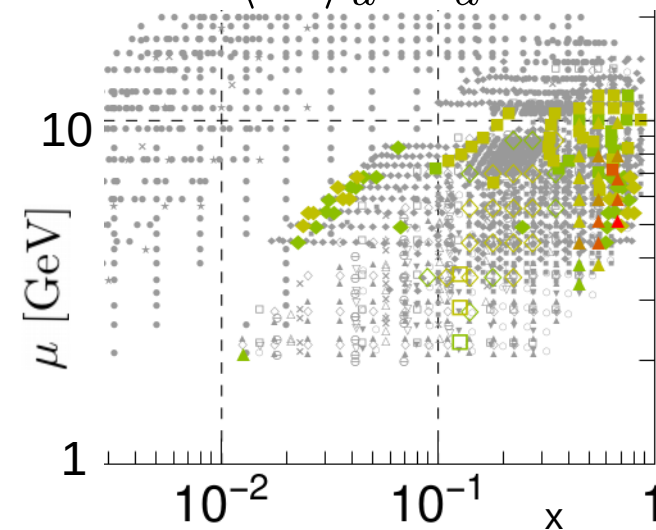
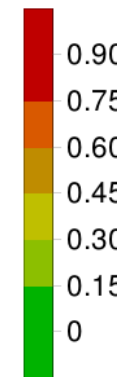
$|S_f|$  for  $\langle x^1 \rangle_{u^+ - d^+}$ , CT14HERA2

- We focus on **isovector** (u-d) PDF combinations

→ on the lattice, these are more readily computed since flavor non-singlet combinations do not receive disconnected insertions

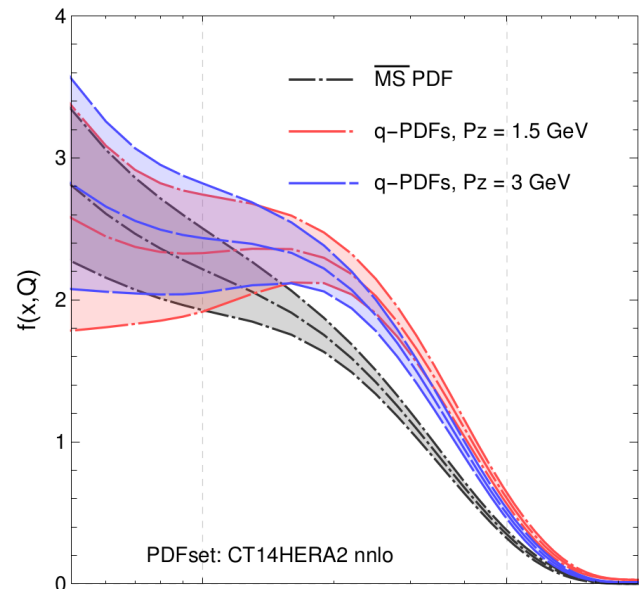
- Moments of higher order are constrained by higher  $x_i$  fixed-target data:

$\langle x^3 \rangle_{u^+ - d^+}$

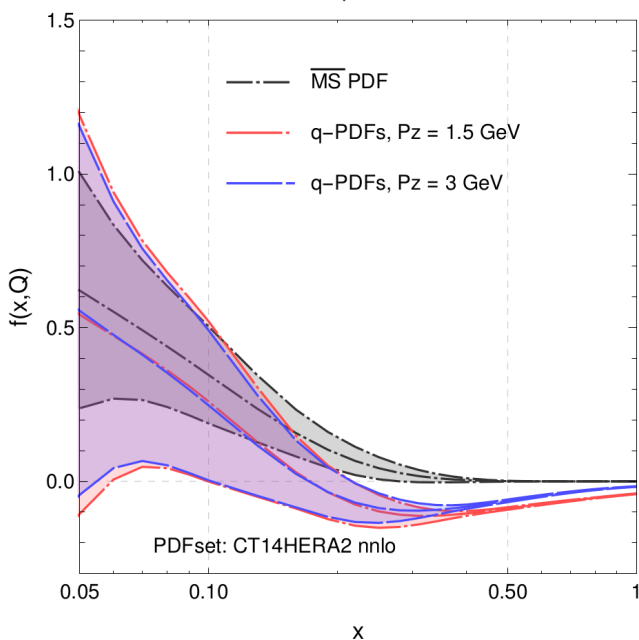


$$\bar{x}_{|S_f|} = \frac{\sum_i x_i |S_f^i|}{\sum_i |S_f^i|} \quad (\text{grows with moment order, } n)$$

u-d at  $\mu_F = 3\text{ GeV}$

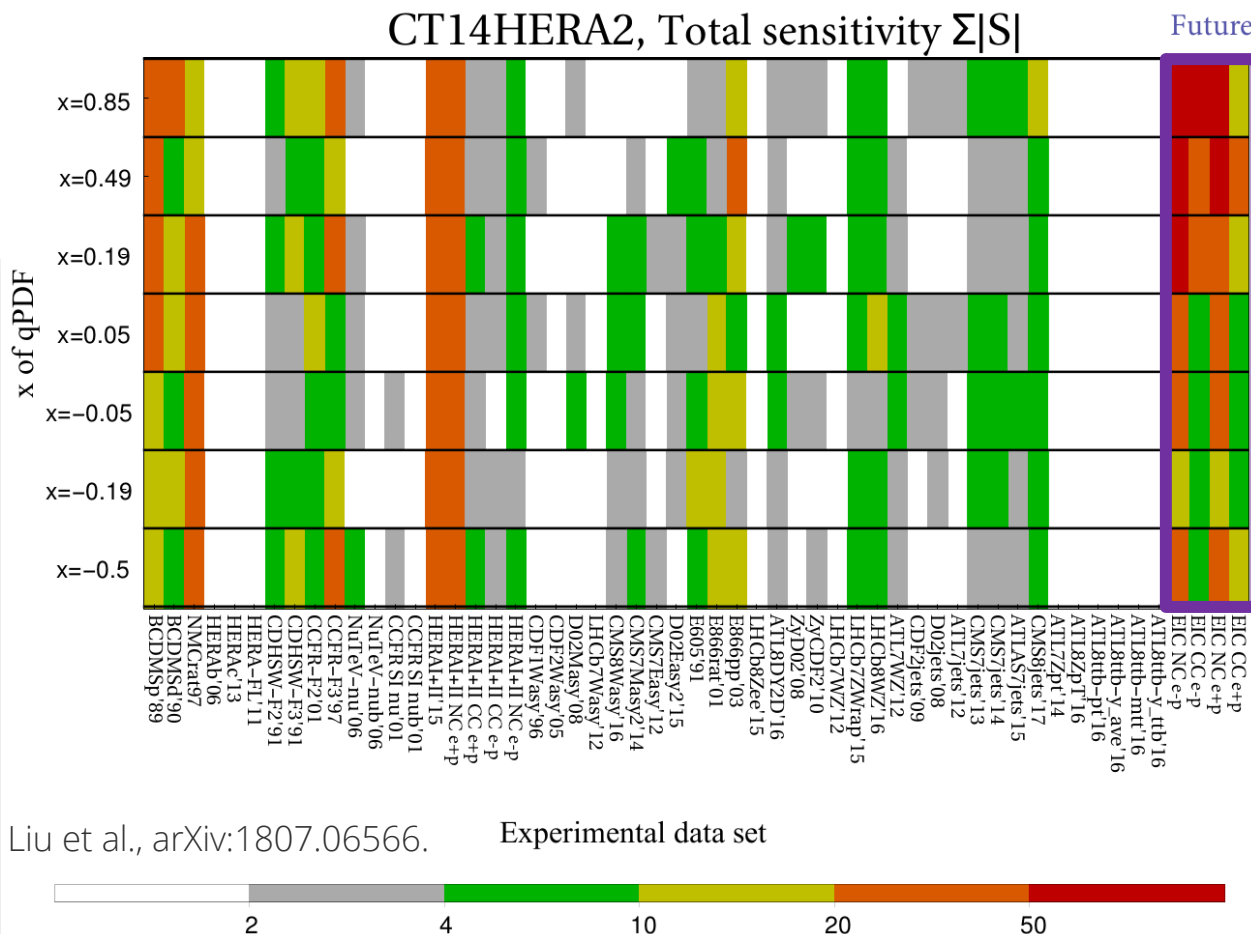


$\bar{d}-\bar{u}$  at  $\mu_F = 3\text{ GeV}$



$$\bar{q}(x) = -q(-x) \rightarrow q(x) \equiv \begin{cases} u(x) - d(x), & x > 0 \\ \bar{d}(|x|) - \bar{u}(|x|), & x < 0 \end{cases}$$

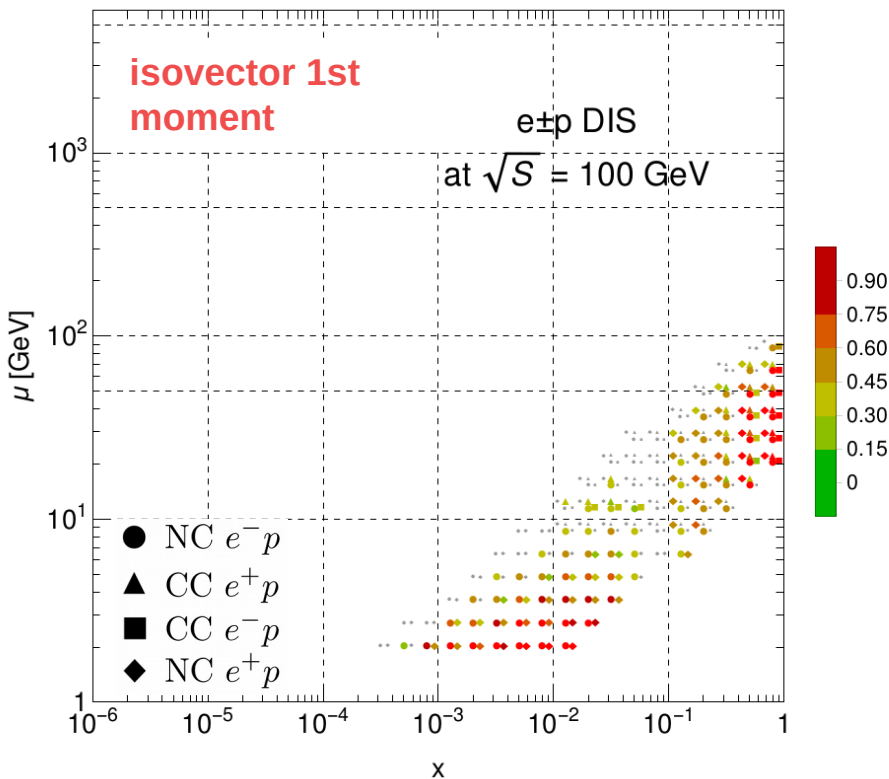
$P_z = 1.5\text{ GeV}; \mu_F = 3\text{ GeV}$



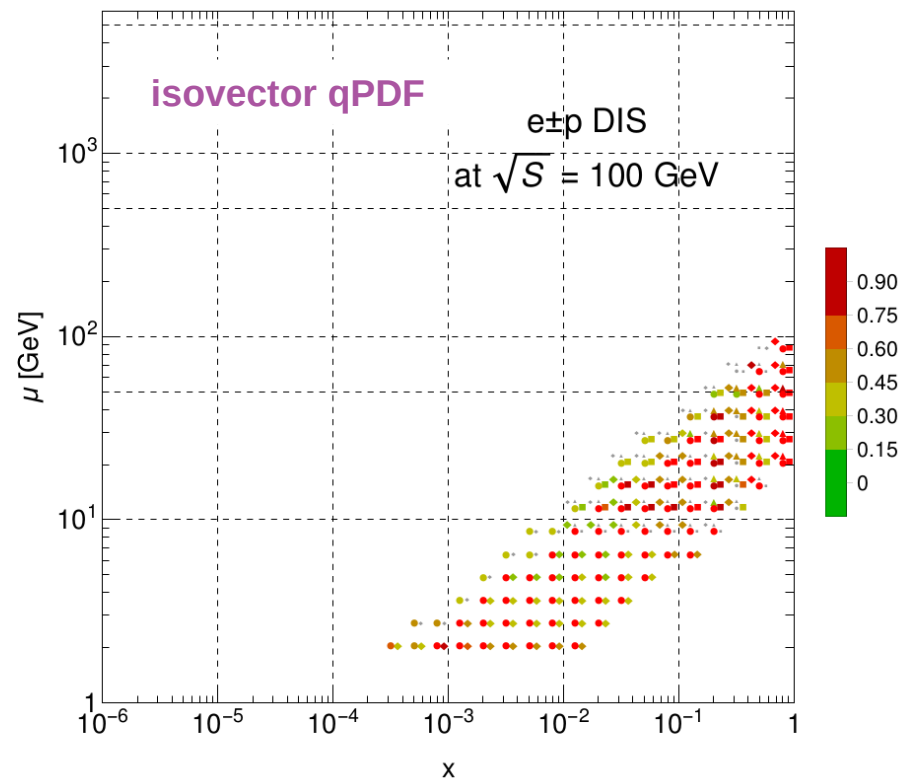
# An EIC would drive lattice phenomenology

- A high-luminosity lepton-hadron collider will impose very tight constraints on many lattice observables; below, the isovector first moment and qPDF
- Many of the experiments most sensitive to PDF Mellin moments and qPDFs involve nuclear targets → eA data from EIC would sharpen knowledge of nuclear corrections

$|S_f|$  for  $\langle x^1 \rangle_{u^+ - d^+}$ , CT14HERA2



$|S_f|$  for  $[\tilde{u} - \tilde{d}](x=0.85, P_z=1.5\text{GeV})$ , CT14HERA2



→ “EIC impact on tomography and HEP phenom.,” Session **C09**: Sat., April 13<sup>th</sup> – 1:30pm